

Hepatitis C: transcriptional response and interferon signalling in human liver

Inauguraldissertation

zur
Erlangung der Würde eines Doktors der Philosophie
vorgelegt der
Philosophisch-Naturwissenschaftlichen Fakultät
der Universität Basel

von

Tuyana Boldanova
aus Irkutsk, Russland

Basel, 2017

Genehmigt von der Philosophisch-Naturwissenschaftlichen Fakultät
auf Antrag von

Fakultätsverantwortlicher: Prof. Dr. med. M. H. Heim

Korreferent: Prof. Dr. phil. M. N. Hall

Basel, den 13.12.2016

Prof. Dr. J. Schibler
Dekan der Philosophisch-Naturwissenschaftlichen Fakultät

Dedicated to my dad
(Посвящается моему папе)

Acknowledgments

Firstly I would like to express my gratitude to Markus Heim for his amazing support of my PhD study. For his knowledge, motivation, encouragement and guidance in all time of research and writing of the thesis. His love for science and medicine is very inspiring.

A special thank to Anamaria Necsulea from School of Life Sciences, École Polytechnique Fédérale de Lausanne for our collaboration. Her expertise and immense knowledge of bioinformatics and biology are outstanding.

I am very grateful for the support of Stefan Wieland during writing of the thesis and his tough but fair comments.

I would like to thank all current and former members of our laboratory and collaborators: Michael Dill, Francois Duong, Ilona Krol, Sonja Rothweiler, David Semela, Magdalena Filipowicz, Vijay Shanker, Xuya Wang, Isabel Fofana, Diego Calabrese, Benedetta Campana, Tanja Blumer, Sandro Nuciforo, Mairene Coto, Qian Chen, Luigi Terracciano, Christian Beisel.

I thank Sylvia for helping me in samples collection for my PhD study, motivating me during difficult moments and keeping our laboratory organized.

Thank you Aleksei for the tea breaks, your friendship and interesting conversations about science and life.

I extend a special thank you to my friend Gaia for introducing me to the laboratory, performing my very first experiment with me and making our lab life stylish, interesting and funny.

A big thank you to my beloved family and friends for the great support and encouragement.

Contents

Abbreviations

Summary

1. Introduction

1.1. Hepatitis C Infection

1.1.1. Epidemiology and natural history

1.1.2. Structure

1.1.3. Model systems in Hepatitis C

1.1.4. Treatment

1.2. Interferon signaling

1.2.1. Interferons and their receptors

1.2.2. Induction of interferons

1.2.3. Interferon signaling and interferon regulated genes

1.3. Innate and adoptive immune response in Hepatitis C infection

1.3.1. Innate and adoptive immune response in acute Hepatitis C

1.3.2. Innate immune response in chronic hepatitis C

1.3.3. Non-response to PegIFN- α in CHC patients with an activated endogenous IFN system in the liver

1.3.4. Genetic variations and treatment outcome

2. Aims of the MD-PhD Project

3. Materials, Methods and Results

Transcriptional response to hepatitis C virus infection and interferon alpha treatment in the human liver (Manuscript under review, 2016)

4. Conclusion

5. References

6. Curriculum vitae

Abbreviations

AHC	acute hepatitis C
ALT	alanine-aminotransferase
CHC	chronic hepatitis C
DAA	direct-acting antivirals
DNA	deoxyribonucleic acid
GAA	gamma-activation sequence
GSEA	gene set enrichment analysis
GWAS	genome-wide association study
HCC	hepatocellular carcinoma
HCV	hepatitis C virus
IFN α R	Interferon alpha receptor
IFN- α	Interferon alpha
IFN- γ	Interferon gamma
IFN- λ	Interferon lambda
IRF	Interferon regulatory factor
IRS	internal ribosome entry site
ISG	Interferon stimulated gene
ISRE	IFN-stimulated response element
Jak	Janus kinase
lncRNA	Long non-coding RNA
MAVS	mitochondrial antiviral signaling protein
mRNA	messenger RNA
miRNA	microRNA
PAMP	pathogen-associated molecular pattern
PBMC	peripheral blood mononuclear cell
pegIFN α	pegylated Interferon alpha
pSTAT1	phosphorylated STAT1
RNA	ribonucleic acid
SNP	single nucleotide polymorphism
SOCS	suppressor of cytokine signaling
STAT	signal transducer and activator of transcription
SVR	sustained virologic response
TLR	toll-like receptor
TRIF	TIR-domain-containing adapter-inducing interferon- β
USP18	Ubiquitin-specific peptidase 18

Summary

Because of its worldwide impact on human health, hepatitis C virus (HCV) is among the most intensively studied human pathogens. Humans are the only natural host for HCV and chimpanzees the only animal model. Therefore, HCV research is mostly restricted to *in vitro* systems. In particular, a robust *in vitro* HCV infection system has enabled the accumulation of an impressive body of knowledge on basic HCV biology and viral-host interactions *in vitro*. Not unexpectedly however, little research on the host-virus interaction and the impact of antiviral therapy in the human liver has been performed mostly due to the challenges and difficulties associated with collection and sampling of appropriate human liver tissue.

In the first part of our work we investigated the impact of HCV infection on the cellular homeostasis of hepatocytes *in vivo*. The challenge for such an analysis lies in separating direct responses to viral infection in the infected hepatocytes from the innate and adaptive immune responses associated with HCV infection. Furthermore, the strength of the immune response varies considerable from patient to patient further complicating separation of direct and indirect responses to HCV infection. We therefore carefully selected a set of biopsies without detectable immune response and compared high-throughput transcriptome sequencing profiles of these biopsies with biopsies from non-infected patients. These studies revealed that gene expression changes mainly reflect the presence of immune cell infiltrates in the HCV group without detectable immune response. However, HCV infection does not trigger any significant gene expression changes in the infected cells suggesting that many of the HCV induced changes previously observed *in vitro* do not occur in the HCV-infected liver. This discrepancy most likely is a reflection of the much higher viral RNA content per cell typically observed in *in vitro* systems compared to the viral load in the hepatocytes in the HCV infected liver.

In the second part we investigated a long-standing conundrum in the field regarding the inability of the endogenous IFN system activation to eradicate HCV infections. Interferon alpha (IFN α) has been the backbone of anti-HCV therapy for the last 25 years. Till today it is unclear, why recombinant IFN α injected during therapies is a potent antiviral and eradicates HCV in about 50% of patients, whereas the activation of the endogenous IFN

system in the liver is ineffective. We performed an in-depth transcriptome analysis of a unique set of paired liver biopsies, obtained before and at different time points during the first week of antiviral therapy using pegylated interferon alpha (pegIFN α). Our analysis provides strong evidence that quantitative rather than qualitative differences in gene induction are responsible for the failure of the endogenous IFNs and the success of pegIFN α in viral eradication

Finally the role of miR-122 and other non-coding RNAs in response to HCV infection and to IFN α therapy in the liver was investigated. *In vitro* studies have shown that binding of miR-122 by HCV can regulate host gene expression by reducing (sponging) the amount of miR-122 available for gene repression¹. We find that miR-122 targets are not significantly up-regulated in response to HCV infection in the human liver. However, we show that the precursor transcript of miR-122, as well as other long non-coding RNA transcripts that act as precursors for miRNAs, are down-regulated in the infected liver during peg IFN α /ribavirin treatment. These results suggest that the down-regulation of miRNAs could contribute to peg IFN α /ribavirin-mediated clearance of HCV infection.

1. Introduction

1.1. Hepatitis C Infection

1.1.1. Epidemiology and natural history

HCV infections are a major cause of liver-related morbidity and mortality. An estimated 160 million persons are chronically HCV infected worldwide and are at increased risk of developing liver fibrosis, cirrhosis and hepatocellular carcinoma². HCV was characterized in 1989 using a novel experimental approach in which a cDNA expression library that had been constructed from the plasma of a patient with post-transfusion non-A, non-B hepatitis was screened for the unidentified agent³. Populations at risk of acute hepatitis C were patients who received blood products prior to 1990, before routine screening of blood products for HCV. Thus, in Europe and the USA, seroprevalence increases with age and peaks in 55–64 year old patients⁴. Since the introduction of routine screening of blood products and sterile injection needles in the 1990s, the principal cohorts of newly infected patients has changed. The majority of patients presenting as new cases in developed countries now are people who inject drugs and men who have sex with men⁵. Despite considerable research efforts, a prophylactic vaccine is still not available.

The acute phase is often clinically mild and therefore rarely diagnosed. (Figure 1). The initial features are non-specific flu-like symptoms, while more specific viral hepatitis symptoms such as jaundice, dark urine and abdominal discomfort only occur in a minority of individuals. Accurate studies of the time course for clearance of acute hepatitis C infection are difficult to carry out because of the silent onset of the acute disease. In the available studies, the rate of spontaneous resolution of HCV infections is reported to be between 15–40%^{6,7,8}.

Chronic HCV infection is defined as persistence of HCV RNA in the blood for more than six months. Chronic hepatitis is the most common outcome of HCV infection and may lead to fibrosis and cirrhosis of the liver. It is generally a slowly progressive disease characterized by persistent hepatic inflammation leading to the development of cirrhosis in approximately 15–25% of patients over 20–30 years of HCV infection. (Published data are highly variable with progression rates to cirrhosis between 2–3%

and 51% over 22 years^{9, 10}.) Development of hepatic fibrosis in hepatitis C is multifactorial with many co-factors, such as age at infection, male gender, alcohol consumption, obesity, insulin resistance, type 2 diabetes, co-infection with hepatitis B or HIV, immunosuppressive therapy or genetic factors potentially increasing an individual's risk of developing significant fibrosis or cirrhosis¹¹. Spontaneous clearance in the chronic phase of infection is extremely rare¹². Once cirrhosis is established, the disease progression remains unpredictable: cirrhosis can remain indolent for many years in some patients whilst progressing in others to hepatocellular carcinoma, hepatic decompensation and death. Hepatic decompensation occurs at a rate of 3-6 % per year, and decompensated cirrhosis has an annual mortality rate of 15-20%¹³. HCC develops with an annual rate of 1-5%. Successful treatment of CHC results in marked improvements in liver inflammation and in fibrosis stage¹⁴.

Since the majority of the people with persistent infection are unaware of the infection, screening programs will be required to identify patients and to prevent silent progression of the disease^{2, 4}. Given the lack of a vaccine, the burden of disease and the high number of chronically infected individuals, successful antiviral treatment will no doubt be an integral part of controlling this disease.

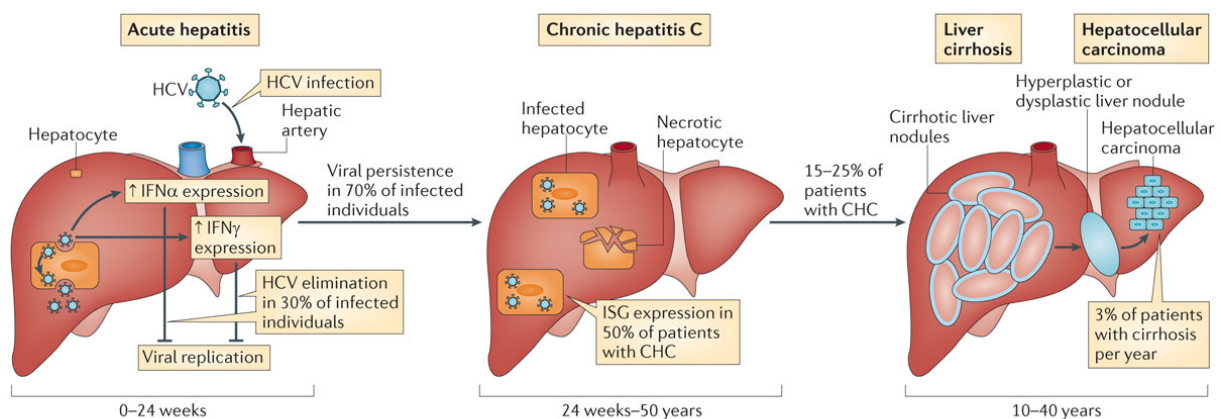


Figure 1: Natural history of CHC¹⁵

1.1.2. HCV structure and life cycle

HCV is an enveloped positive-strand RNA virus belonging to the family of Flaviviridae and only infects humans and chimpanzees. Hepatocytes are the main target cell for HCV, although low level infection of cells of the immune system has also been reported¹⁶. HCV infection is a highly dynamic process with a viral half-life of only a few hours and production and clearance of an estimated 10^{12} virions per day in a given individual¹⁷. This high replicative activity as well as the high error rate of the viral RNA-dependent RNA polymerase are responsible for the broad genetic variability of the isolated HCV samples recognized as viral quasispecies¹⁸. Phylogenetic analysis of HCV isolates enabled viral classification into seven major genotypes and more than 100 subtypes¹⁹.

The HCV genome is a 9.6kb positive-strand RNA molecule that is composed of a 5'-non-coding region (NCR) containing an internal ribosome entry site (IRES) that drives translation of a single open reading frame encoding the structural as well as non-structural proteins and is followed by a 3'-NCR. (Figure 2). The polyprotein is cleaved by cellular and viral proteases to yield the structural core protein and envelope glycoproteins E1 and E2 that form the viral particle and seven non-structural proteins. The non-structural proteins include the p7 ion channel, the NS2-3 protease, the NS3 serine protease and RNA helicase, the NS4A polypeptide, the NS4B and NS5A proteins and the NS5B RNA-dependent RNA polymerase (RdRp)²⁰.

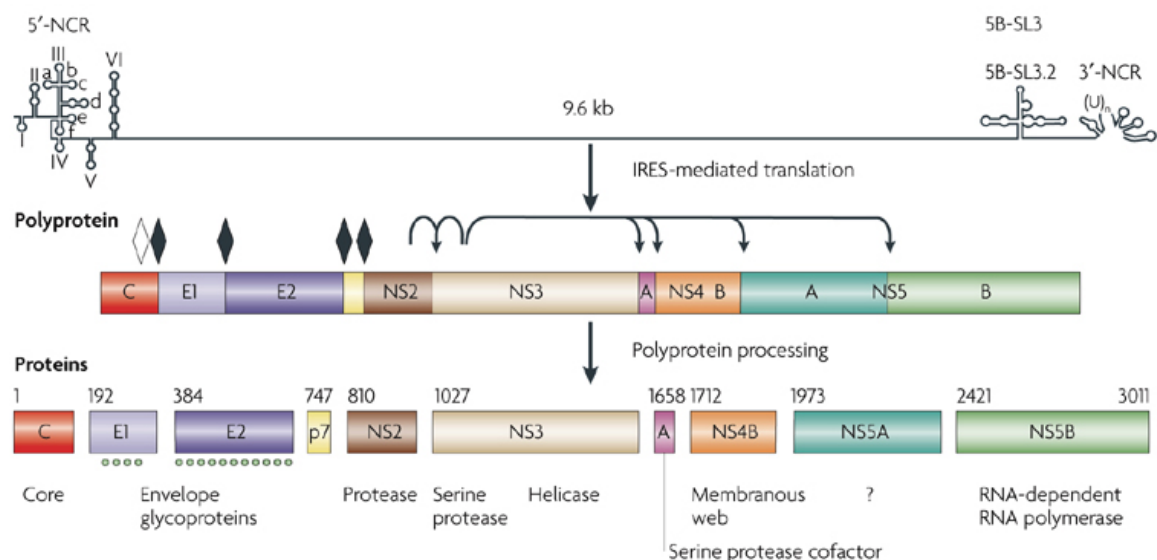


Figure 2: Structure of HCV²⁰

The HCV life cycle is only partly understood. Briefly, as shown in Figure 3, the HCV virion circulates in the bloodstream either as a free particle or surrounded by host low-density lipoproteins²¹, attaches onto the target cell membrane by sequential binding of various receptor molecules, and enters into the cell by a clathrin-mediated endocytosis process. Disruption of the viral capsid in the endocytic compartment releases RNA genome of positive polarity into the cytoplasm. Upon virus uncoating the IRES-dependent translation of HCV proteins is initiated on the template of the viral genome. HCV non-structural proteins assemble into replication complexes on the membranes of the endoplasmic reticulum, inducing formation of specific structures known as membranous web^{22, 23}. The positive-strand RNA is copied by the NS5B RdRp into a negative-strand intermediate forming a double-strand replicative form, which serves as template for the production of new positive-strand genomes. Newly synthesized positive-strand viral RNA translocates to the surface of the lipid droplets, where virion assembly takes place^{24, 25, 26}. The viral particles leave the cell in a complex with lipids making use of the very-low-density lipoproteins secretion pathway^{21, 27, 28}.

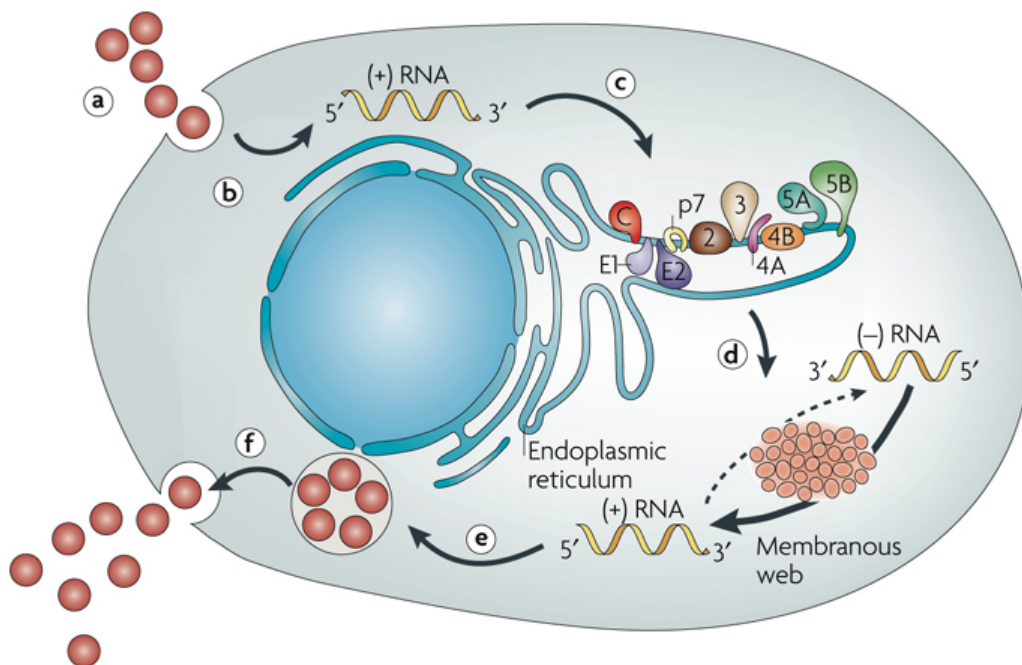


Figure 3: Lifecycle of HCV²⁰. Virus binding and internalization (a); cytoplasmic release and uncoating (b); IRES-mediated translation and polyprotein processing (c); RNA replication (d); packaging and assembly (e); virion maturation and release (f).

Several host cell factors are required for virus translation, replication and production. These include liver-specific microRNA-122 (miR-122), which was shown to interact with the 5'-NCR of the HCV genome and increase HCV abundance in replicon models²⁹. miR-122 was also implicated in HCV translation, reportedly by enhancing the association of ribosomes with the viral RNA³⁰. miR-122 associates with host Argonaute 2 to bind the HCV RNA, and through this interaction stabilizes the viral RNA³¹ and most likely protects its 5'-NCR from degradation³². It was reported, that HCV has also sponge effect in depleting the host cell for miR-122 resulting in global derepression of host miR-122 targets¹.

1.1.3. Model systems in Hepatitis C

Because of their substantial impact on human health, HCV infections have been extensively studied and became widely used model systems to investigate host-virus interactions³³.

In vitro models

Since the discovery of HCV in 1989³, the lack of a suitable cell culture and small animal model systems represented a major obstacle in studying the biology of the virus and developing prophylactic and therapeutic interventions. Patient-derived HCV isolates failed to initiate productive infection in cell culture. In 1997 HCV molecular clones that were infectious in chimpanzees were developed, however these viral genomes did not produce viral particles in cell culture^{34, 35}. In 1999, the group of Bartenschlager developed an efficient cell culture replication model of HCV. These HCV replicons contained adaptive mutations that prevented productive replication in chimpanzees³⁶. Moreover, the system did not support the full viral life cycle and did not produce infectious viruses. The breakthrough came with the serendipitous discovery that an isolate from a Japanese patient with fulminant hepatitis could replicate in Huh7 derived cell lines without the requirement for cell culture adaptive mutations and produced fully infectious viral particles that were infectious in chimpanzees^{37, 38, 39}. Following this initial observations, a number of improved derivatives of the original genotype 2a HCV clone have been generated and successfully tested in additional cell culture model. Of note, primary human hepatocytes can also be infected, albeit with much lower efficiency of infection and replication, and are considered to represent a more physiological experimental system^{40, 41, 42}. However, poor availability of these cells, high costs, short survival (up to 2 weeks) and the relative poor permissiveness for HCV infection have

limited HCV studies in PHH. Recently, hepatocyte-like cells derived from induced pluripotent stem cells (iPSC) and human embryonic stem cells (hESC) have been shown to be susceptible to HCV infection and could potentially offer improved *in vitro* HCV infection systems in the future^{43, 44}.

In vivo models

Besides humans, experimental infection of chimpanzees has played a pivotal role in the discovery and characterization of HCV and deciphering host-virus interactions, particularly cellular immunity, and also preclinical testing of antiviral treatment strategies⁴⁵. However, contrary to humans, only very few chimpanzees develop chronic HCV infection and to date no fibrosis and only one case of HCC has been observed. Furthermore, studies involving chimpanzees are very restricted due to growing ethical constraints, limited availability and high costs. Thus, a continuous effort in establishing alternative animal model systems for HCV infection is ongoing.

Alternatives to humans and chimpanzees for the study of HCV biology *in vivo* could be found in HCV-related viruses that infect other species (HCV homologs)^{46, 47} (Figure 4). However, it remains to be examined whether the pathogenesis of these viruses parallels that seen for HCV in humans. Besides exploring viral homologs as an HCV model, generating a mouse model that fully supports HCV infection has been extensively pursued for many years⁴⁸. These efforts include complementary approaches including adapting HCV to the mouse liver, establishing HCV replicating transgenic mice and establishing human xenograft mice that would not only allow to study HCV infection but also the human immune response to the infection^{49, 50, 51} (Figure 4). Despite these efforts, no robust and reliable small animal model of HCV infection has yet been reported.

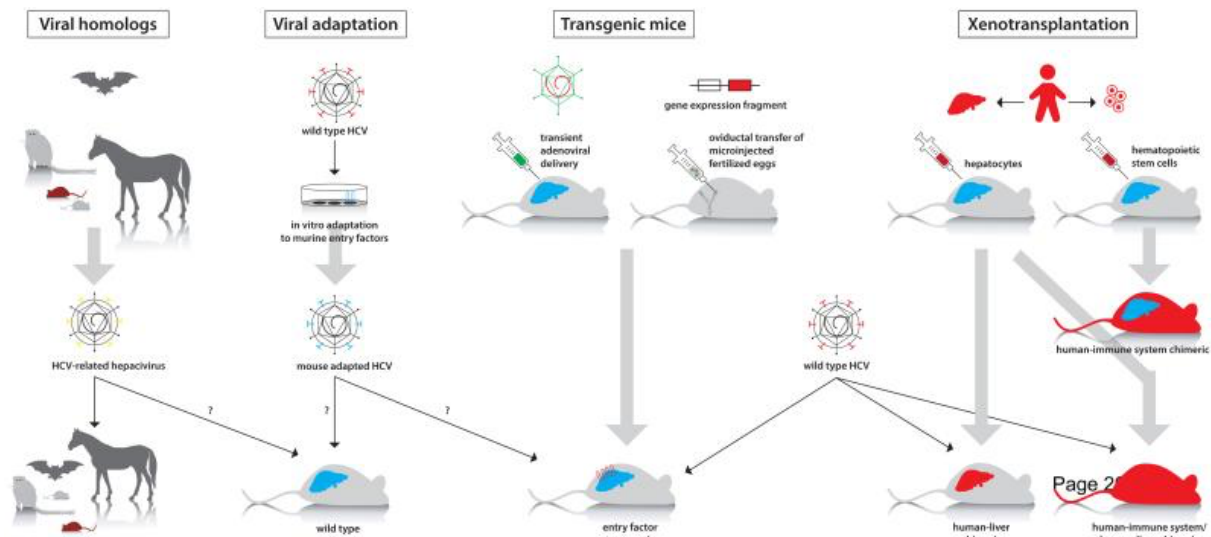


Figure 4: Different approaches to study HCV in animal models⁴⁸.

First panel: HCV-related viruses that infect animal species such as wild mice, rats, tamarins, bats and horses. These infections can be studied in their natural host, or eventually immune competent laboratory inbred mouse strains. Second panel: in vitro adaptation of HCV to mouse hepatoma cells may allow the isolation of viral variants that can establish an infection in wild type mice. Third panel: transient or stable expression of human factors that are essential to support infection of wild type HCV. Fourth panel: in xenotransplantation models, the genetic background of the host permits repopulation of the liver upon transplantation of human hepatocytes. Additional transplantation of HLA-compatible hematopoietic stem cells results in dually reconstituted mice.

Given the difficulties of working with and lack of suitable animal models, it is not surprising that HCV-host cell interactions have been mainly studied in cell culture systems, and that only few of these findings have been evaluated in the human liver.

1.1.5. Treatment

The main goal of treatment for chronic HCV is cure, and thus prevention of disease progression. Sustained virological response (SVR), defined as undetectable HCV RNA 12–24 weeks after completion of antiviral therapy is associated with reduction of both all-cause and liver-related mortality from HCV⁵².

For the past 25 years, recombinant interferon- α (IFN α) has been the main component of HCV antiviral therapy. Treatment efficacy improved stepwise with pegylation of IFN α and its combination with other antiviral drugs¹⁵. However, low SVR rate of ~50%, depending on genotype and substantial drug toxicity limited the efficacy of this

treatment⁵³. The introduction of direct-acting antiviral drugs (DAAs), with two protease inhibitor (PI) drugs licensed in 2011, has increased the number of patients who respond to treatment, and marks a new era of HCV therapy^{54, 55, 56} (Figure 5).

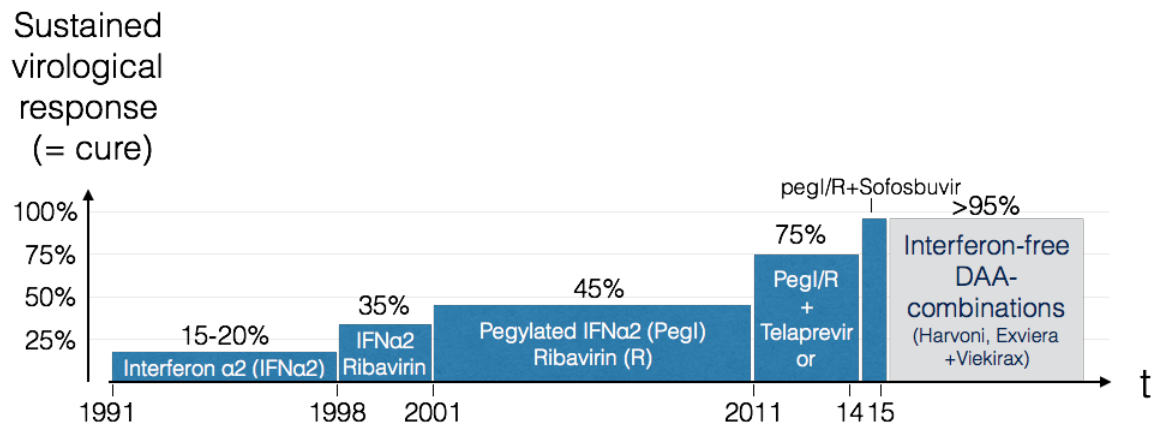


Figure 5: Changes in standard of care for HCV, and improvements in numbers of sustained virological responses¹⁵

Early use of recombinant IFN monotherapy

Already in 1986, before HCV was cloned, the therapeutic efficacy of recombinant human IFN α was shown in a pilot study of ten patients with NANBH⁵⁷. In the first two randomized controlled trials recombinant IFN α was injected at doses of 1 to 3 million units three times per week for 24 weeks. In only 10-25% of patients sustained alanine transaminase (ALT) normalization occurred^{58, 59}. Of note, the response to treatment in these early trials was assessed by measuring ALT levels in the serum, which reflected the biochemical response to HCV infection. It was only in 1989 that the molecular cloning of HCV made it possible to develop polymerase chain reaction (PCR)-based assays to measure the viral load in the serum instead.

Virological responses to IFN α -based treatments, depending on measured HCV RNA levels in the serum, classified into three general groups: non-response (including null-response and partial response); on-treatment response and relapse; and on-treatment response with SVR after treatment (Figure 6)¹⁵.

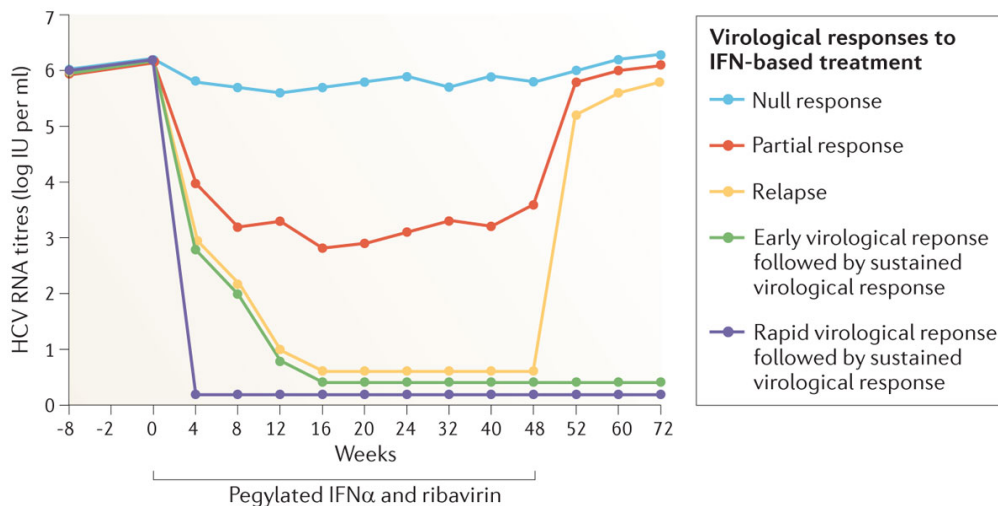


Figure 6: Virological response to IFN-based treatment¹⁵.

After 12 weeks of treatment of CHC with a combination of pegIFN α and ribavirin, some patients show a less than 2 log decrease in the titres of HCV, as measured in international units (IU) per ml of serum, which is classified as a 'null response'. These patients are considered to be true non-responders to pegIFN α treatment. Partial responders have a decrease in viral load of more than 2 log IU per ml at the same time point, but HCV RNA remains detectable in the serum throughout the entire period of time that they are being treated. Both null-responders and partial responders are classified together as non-responders. Relapsing patients have undetectable levels of HCV RNA in the serum during their treatment but become positive for HCV RNA after the end of their treatment. A SVR is determined by a lack of detectable HCV RNA levels in the serum of patients for 6 months after treatment. Patients with an early virological response test negative for HCV RNA after week 12 of treatment and have more than 75% probability of generating an SVR. Patients with a rapid virological response test negative for HCV RNA after 4 weeks of treatment and have more than a 90% chance of generating an SVR.

Combination of IFN and Ribavirin (RBV)

Ribavirin is a nucleoside analogue with a known broad range of antiviral activities. It had already been tested as a monotherapy for CHC in the early 1990s and was found to transiently reduce ALT levels during treatment. In 1998 the first randomized controlled trial that included 912 patients showed that the combination of subcutaneously injected IFN α 2b with daily oral administration of RBV achieved an SVR in 38% of treated patients, which was an increase of more than 20% compared with IFN α 2b monotherapy⁶⁰. After this study the combination of IFN α 2b and RBV became the new standard of care. However, it still remains unclear how RBV boosts the response to IFN α .

Pegylated IFN α

Pegylation of IFN α by attaching a polyethyleneglycol molecule significantly improved the half-life and thus the pharmacokinetics of IFN α without any loss in biological activity^{53,54}. This allowed for a reduction of the injection frequency from daily to weekly and at the same time increased the antiviral efficacy of IFN α by about another 10–15%⁶¹. It is assumed, that the sustained high serum concentration of pegIFN α provide for interrupted antiviral activity through a permanent stimulation of the IFN signaling pathways, whereas the serum concentrations of standard IFN- α (with an elimination half-life of 4 to 10 hours) decline below pharmacologically active levels in the second half of each 48-hour dosing interval^{61 62}. However, there is no experimental evidence to support this hypothesis. On the contrary, IFN α -induced signalling through the JAK–STAT pathway becomes refractory in a matter of hours⁶³, and in mice hepatocytes remain unresponsive to further stimulation with high doses of IFN α for several days^{64, 65}. Whatever the mechanisms, pegIFN α was significantly more effective and in combination with ribavirin achieved SVRs of 56% of treated patients, an increase of > 10 % compared to conventional IFN α 2a.⁵⁴ In 2002, the combination of pegIFN α with ribavirin for 6 to 12 months therefore became the standard of care protocol for the subsequent decade.

Direct-acting antiviral agents (DAAs)

In the last years, pegIFN α and ribavirin have been gradually replaced by a new and very potent class of DAAs. In contrast to IFN α , which induces the body's innate antiviral immune response, DAAs are designed to directly inhibit viral proteins involved in the HCV life cycle. Three important HCV DAA classes are highlighted: (1) NS3/4A protease inhibitors, which inhibit HCV polyprotein processing, (2) NS5B polymerase inhibitors, which inhibit HCV RNA replication, and (3) NS5A inhibitors, which inhibit viral replication and assembly, although the precise mechanism of action is unknown⁶⁶. In 2011, the first two DAAs that act as NS3/4A protease inhibitors (PI) were developed, boceprevir and telaprevir. In combination with pegIFN α and ribavirin these triple-drug management could achieve SVR in more than 70%^{55,67}. Treatment with first-generation PIs had substantial tolerability issues with additional side effects, including severe anemia, serious skin reactions or rash, and dysgeusia, which added to the underlying tolerability issues associated with pegIFN and RBV. Development and implementation of novel DAAs progress fast. Because of the considerable toxicity of recombinant IFN α , major efforts are underway to develop IFN-free treatments. In 2013 two additional

DAAAs were approved (Sofosbuvir und Simeprevir). In 2014, multiple IFN-free regimens (in some cases, also RBV-free) became available for the treatment of HCV genotype 1 infection (Table 1). The approval of these DAAs further transformed the landscape for the treatment of HCV, leading to both improved efficacy and tolerability. IFN-free regimens allow shorter treatment duration with SVR rates reaching more than 90%^{68, 69}. Whether such IFN-free regimens will completely replace recombinant IFNs in all patient subgroups is unclear, since many of the next-generation drugs are still in the early phase of clinical development and their overall efficacy and safety in larger patient groups is not yet known. Specific concerns include drug–drug interactions, efficacy in patients that are also under immunosuppressive therapy (after organ or haematopoietic stem cell transplantation, or in patients with severe autoimmune diseases) or in patients with impaired kidney function¹⁵.

Drug Class	Generic Name	Trade Name	HCV Genotype With Approved Indication
NS3A/4A protease inhibitors	Simeprevir	Olysio®	1, 4
	Paritaprevir (fixed-dose combination product with ritonavir, ombitasvir, and copackaged with dasabuvir)	Viekira Pak®	1
	Paritaprevir (fixed-dose combination product with ombitasvir, ritonavir)	Technivie®	4
	Grazoprevir (fixed-dose combination product with elbasvir)	Zepatier™	1, 4
NS5B polymerase inhibitors —nucleotide	Sofosbuvir	Sovaldi®	1, 2, 3, 4
NS5B polymerase inhibitors —nonnucleoside	Dasabuvir (copackaged with fixed-dose combination product ombitasvir, paritaprevir, ritonavir)	Viekira Pak®	1
NS5A inhibitors	Ledipasvir (fixed-dose combination product with sofosbuvir)	Harvoni®	1, 4, 5, 6
	Ombitasvir (fixed-dose combination product with paritaprevir, ritonavir, and copackaged with dasabuvir)	Viekira Pak®	1
	Ombitasvir (fixed-dose combination product with paritaprevir, ritonavir)	Technivie®	4
	Daclatasvir	Daklinza™	1, 3
	Elbasvir (fixed dose combination product with grazoprevir)	Zepatier™	1, 4
	Velpatasvir (fixed-dose combination product with sofosbuvir)	Eplusa®	1, 2, 3, 4, 5, 6

Table 1. Currently Available HCV DAAs by Drug Class

1.2. Interferon signaling

1.2.1. Interferons and their receptors

Isaacs and Lindenmann identified IFN in 1957 during their studies of the phenomenon of viral interference characterized as the ability of an active or inactivated virus to interfere with the growth of an unrelated virus⁷⁰. IFNs are a family of cytokines classified as type I, II or III IFNs based on the specific cell surface receptors they recognize. Human type I IFNs include 12 highly similar members of the IFN α -family, a single IFN- β as well as IFNs- ϵ , κ , ω and ν . Type I IFNs bind to the IFN- α /IFN- β receptor (IFNAR) that consists of the two subunits IFNAR1 and IFNAR2⁷¹. IFNAR is ubiquitely expressed on virtually all cells in the body. There is only one type II IFN, IFN- γ . It is produced mainly by NK and T cells in response to stimulation with antigens or mitogens^{72,73}. IFN γ binds to a distinct receptor, the interferon gamma receptor (IFNGR) consisting of the two subunits IFNGR1 (previously called α chain)⁷⁴ and IFNGR2 (previously called β chain or accessory factor)^{75,76}. More recently, a type III IFNs have been described. The 3 members of the type III class, IFN λ 2, IFN λ 3 and IFN λ 1(also known as IL28A, IL28B and IL29 respectively), signal through the IFN- λ receptor consisting of the IL-10R2 chain shared with the IL-10 receptor, and a unique IFN λ chain^{77,78}. Type I IFNs and type III IFNs are produced by cells infected with viruses and by key sentinel cells of the innate immune system such as macrophages and dendritic cells (DCs). Importantly, macrophages and DCs do not have to be infected by viruses in order to produce IFNs. Instead, they constantly sample the extracellular milieu for the presence of foreign materials such as virus containing remnants of apoptotic cells and intact viral particles⁷⁹. It has also been postulated that type III IFNs might be induced by stimulation of cells with type I or III IFN, suggesting that this class of cytokines belongs at the same time to the group IFN-stimulated genes⁸⁰.

1.2.2. Induction of interferons

Cells produce IFN α , IFN β and IFN λ in response to infection by a variety of viruses. Two important pathways that detect components of viral genomes and trigger type I and type III IFN expression have been discovered and characterised in recent years. These include the toll-like receptor (TLR) dependent pathway^{81,82} and the cytosolic pathway triggered by binding of viral RNA to the RNA helicases retinoic acid inducible gene-I (RIG-I) and melanoma differentiation antigen 5 (MDA5)⁸³. Both pathways converge to

activate the key transcription factors NF- κ B and the interferon regulatory factor (IRF) 3 and 7. Activated IRF3 and NF- κ B bind to response elements in the promoters of type I and III IFN genes. All types of IFNs induce an antiviral state by the transcriptional activation of hundreds of genes called interferon stimulated genes (ISGs)⁸⁴. The specific set of induced ISGs depends on the IFN and the cell type.

1.2.3. Interferon signaling and interferon regulated genes

IFN receptors connect to the Jak-STAT pathway to transmit signals from the cell surface to the nucleus (Figure 7)⁸⁵. All IFNs activate STAT1 to form homodimers that translocate into the nucleus and bind to promoter regions containing a specific gamma-activated sequence (GAS) to activate the transcription of downstream genes, so called interferon stimulated genes (ISGs)^{86, 87}. Type I and III IFNs additionally induce the heterotrimeric transcription factor IFN stimulated gene factor 3 (ISGF3) that consists of STAT1, STAT2, and IRF9 and binds to IFN-stimulated response elements (ISRE) in the promoters of classical ISGs^{85, 88, 89, 90} (Figure 7). The sets of genes induced by type I and III IFNs in the same cell are almost identical, and partially overlap with the distinct set of the IFN- γ -induced gene^{91, 92}. Besides the gene set specificity in a given cell, the overall number of regulated is different in different cell types. For instance, pegylated IFN- α triggers induction of up to 300 genes in the liver, but nearly 2000 genes in peripheral blood mononuclear cells (PBMCs)⁹³.

Prolonged and intense IFN response can be detrimental and the Jak-STAT pathway is tightly controlled by several IFN-inducible negative feedback mechanisms in order to protect the organism from deleterious consequences of exaggerated immune activation. Important negative regulators include SOCS, USP18, PIAS and TcPTP. Suppressor of cytokine signalling (SOCS) proteins are rapidly induced by activated STATs and provide an early negative feedback loop^{94, 95, 96}. Ubiquitin-specific peptidase 18 (USP18, also designated UBP43) is another important negative regulator in type I IFN signaling⁹⁷. USP18 is a key mediator of the refractoriness of liver cells to continuous stimulation with IFN- α ⁶⁵. USP18 is not induced by IFN- γ , and does not inhibit IFN- γ or IFN- λ signalling⁶⁴.

Genes induced by IFN stimulation contribute to the establishment of the so-called antiviral state. IFN stimulation typically leads to up- and down-regulation of several hundred genes, many of which are regulated in a cell-type specific manner. Only a small

number of the IFN-induced antiviral effectors have been studied in detail to reveal their mode of action in inhibiting viral infections. To date, four main effector pathways of the IFN-mediated antiviral response have been described. These include pathways triggered by the Mx GTPase, the ISG15 ubiquitin-like protein, the OAS-RNaseL system and protein kinase R⁸⁴.

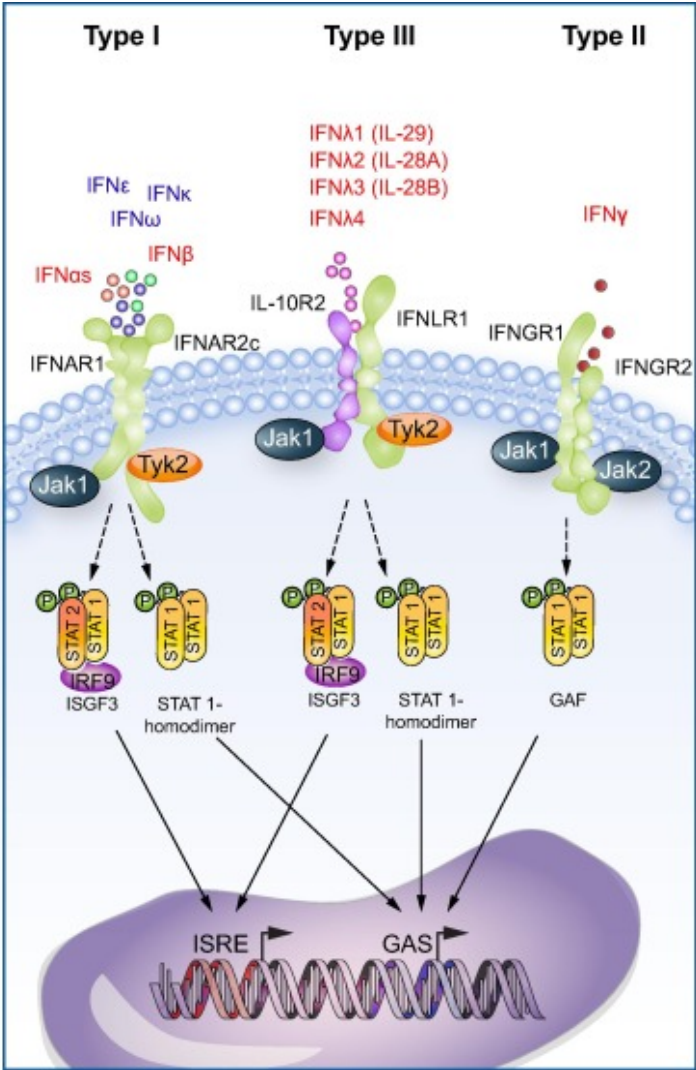


Figure 7: IFN Signaling through the Jak-STAT Pathway

1.3. Innate and adoptive immune response in Hepatitis C infection

1.3.1. Innate and adaptive immune response in acute HCV (AHC) infection

The acute phase of HCV infection is divided in an early acute phase prior to the activation and recruitment of HCV specific T cells in the liver, and a late acute phase, characterized by the adaptive immune response (Figure 8). Innate immune responses are the first line of defense against pathogens including viral infections. IFNs are the central cytokine mediators responsible for the induction of an innate antiviral state within cells and also for the activation and regulation of the cellular components of the innate immune system such as natural killer (NK) cells⁹⁸. However, little is known about the early induction of innate immune responses in HCV infection because the acute phase of HCV infection is only infrequently diagnosed due to the very mild and unspecific clinical manifestation. Furthermore, the few prospective studies of acute HCV infection that were done with health-care workers after accidental needle stick injury typically focused on the analysis of the adaptive immune response to HCV infection. Our current understanding of the early hepatic events during HCV infection derives from studies using serial liver biopsy and blood samples obtained from experimentally infected chimpanzees^{99, 100, 101, 102}. High HCV viral titers have been observed in chimpanzee serum and liver already within days after inoculation. After a very rapid increase in the first 2 weeks after an infection, HCV viral loads remain stable for several weeks, until the emergence of a cellular immune response in the liver. Transcriptomic analysis of the liver biopsy derived RNA revealed induction of type I IFN response in the early acute phase of infection. The extent and duration of the ISG induction was positively correlated with the viral load. However, despite this apparent and strong innate immune response during the acute phase of HCV infection, the infection is not cleared in most cases. Although there is evidence that HCV could trigger IFN production in the cells it infects, this has so far not been proven and the cellular source and type of IFN that triggers the massive ISG induction during acute HCV infection still remains to be identified. While several reports suggest that HCV triggers type III IFN induction in primary human PHH it infects^{42, 103, 104}, other groups reported that plasmacytoid dendritic cells, stimulated by cell-cell contact with infected hepatocytes, might be the source of primarily type I IFNs¹⁰⁵. More recent studies detected up-regulation of mRNA of type III (but not type I) IFNs in liver biopsies of chimpanzees and an increase of type III IFN protein, primarily IFN- λ 1 (IL29), in the serum of chimpanzees.

In contrast to the innate immune responses that are induced within days after infection, adaptive immune responses, that correspond to the late acute phase become detectable, for reasons not yet clearly understood, only after 6–8 weeks^{101, 106, 107} (Figure 8). This phase lasts 4–10 weeks and is clinically characterized by elevated transaminases and sometimes icterus, and leads to clearance of the infection in about 30% of infected individuals. There is general consensus from a number of immunological studies that HCV elimination requires sustained, strong and multispecific HCV-specific CD4+ and CD8+ T cell responses⁷⁹. The combination of non-cytolytic inhibition of virus replication and production reduces viral spread while the adaptive response eliminates the still infected cells¹⁰⁸.

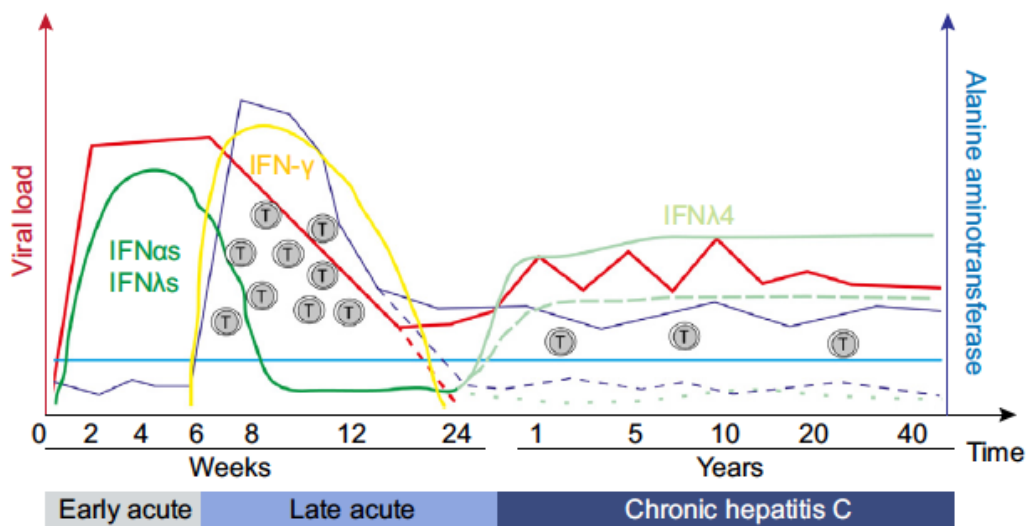


Figure 8: Natural course of HCV Infection

1.3.2. Innate immune response during chronic HCV infection

The chronic phase of HCV infection is primarily characterized by a largely ineffective cellular immune response probably caused by a combination of T cell exhaustion and emergence of viral escape mutants. Even though the IFN system is still activated in the liver, it is not sufficient to clear the virus (reviewed in⁷⁹). In humans who develop chronic infection, ISG induction varies considerably between individuals. In about half of Caucasian patients, hundreds of type I or III ISGs are constantly expressed at high levels in the liver, whereas the other half has no detectable induction of the innate immune

system¹⁰⁹. Apart from a strong association of allelic variants near the IFN- λ 4 gene with ISG induction, little is known about the factors that determine the activation level of the IFN system.^{110, 111, 112.}

HCV persists for decades despite the expression of hundreds of ISGs⁹³. Furthermore, in contrast to what is seen during AHC, there is no significant correlation between serum or intrahepatic viral loads with ISG expression levels¹⁰⁹. The interplay between viral replication levels and ISG induction in the liver is still unknown, Nevertheless, intrahepatic ISG expression seems to be maximal in, but not restricted to the HCV infected cell as determined by simultaneous HCV RNA and ISG mRNA by fluorescent in situ hybridization suggesting that HCV itself is the main driver of the observed innate response¹⁰⁹.

1.3.3. Non-response to PegIFN- α in CHC patients with an activated endogenous IFN system in the liver

It is known that patients with an activated endogenous IFN system are poor responders to IFN- α based therapies^{93, 113, 114}. Analysis of paired liver biopsies obtained before and 4 h after the first injection of PegIFN- α 2 revealed that patients with an activated endogenous IFN system had hundreds of ISGs expressed at high levels already before treatment. Staining of these biopsies for the phosphorylated form of STAT1 showed a faint staining in nuclei of hepatocytes in pre-treatment biopsies, and no further increase of phospho-STAT1 signals 4 h after PegIFN- α injections. In contrast, no phospho-STAT1 signals were detected in pre-treatment biopsies of patients without activated endogenous IFN system, but PegIFN- α injections induced a very prominent and strong activation and nuclear translocation within 4 h⁹³. The reason for the refractoriness of IFN- α induced Jak-STAT signaling is not entirely clear, but there is evidence that USP18 is an important factor¹¹⁵. USP18 was strongly expressed in a large number of hepatocytes in liver biopsies from patients with CHC and a pre-activated endogenous IFN system ¹¹⁵.

1.3.3. Genetic variations and treatment outcome

Genome wide association studies revealed that genetic variants near the interleukin 28B (IL28B) strongly associated not only with spontaneous clearance of the infection, but also with the success rate of PegIFN- α /ribavirin antiviral treatment^{116, 117, 118, 119, 120}. IL28B corresponds to IFN λ 3, further analysis however revealed that an additional polymorphism located within IFN λ 4 gene has even stronger predictive value¹²¹. The IFN λ 4 gene harbors several genetic variants in human populations, including a frameshift mutation that abrogates the production of the IFN λ 4 protein. Paradoxically, the IFN λ 4-producing genotype is associated with poor response to PegIFN- α /ribavirin^{110, 116, 120}. The variability within the IFN λ s seems to result primarily from two polymorphisms (rs368234815 and rs117648444) that determine three haplotypes, each associated with a different pattern of IFN λ 4 expression (Figure 9)¹¹⁰. The first, TT G haplotype is predicted not to produce IFN λ 4 and patients have low ISG expression in the liver and, surprisingly, a higher incidence of spontaneous clearance. Likewise, they show a better response rate to IFN-based treatment. The second, Δ G G haplotype is predicted to express the IFN λ 4-P70 variant and patients produce important amounts of ISG in the liver and have a low ability to clear HCV. The third, Δ G A haplotype is predicted to express the IFN λ 4-S70 variant and patients have an intermediate ability to clear HCV. It is presently not known why the activation of the endogenous IFN system in the liver in patients with the IFN λ 4-producing genotype is ineffective against HCV, whereas pegIFN α -induced ISG expression results in viral eradication in so many patients.

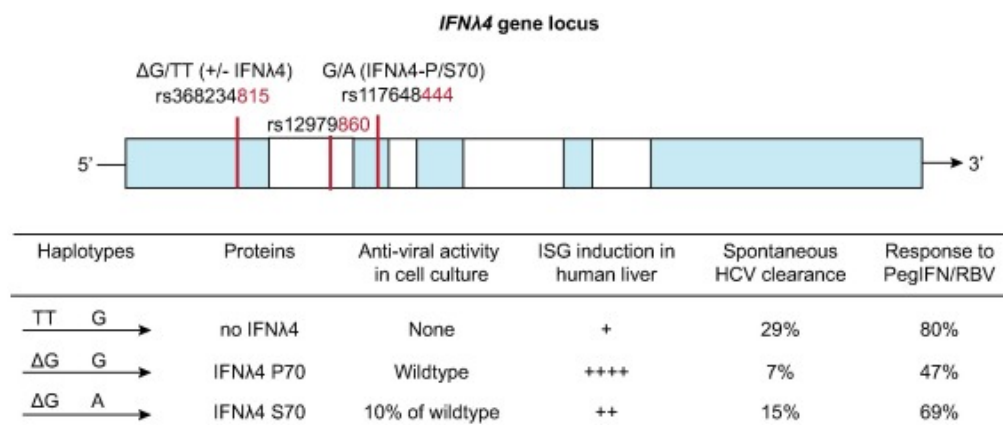


Figure 9: Genetic polymorphisms in the IFN λ 4 gene determine IFN stimulated gene induction and viral clearance. The rs368234815 and rs117648444 polymorphisms determine 3 haplotypes that predict a different expression of IFN λ 4 (none, 70P variant and 70S variant).

2. Aims of the MD-PhD project

The overall aim of the project was to investigate the host response to hepatitis C virus (HCV) infection in the human liver by a systematic analysis of the transcriptome using liver biopsies of patients with HCV infection and of controls.

The analysis focused on 4 aspects:

1. The cell intrinsic adaptations in HCV infected hepatocytes.
2. The induction of IFN stimulated genes (ISGs) and long noncoding RNAs in the liver of patients with chronic hepatitis C (CHC).
3. The induction of ISGs and long noncoding RNAs in patients treated with pegIFN α and comparison of these data to RNA seq data from patients with an activated endogenous IFN system.
4. The contribution of miRNAs to ISG expression induced by pegIFN α .

In the first part of our study we aimed to disentangle the direct and indirect effects of HCV infection on the cellular gene expression profile. We therefore carefully selected a set of biopsies without detectable immune response and compared high-throughput RNA sequencing profiles of these biopsies with biopsies from non-infected patients.

In the second part of the study, RNA seq data from liver biopsies of patients with a strong induction of the endogenous IFN system were compared to controls.

In the third part, a number of patients were biopsied before and at different time points during the week after the first injection of pegIFN α . This study design allowed a unique insight into pharmacodynamics effects of pegIFN α in the human liver. The data were then compared to the RNA seq data from patients with a strong activation of the endogenous IFN system with the aim to identify the differences between exogenous and endogenous ISG induction responsible for viral eradication by pegIFN α treatments.

In the fourth part, we addressed the role of miRNAs in pegIFN α induced gene regulation in the liver.

3. Materials, Methods and Results

Transcriptional response to hepatitis C virus infection and interferon alpha treatment in the human liver

Tujana Boldanova^{1,2}, Aleksei Suslov¹, Markus H. Heim^{1,2*} and Anamaria Necsulea^{3*}

¹Department of Biomedicine; and ²Division of Gastroenterology and Hepatology, University Hospital Basel; University of Basel, 4031 Basel, Switzerland

³Laboratory of Developmental Genomics, School of Life Sciences, École Polytechnique Fédérale de Lausanne, 1015 Lausanne, Switzerland.

* equal contribution

Abstract

Hepatitis C virus (HCV) is widely used to investigate host-virus interactions. Cellular responses to HCV infection have been extensively studied *in vitro*. However, in human liver, interferon (IFN) stimulated gene expression can mask direct transcriptional responses to infection. To better characterize the direct effects of HCV infection *in vivo*, we analyze the transcriptomes of HCV-infected patients lacking an activated endogenous IFN system. We show that expression changes observed in these patients predominantly reflect immune cell infiltrates rather than cell-intrinsic pathways. We also investigate the transcriptomes of patients with endogenous IFN activation, which paradoxically cannot eradicate viral infection. We find that most IFN-stimulated genes are induced by both recombinant IFN therapy and the endogenous IFN system, but with lower induction levels in the latter, indicating that the innate immune response in chronic hepatitis C is too weak to clear the virus. We show that coding and non-coding transcripts have different expression dynamics following IFN treatment. Several microRNA precursors, including miR-122, are significantly down-regulated in response to IFN treatment, suggesting a new mechanism for IFN-induced expression fine-tuning.

Introduction

Hepatitis C virus (HCV) infections are a major cause of liver-related morbidity and mortality. An estimated 160 million persons are chronically infected worldwide and are at risk to develop liver cirrhosis and hepatocellular carcinoma(Lavanchy, 2011). Because of their substantial impact on human health, HCV infections have been extensively studied. HCV is now one of the most widely used model systems to investigate host-virus interactions(Colpitts et al, 2015). HCV is transmitted through blood and infects and replicates in hepatocytes. Due to the lack of a small animal model and of the difficulties inherent to working with human samples, HCV-host cell interactions have been mainly studied in a cell culture system, specifically in Huh7-derived hepatoma cells infected with the JFH1 isolate of the virus(Colpitts et al, 2015; Lindenbach et al, 2005; Wakita et al, 2005; Walters et al, 2009; Zhong et al, 2005). Experiments in this *in vitro* system have identified a large number of host factors that are required for viral replication or that have antiviral properties(Colpitts et al, 2015). This experimental system also brought important insights into the virus-host interactions that may contribute to pathogenesis, for example revealing cell cycle perturbations in HCV-infected cells(Walters et al, 2009). However, few of these findings have been evaluated in the human liver.

Studying HCV infections *in vivo* presents important challenges. An intrinsic difficulty comes from the immune response, which is a strong confounding factor in analyses of human liver biopsies. Gene expression differences between HCV-infected and uninfected livers are the result of direct HCV-induced cell-autonomous adaptive responses in infected cells and of more global changes that result from the immune response in the liver. The chronic phase of HCV infections is characterized by a largely ineffective cellular immune response combined with a highly variable interferon lambda (IFN λ) mediated innate immune response(Heim & Thimme, 2014). A significant proportion of patients are characterized by an endogenous activation of the interferon (IFN) system, in which hundreds of classical IFN-stimulated genes (ISGs) are strongly induced(Heim & Thimme, 2014). The presence of the endogenous IFN system activation can mask more subtle changes that occur as a direct consequence of viral infection and replication in HCV-infected cells. The confounding effect of the immune answer is aggravated by the fact that the percentage of HCV-infected hepatocytes rarely exceeds 50% and often is

below 20%, whereas ISG expression can be observed in up to 95% of cells(Wieland et al, 2014). To better understand the molecular consequences of HCV infection *in vivo*, it is thus important to disentangle the direct cellular response to viral infections from the transcriptional signature of the immune response, and in particular of the endogenous IFN system activation.

The endogenous activity of the IFN system is also highly relevant for therapeutic choice in chronic hepatitis C (CHC). Until the recent introduction of direct antiviral drugs for the treatment of CHC, recombinant pegylated IFN alpha 2 (pegIFNa) had been an essential component of the standard of care for CHC for over 25 years, and it is still used in many parts of the world. Treatment with pegIFNa and ribavirin achieved cure rates between 30-80%, depending on the viral genotype, pretreatment patient history and stage of liver fibrosis(Heim, 2013). The success of the treatment is also highly dependent on the genetic background of the patients. Genome-wide association studies revealed significant associations between polymorphisms in the *IFNL4* gene and response to pegIFNa/ribavirin(Bibert et al, 2013; Prokunina-Olsson et al, 2013; Terczynska-Dyla et al, 2014). The recently discovered IFNL4 protein has strong antiviral properties and stimulates ISG production through binding to the IFN lambda receptor(Hamming et al, 2013; Prokunina-Olsson et al, 2013). The *IFNL4* gene harbors several genetic variants in human populations, including a frameshift mutation that abrogates the production of the IFNL4 protein(Terczynska-Dyla et al, 2014). Paradoxically, the IFNL4-producing genotype is associated with poor response to pegIFNa/ribavirin, whereas mutated alleles coding for an IFNL4 variant with strongly reduced biological activity or even a complete loss of function are associated with very good spontaneous and treatment-induced resolution rates(Terczynska-Dyla et al, 2014). These observations are consistent with earlier findings that patients who have a strong endogenous induction of ISGs during the chronic phase of HCV infection do not respond to therapeutically injected pegIFNa(Asselah et al, 2008; Chen et al, 2005; Sarasin-Filipowicz et al, 2008). It is presently not known why the activation of the endogenous IFN system in the liver in patients with the IFNL4-producing genotype is ineffective against HCV, whereas pegIFNa-induced ISG expression results in viral eradication in so many patients.

In this study, we aimed to disentangle the direct and indirect effects of HCV infection on gene expression patterns, by performing a detailed characterization of the gene

expression changes associated with HCV infection, endogenous IFN system activation and pegIFNa treatment in the human liver. With this objective, we generated and analyzed high-throughput transcriptome sequencing profiles from liver biopsies derived from different categories of HCV-infected and non-infected patients, prior to and during treatment. First, to unveil HCV-induced cell-autonomous effects and to separate them from IFN-induced changes in the transcriptome, we selected liver biopsies from CHC patients without hepatic ISG induction, and compared them with un-infected control biopsies. Second, we examined the transcriptomic changes associated with the endogenous activation of the IFN system in a subset of CHC patients. Finally, we analyzed the gene expression changes resulting from pegIFNa/ribavirin treatment, by comparing transcriptome data from liver biopsies obtained before treatment and at different time points during the first week of therapy. We found that the transcriptional profiles associated with endogenous IFN activation and with pegIFNa/ribavirin treatment share a core set of IFN-stimulated genes, although quantitative differences can be found in gene activation levels.

Throughout our study, we investigated the differential expression patterns of both protein-coding genes and non-coding RNAs, aiming to clarify the regulatory mechanisms underlying the transcriptomic changes induced by HCV infection and pegIFNa treatment. In particular, we evaluated the roles of microRNAs (miRNAs) in the regulation of the hepatocellular and immunological host response to HCV infection. Interestingly, we found that the precursor transcripts of several miRNAs (including miR-122, which is required for HCV replication (Jopling et al, 2005)) are down-regulated following pegIFNa treatment in the human liver. Consistently, we observe a subtle up-regulation of the corresponding miRNA target genes, indicating that the expression changes observed for the precursor transcripts are reflected in the mature miRNA levels. Although these findings warrant further validation, we propose that the down-regulation of miRNA precursors, in particular of miR-122, may contribute to efficiency of HCV clearance by pegIFNa/ribavirin treatment.

Results

Expression patterns of interferon-stimulated genes define two classes of CHC patients

Previous studies focusing on the response to interferon (IFN) treatment in chronic hepatitis C (CHC) revealed the existence of a subset of patients with high endogenous levels of interferon-stimulated genes (ISGs)(Sarasin-Filipowicz et al, 2008). This distinction between two categories of CHC patients is highly relevant when seeking to determine the molecular consequences of HCV infection in the human liver, which otherwise can be confounded by the endogenous activation of the IFN system. We thus analyzed the expression levels of ISGs in the examined CHC patients. To do this, we mined a previously published dataset of ISGs(Dill et al, 2014) and extracted a set of genes that are strongly up-regulated in the human liver upon pegIFNa treatment, requiring a minimum expression fold change of 2 across all studied time points. We thus obtained a set of 20 strong ISGs and we assessed their expression levels in 28 liver biopsies (including control non-infected samples, termed hereafter non-CHC) in our dataset (Fig. 1a, Supplementary Table 1).

A hierarchical clustering approach applied on centered and scaled gene expression levels confirmed the existence of two main groups of patients (Fig. 1a). The first group, characterized by overall low ISG transcript levels, comprised 21 samples, including all 6 non-CHC liver biopsies and 15 of the CHC samples. Importantly, no clear distinction was found between the non-CHC and the CHC samples in this group. The second group, consisting of 7 CHC samples, displayed higher expression levels across the 20 analyzed ISGs (Fig. 1a). Importantly, we note that this separation between two groups of patients cannot be explained by the HCV genotype carried by the CHC patients, as all four genotypes were found in the 7 patients with high ISG levels (Fig. 1a). Similarly, analysis of the inflammation and fibrosis METAVIR scores(Bedossa & Poynard, 1996) and of the HCV viral load indicated that these factors cannot explain the patient grouping (Fig. 1a,b). To verify that the clustering of CHC samples was not dependent on the set of genes used as markers, we performed a principal component analysis on 360 genes associated with Gene Ontology (GO) categories related to response to interferon (Methods). This

analysis confirmed that our sample sub-classification is robust with respect to the choice of the ISG input dataset (Supplementary Fig. 1).

Gene expression changes induced by HCV in the absence of the endogenous IFN system activation

We first aimed to investigate the gene expression changes induced by HCV infection, without the confounding effect of the activation of the endogenous IFN system, and without the confounding effects of strong inflammation or fibrosis. We thus compared gene expression levels between 6 non-CHC and a subset of 7 CHC low ISG samples with METAVIR scores \leq A2F3, using the Wald test for differential expression implemented in DESeq2 (Love et al, 2014) and a sample randomization procedure to minimize outlier effects (Methods). We identified 179 robustly differentially expressed protein-coding genes, at a false discovery rate (FDR) threshold of 10% and requiring an absolute fold change above 1.5 (Fig. 2a, Supplementary Table 2). With the same parameters, we discovered 14 long non-coding RNAs (Methods) and 43 genes with unclear classification (including pseudogenes and other classes of non-coding RNAs, Methods) that were robustly differentially expressed between the two sample categories (Fig. 2a). Most differentially expressed protein-coding genes were up-regulated in the CHC low ISG patients compared to controls, reaching a maximum fold change of 8.

We next examined the protein-coding genes with the highest absolute fold change between the two groups of samples (Fig. 2b). The strongest up-regulated genes included genes typically expressed in immune system cells, including *IGHG1*, *IGHG3*, *CD27*, *CD5*, etc. (Fig. 2b). Genes specifically associated with defense against viral infections, such as *OASL*, were also strongly up-regulated (Fig. 2b). A gene ontology (GO) analysis for up-regulated protein-coding genes revealed strong enrichment for biological processes related to lymphocyte and leukocyte activation, including more specific terms like T-cell and B-cell activation (Supplementary Table 3). In contrast, down-regulated genes were enriched for processes related to the protein activation cascade, response to stimulus or complement activation, although these patterns were driven by only a few genes (Supplementary Table 3).

We then analyzed the expression patterns of these genes in the broad collection of human tissue transcriptomes of the GTEx consortium (Mele et al, 2015). In agreement with the GO association with immune system cells, up-regulated genes were most highly expressed in the whole blood, in the lymphocytes or in the spleen (Fig. 2c), while down-regulated genes generally reached maximum expression in the liver or in adipose tissue (Fig. 2c). Moreover, an analysis of the transcription factor binding motifs over-represented in the promoters of the genes up-regulated in low ISG patients revealed the presence of several transcription factors associated with immune system cells, including members of the ETS family, the E2A, NFKB and SPIB transcription factors (Supplementary Fig. 2a). No motif enrichment was found for genes down-regulated in CHC low ISG samples. Taken together, these results indicate that the gene expression changes observed in this class of HCV-infected patients largely result from the recruitment of immune system cells into the liver.

To further explore the regulatory mechanisms driving differential gene expression patterns, we examined the behavior of microRNA (miRNA) target genes. Experiments in Huh7 hepatocellular carcinoma cells recently showed that HCV functionally sequesters miR-122, thus reducing its binding to endogenous target genes and leading to their up-regulation (Luna et al, 2015). To assess whether this observation also holds *in vivo*, we analyzed the expression fold change of predicted miRNA targets in CHC low ISG samples compared to non-CHC samples (Fig. 2d). We analyzed a set of microRNAs expressed in normal and/or HCV-infected human livers (Hou et al, 2011) and a set of evolutionarily conserved miRNA targets predicted computationally with TargetScan (Agarwal et al, 2015) (Supplementary Table 4, Methods). We found that miR-122 targets had significantly higher fold changes (median 0.045) than targets of other expressed miRNAs (median -0.015, Wilcoxon rank sum test, p-value 0.018) and than genes not targeted by this set of liver miRNAs (median -0.14, Wilcoxon rank sum test, p-value < 1e-10, Fig. 2d). These observations are compatible with the reported subtle de-repression of miR-122 target genes in the presence of HCV infection (Luna et al, 2015). However, we also found that miR-122 targets have comparable expression fold changes with the targets of other highly expressed miRNAs, such as miR-192, let-7 or miR-199 (Fig. 2d). Similar conclusions were reached when analyzing a set of miRNA targets identified in Huh7 cells using high-throughput sequencing of RNA isolated by crosslinking immunoprecipitation (Luna et al, 2015) (Supplementary Fig. 2b,

Supplementary Table 4). Overall, the fold expression change was positively correlated with the number of distinct miRNA families that are predicted to target each gene (Supplementary Fig. 2c). This observation cannot be simply explained by the previously reported sequestration of miR-122 by HCV, but may reflect the expression or functional characteristics of genes targeted by multiple miRNA families. Our results thus reveal a potential confounding factor in the up-regulation of miR-122 targets following HCV infection.

Gene expression patterns associated with endogenous IFN system activation

We next investigated the gene expression changes driven by the combined effect of HCV infection and endogenous IFN system activation. To do this, we contrasted gene expression levels between non-CHC and CHC high ISG samples (Methods). Using the same parameters as above, we observed numerous differentially expressed genes in the high ISG patients, including 503 protein-coding genes, 80 candidate long non-coding RNAs and 125 other genes (Fig. 3a, Supplementary Table 2). The observed expression fold changes and significance levels spanned a wider range than for the comparison between non-CHC and CHC low ISG patients (Fig. 2a and 3a). As expected, the most highly up-regulated protein-coding genes were known ISGs, including *LAMP3*, *IFI27* and *RSAD2* (Fig. 3b). The up-regulated long non-coding RNAs included a previously described interferon-inducible transcript, *NR1R* (Kambara et al, 2014) (Fig. 3c).

Gene ontology analyses showed a strong enrichment for genes involved in immune system processes, in particular response to virus and type I interferon signaling pathway (Supplementary Table 3). Interestingly, the GO categories found to be enriched among the genes up-regulated in CHC low ISG patients were generally also over-represented in this second comparison, although the enrichment was much weaker than the one observed for the interferon pathway (Supplementary Table 3). In agreement with these observations, we found that interferon-stimulated response element (ISRE) motifs and IFN-regulatory factors (IRF) motifs were strongly over-represented in the promoters of the genes up-regulated in CHC high ISG samples (Supplementary Fig. 3). However, we also observed a significant enrichment for NFkB and ERG motifs (Supplementary Fig. 3), indicating the presence of immune cells in these high ISG

samples. The promoters of down-regulated genes were enriched in binding sites for two liver-specific transcription factors, HNF4a and HNF1, indicating that most down-regulated genes are hepatocyte-specific genes (Supplementary Fig. 3). As in the comparison between non-CHC and CHC low ISG samples (see above), we found no evidence for a specific de-repression of miR-122 target genes (Fig. 3d).

Overall, genes differentially expressed between CHC low ISG and non-CHC samples were recovered in the comparison between CHC high ISG and non-CHC samples (Fig. 4). Specifically, we found that 114 (64%) of the 179 protein-coding genes that differed (up or down) between CHC low ISG and non-CHC samples were also differentially expressed between CHC high ISG and non-CHC samples (Fig. 4a). The remaining genes that were only differentially expressed in low ISG compared to non-CHC patients generally displayed consistent fold changes in both comparisons, but did not pass the FDR threshold when comparing CHC high ISG and non-CHC samples (Fig. 4b-d). In contrast, most of the genes that were uniquely up-regulated or down-regulated in CHC high ISG patients compared to controls had only weak expression changes in the comparison between CHC low ISG and control samples (Fig. 4b, e, f). These observations are consistent with the presence of a unique expression signature associated with the group of high ISG patients (Fig. 1a). To further define this expression signature, we directly compared the two groups of CHC samples (Supplementary Fig. 4, Supplementary Table 2). We found numerous genes with significant expression changes, including 176 protein-coding genes and 21 lncRNA candidates (Supplementary Fig. 4). As expected, we observed a strong enrichment for biological processes associated with defense response to virus and type I interferon signaling pathway among the genes up-regulated in high ISG (Supplementary Table 3).

Gene expression patterns associated with HCV infection *in vivo* and *in vitro*

We next sought to compare the transcriptional responses following HCV infection *in vivo* and *in vitro*. A previous genome-wide analysis of differential gene expression in HCV-infected Huh-7.5 cells revealed that numerous genes involved in cell death, cell cycle and cell growth/proliferation are mis-regulated following viral infection (Walters et al, 2009). Although our unsupervised gene ontology analyses did not reveal enrichments

for cell cycle-associated categories among the genes differentially expressed in CHC samples (Supplementary Table 3), we found significant intersections between the sets of genes that are differentially expressed following HCV infection *in vivo* and *in vitro*. Specifically, out of 698 protein-coding genes differentially regulated in HCV-infected Huh-7.5 cells (Methods), we found that 25 (3.6%) were differentially expressed between control and CHC low ISG samples and 48 (6.9%) were differentially expressed between control and CHC high ISG samples (FDR<0.1, Supplementary Table 5). The extent of the overlap was significantly higher than expected by chance given the total number of differentially expressed genes, in both cases (Chi-square test, p-value <1e-9). The common differentially regulated genes included several genes associated with cell death and cell cycle, such as *UBD*, *TNFRSF9*, *BIRC3*, *JUN*, *FOS* etc. (Supplementary Table 5). Differentially expressed genes shared between HCV-infected Huh7.5 cells and high ISG liver biopsies include classical ISGs, such as *MX1*, *ISG15*, *IFIT1* etc. (Supplementary Table 5), as expected given the previously reported induction of interferon-stimulated genes in these cells (Walters et al, 2009).

Gene expression changes induced by pegIFN α treatment

We next analyzed the gene expression changes induced by pegIFN α /ribavirin treatment in the human liver, by comparing the expression profiles of control and post-treatment biopsies at five different time points ranging from 4 hours to 144 hours post-treatment (Methods). We considered genes to be differentially expressed if they displayed an absolute fold change of at least 2, at a FDR rate of 5% and an RPKM value above 1 in at least one of the compared samples (Methods). With these stringent criteria, we observed numerous expression changes at all time points, in particular for protein-coding genes, but also affecting other categories of transcripts (Fig. 5, Supplementary Table 6). As previously reported (Dill et al, 2014), most differentially expressed protein-coding genes were observed at 16 hours post-treatment, followed by the 4 hours time point (Fig. 5a). We observed a different temporal dynamics for differentially expressed non-coding transcripts, for which the number of detected up-regulated genes was highest at the 4 hours time point and decreased afterwards (Fig. 5a). Strikingly, for all gene categories the vast majority of down-regulated genes were observed 16 hours after treatment, with only few detected cases elsewhere (Fig. 5a).

At all time points, we found strong enrichments in GO categories related to the type I interferon signaling and response to virus pathways among the genes that were up-regulated following pegIFNa treatment (Supplementary Table 7), as expected. Consistently, we observed that interferon-stimulated response element (ISRE) motifs and IFN-regulatory factors (IRF) motifs were strongly enriched in the promoters of up-regulated protein-coding genes, at all time points (Supplementary Fig. 5a-e). For down-regulated genes, we found significant (FDR<0.1) enrichments in functional categories related to small molecule biosynthetic process and lipid metabolism, but only for the 16h time point (Supplementary Table 7).

We next compared the sets of differentially expressed genes observed for the different time points. We observed that almost 60% of the up-regulated protein-coding genes passed our differential expression thresholds at a single time point (Fig. 5b). For up-regulated lncRNAs and other non-coding genes, the time point-specificity was even stronger (Fig. 5b). However, we were able to identify a core set of 60 genes that are up-regulated at 4 or more time points, including 31 genes up-regulated at all analyzed time points (Supplementary Table 8). Interestingly, 3 lncRNAs were found to be significantly up-regulated at all time-points (Supplementary Table 8, Supplementary Fig. 5f-h). However, two of these lncRNAs (including *NRIR*, a lncRNA previously proposed to act as a negative regulator of interferon response (Kambara et al, 2014)) are found downstream of interferon-stimulated protein-coding genes (*CMPK2* and *BST2*), and our RNA-seq data suggests that their induction may be at least in part due to leaky transcription from the upstream gene (Supplementary Fig. S5f-g). No such neighborhood effects were observed for the third lncRNA, which is found upstream of *RHOT1* (Supplementary Fig. S5h). In contrast with the tendency of up-regulated genes to be shared across time points, down-regulated genes were time point-specific in more than 80% of cases, for all three categories of genes (Fig. 5b), and only two genes (including *CD1C* and a newly annotated long non-coding RNA) were down-regulated at 4 time points (Supplementary Table 8).

Comparison between pegIFNa treatment and endogenous IFN system activation

The induction of hundreds of ISGs in patients with CHC has little impact on viral replication, whereas treatment of patients with recombinant pegIFNa achieves high cure rates specifically in patients without an activation of the endogenous IFN system in the liver (Heim, 2013; Heim & Thimme, 2014). To investigate the molecular differences between these two modes of IFN system activation, we compared the transcriptional response to pegIFNa treatment with the one elicited by the endogenous IFN system activation. We first extracted the genes that are significantly up- or down-regulated following pegIFNa treatment, at each time point, and analyzed their expression differences between CHC low ISG and CHC high ISG patients (Fig. 6, Supplementary Table 9). We found that the vast majority of genes that are up-regulated upon pegIFNa treatment are also induced in high ISG patients (Fig. 6, Supplementary Table 9). In numerous cases, these differences were also statistically significant (FDR<10%) in the comparison between low ISG and high ISG patients (Fig. 6). However, the level of gene induction was significantly stronger in the pegIFNa treatment analysis (Fig. 6a), as were the absolute levels of gene expression in the corresponding samples (Fig. 6c). In other words, the ISG expression levels reached after pegIFNa/ribavirin treatment are higher than the ones observed in patients with high endogenous ISG levels. In contrast, genes that were down-regulated upon pegIFNa treatment were only rarely down-regulated in high ISG compared to low ISG patients (Fig. 6b,d). Similar conclusions were reached when extracting genes that are significantly differentially expressed between low ISG and high ISG patients and analyzing their expression patterns following pegIFNa treatment (Supplementary Fig. 6). These observations suggest that the endogenous IFN system activation and its external stimulation with pegIFNa/ribavirin treatment have qualitatively similar effects on the gene expression patterns on the human liver transcriptomes. However, numerous quantitative differences in the two transcriptional responses can be observed, with stronger ISG induction levels following pegIFNa/ribavirin treatment.

To further investigate the inability of the endogenous IFN system activation to cure HCV infections, we analyzed the expression patterns of a set of genes proposed to act as antiviral effectors, selected based on their capacity to inhibit HCV replication in human cell lines (Metz et al, 2012; Metz et al, 2013; Schoggins et al, 2011) (Methods). We

analyzed the expression of these genes in our samples (Fig. 7, Supplementary Table 10). We found that their expression levels in pegIFNa/ribavirin-treated samples and in high ISG samples were strongly positively correlated (Fig. 7a). However, a number of these candidate ISGs were indeed significantly more stimulated by pegIFNa than by endogenous IFNs in high ISG patients (Fig. 7a, Supplementary Table 10). In particular, 6 genes (*IRF1*, *IRF2*, *IRF7*, *IRF9*, *OASL*, *IFITM3*) that were reported as antiviral effectors in at least two publications (Metz et al, 2013; Schoggins et al, 2011) did not differ significantly between low ISG and high ISG samples. However, with the exception of *IRF2*, all of them appeared to be induced in high ISG patients compared to controls or low ISG patients, albeit at weak levels. Thus we could not identify ISGs that are exclusively induced by pegIFNa and that could be *bona fide* anti-HCV effector genes.

Down-regulated microRNA host genes following pegIFNa treatment

Our analysis of the dynamics of differentially expressed genes following pegIFNa treatment revealed that numerous non-coding transcripts are down-regulated, in particular at the 16h time point (Fig. 5a). We noticed that these down-regulated genes include several miRNA “host” genes (defined as non-coding transcripts that have sense exonic overlap with annotated miRNAs, Methods). In total, 11 miRNA host genes were significantly differentially expressed (FDR<0.05) for at least one time point, and all instances were down-regulated rather than up-regulated (Fig. 8a). Strikingly, these down-regulated precursors include the “host” gene of miR-122, which enhances HCV replication in human hepatocytes (Jopling et al, 2006) (Fig. 8a,b). The estimated decrease in expression levels is likely not due to differential processing of the mature miRNA out of the precursor transcript, as consistent differences between baseline and post-treatment biopsies were observed along the entire gene length (Fig. 8b, Supplementary Fig. 7). Among the other miRNAs whose precursor genes are down-regulated upon pegIFNa treatment, miR-146a is a striking example, with significant down-regulation (at 10% FDR) for 3 out of the 5 analyzed time-points (Fig. 8a).

Our RNA-seq dataset does not allow us to determine whether the observed down-regulation of miRNA precursor genes affects the pool of mature miRNAs in the cells. To indirectly test this hypothesis, we reasoned that a decrease in mature miRNA expression

levels should positively affect the expression of their target genes. We thus analyzed the behavior of predicted miRNA target genes in response to pegIFNa/ribavirin treatment, at the 16h time-point (for which most miRNA host down-regulation events were observed, Fig. 8a). As above, we analyzed microRNAs expressed in normal and/or HCV-infected human livers(Hou et al, 2011) and their conserved targets predicted computationally with TargetScan(Agarwal et al, 2015) (Methods). Strikingly, out of 57 miRNA families with at least 100 conserved target genes, the three highest median expression fold changes were found for miRNAs whose precursor genes were down-regulated following treatment: miR-122, miR-331 and miR146a/b (Fig. 8c). High median fold changes were also observed for miR-214 and miR-192 (Fig. 8c).

Discussion

Hepatitis C virus (HCV) is one of the most widely used model systems to investigate host-virus interactions. The adaptive changes to HCV infections have been studied extensively in cell culture systems. For example, a comprehensive analysis of gene expression in HCV infected Huh-7.5 cells reported over 800 genes with > 2-fold changes in expression (Walters et al, 2009). Adaptive changes were described in lipid biosynthetic pathways, endoplasmic reticulum stress response, autophagy and cell cycle regulation. However, due to the difficulties inherent to human liver tissue sampling, few of these findings have been validated *in vivo*. To investigate whether the observations obtained in cell culture systems can be confirmed in the human liver, we have collected and analyzed transcriptome data from liver biopsies derived from control and chronic hepatitis C patients, in the absence of and during treatment with pegIFN α /ribavirin.

In the liver, cell-intrinsic adaptive changes to HCV infections are difficult to distinguish from changes induced by the immune response. In experimentally infected chimpanzees, transcriptome analysis revealed a strong induction of hundreds of ISGs in all animals (Bigger et al, 2004). Due to a genetic polymorphism in the IFN14 gene, ISG induction in humans is variable (Prokunina-Olsson et al, 2013; Terczynska-Dyla et al, 2014). In this study, in order to reduce the strong confounding influence of the endogenous IFN system, we analyzed gene expression patterns separately for patients with or without endogenous IFN activation. We found that gene expression changes between uninfected liver samples and low ISG samples mainly reflect the presence of immune cell infiltrates in the latter group. However, even in biopsies from patients without ISG induction (low ISG patients) we could not detect expression changes of genes involved in cellular responses to HCV described in cell culture. For example, a previous large-scale analysis of differential gene expression in HCV-infected Huh-7.5 cells revealed that numerous genes involved in cell death, cell cycle and cell growth/proliferation are mis-regulated following viral infection (Walters et al, 2009), while our differential expression analyses did not reveal enrichments for these functional categories of genes. We therefore used a targeted approach and specifically analyzed genes previously reported to be changed in HCV-infected Huh-7.5 cells (Walters et al, 2009). Specifically, we could identify a core set of 25 genes that are

differentially expressed following HCV infection in both Huh 7.5 cells and in liver samples from patients without IFN system activation. This common gene set included several cell cycle associated genes, such as *UBD*, *ITIH1*, *BIRC3* etc. (Supplementary Table 5)(Walters et al, 2009). Thus, we were able to identify a significant number of genes that respond to HCV infection both *in vivo* and *in vitro*.

How might we explain the differences in HCV-induced expression patterns *in vivo* and *in vitro*? It has been estimated that the number of HCV virions *per* infected cell is between 1 and 8 in the human liver, but can be as high as 500 to 1000 in the Huh-7.5 cell culture model(Stiffler et al, 2009). It is thus conceivable that some of changes described in cell culture are due to the high viral concentration, and do not occur *in vivo*. However, it is also possible that our analysis was underpowered to detect HCV-induced cell-intrinsic changes in gene expression. Changes in infected hepatocytes could be masked by unchanged gene expression in non-infected hepatocytes and non-parenchymal liver cells (endothelial cells, biliary epithelial cells, stellate cells, fibroblasts and Kupffer cells). Non-parenchymal cells provide about one third of the liver mass, and the number of infected hepatocytes can vary from 1% to 55%(Wieland et al, 2014). To minimize the information dilution from uninfected cells, we preferentially included in our study samples from patients with high viral load, because the proportion of infected cells significantly correlates with serum viral load(Wieland et al, 2014). Nevertheless, we cannot exclude that because of these limitations we could not detect some genuine HCV-induced cell-intrinsic changes of gene expression.

We also addressed a long-standing conundrum in the field regarding the inability of the endogenous IFN system activation to eradicate HCV infections. Ever since the discovery that a substantial proportion of patients with CHC have a strong induction of hundreds of ISGs in the liver(Asselah et al, 2008; Chen et al, 2005; Sarasin-Filipowicz et al, 2008) it remained unclear why the endogenous IFN system is ineffective against HCV, whereas therapies with recombinant (pegylated) IFNa were curative in many patients. Two alternative explanations were discussed: Either some critical ISGs are exclusively induced by pegIFNa, or pegIFNa induces the same ISGs but at a higher level than the endogenous IFNs. At first sight, our results indicate that the number of significantly changed ISGs is much higher after pegIFNa compared to those induced by endogenous IFNs (in high ISG samples), suggesting that pegIFNa indeed induces additional ISGs that

are not stimulated by endogenous IFNs. However, most of these “additional” genes were up-regulated in high ISG samples as well, albeit to a lesser degree and therefore not passing the significance threshold. Such quantitative differences were also observed for a number of candidate anti-HCV effector ISGs identified in large screens (Metz et al, 2013; Schoggins et al, 2011). Most of them were significantly stronger induced by pegIFNa compared to endogenous IFNs, but their expression levels were highly positively correlated between samples treated with pegIFNa/ribavirin and samples with high endogenous ISG levels (Fig. 7, Supplementary Table 10). We present 6 candidate antiviral effectors (*IRF1*, *IRF2*, *IRF7*, *IRF9*, *OASL*, *IFITM3*, reported in both publications cited above (Metz et al, 2013; Schoggins et al, 2011)) that do not differ significantly between low ISG and high ISG patients. However, with the exception of *IRF2*, these genes also appear to be slightly induced in high ISG samples compared to low ISG or non-infected samples, although at lower levels (Fig. 7). Of note, *IRF2* stands out because it is induced by pegIFNa at the 4h time point, but appears to down-regulated by endogenous IFNs (Fig. 7). However, *IRF2* is unlikely to be an antiviral effector *sensu stricto*. *IRF2* is a transcriptional regulator involved in IFN induction and in IFN signaling (Ikushima et al, 2013). Our *in vivo* analysis therefore could not reliably identify a set of ISG effectors uniquely up-regulated by pegIFNa that could be responsible for the superior antiviral efficacy of the treatment. Thus, our current analysis for the first time provides strong evidence that quantitative rather than qualitative differences in gene induction are responsible for the failure of the endogenous IFNs and the success of pegIFNa in viral eradication.

We also addressed the contribution of non-coding RNAs to gene regulation in response to HCV infections and to pegIFNa treatments. Most prominent of them is miR-122, because it is an essential host factor for HCV replication (Jopling et al, 2005). The fascinating role of the highly abundant miR-122 in HCV replication and virus-host interaction has recently been enriched by the observation that binding of miR-122 by HCV can regulate host gene expression by reducing (sponging) the amount of miR-122 available for gene repression (Luna et al, 2015). Detailed functional experiments in Huh7 cells brought evidence that HCV infection leads to significant de-repression of miR-122 target genes due to this sponging effect (Luna et al, 2015). At first sight, our *in vivo* transcriptomic analysis appeared to confirm this observation, as miR-122 target genes had higher expression levels in HCV-infected compared to control biopsies, more so than

genes targeted by all other miRNAs and than genes that are not targets of miRNAs (Figure 2,3). However, a closer look revealed the same pattern for other miRNAs highly expressed in the liver (e.g., miR-192, let-7). Because HCV does not bind these other miRNAs, this observation cannot be simply explained by a sponging effect.

An unexpected observation from our analysis of the transcriptional response to pegIFNa/ribavirin treatment was that 11 long non-coding transcripts that act as precursors for miRNAs (miRNA “host” genes) are significantly down-regulated following treatment. Strikingly, the precursor transcript of miR-122 is part of these down-regulated transcripts. Moreover, the genes targeted by these down-regulated miRNAs had the highest median expression fold changes following treatment. This indicates that the expression changes observed for the precursor transcripts are reflected in the mature miRNA levels. This finding is in agreement with previous evidence that IFNbeta treatment decreases mature miR122 levels(Pedersen et al, 2007), and that miR-122 levels are lower in individuals with endogenous IFN system activation(Sarasin-Filipowicz et al, 2009). Interestingly, besides miR-122, several other miRNAs whose host genes are down-regulated have been associated with HCV infections and/or interferon treatment. For example, miR-146a was previously reported to inhibit type I interferon production(Ho et al, 2014; Hou et al, 2009). Its down-regulation following pegIFNa/treatment might thus allow for a sustained activation of ISGs and thus more effective antiviral response. Another example is miR-192, which was previously proposed as a predictor for the response to IFN treatment(Motawi et al, 2015). Finally, it is tempting to speculate that the down-regulation of miR-122 levels might contribute to the efficiency of the pegIFNa/ribavirin treatment in eliminating HCV infections.

In conclusion, this comprehensive gene expression analysis with liver biopsy samples (obtained before and during treatment with pegIFNa) from patients with HCV infection revealed that HCV has no strong effect on the homeostasis of infected cells, that the endogenous IFN response is qualitatively similar to pegIFNa treatment but too weak to clear the infection and that IFN down-regulates miRNA precursor transcripts, thereby fine-tuning ISG expression.

Methods

Patient selection

The study included 25 patients with chronic hepatitis C (CHC) and 6 control patients (not infected with HCV) who underwent a diagnostic liver biopsy in the outpatient clinic of the Division of Gastroenterology and Hepatology, University Hospital Basel. The patients agreed to participate in the study and written informed consent was obtained (approved by the ethics commission of the cantons Basel-Stadt and Basel-Land; approval number EKBBM189/99). All patients with CHC were screened for potential response to treatment using a previously published classification method based on the expression values of *IFI27*, *RSAD2*, *ISG15* and *HTATIP2* (Dill et al, 2011). Patients with high probability of achieving sustained virologic response (SVR) were identified and in case of planned IFN-based treatment they were asked to undergo a second liver biopsy. Nineteen patients agreed to undergo a second biopsy, as follows: after 4h (5 patients), 16h (3 patients), 48h (3 patients), 96h (3 patients) or 144h (5 patients) of the first therapeutic injection of pegylated interferons (pegIFNs). PegIFNs/Ribavirin doses were set according to HCV genotype and body weight based on standard recommendations. PegIFNs were administered subcutaneously once weekly at the initial dose of 1.5 µg/kg body weight of pegIFNα-2b (Essex Chemie) or 180 µg of pegIFNα-2a (Roche). Serum HCV RNA was quantified using the COBAS AmpliPrep/COBAS TaqMan HCV Test and the COBAS Amplicor Monitor from Roche. Diagnosis of control patients was based on clinical, laboratory, and histopathological assessment. For 18 patients, microarray-based expression analyses of the biopsy material were previously published (Dill et al, 2014). One additional patient was included for the 16h time point. Patient characteristics are summarized in Supplementary Table 1.

RNA-seq data generation

Total RNA was extracted from fresh-frozen bulk liver biopsy tissue using Trizol reagent (Invitrogen) and subsequently subjected to DNase treatment using DNA-free™ DNA Removal Kit (Ambion) according to manufacturer's instructions. RNA concentration was determined using NanoDrop 2000 spectrophotometer (Thermo Scientific) and RNA quality/integrity was assessed with an Agilent 2100 BioAnalyzer using RNA 6000 Nano Kit (Agilent Technologies). All 46 RNA samples included in this study had RNA integrity number (RIN) values of >7 (7.1-9.4; median 8.9), with 42 out of 46 samples having RIN

values ≥ 8 . We generated RNA sequencing (RNA-seq) data using the Illumina TruSeq Stranded mRNA protocol, with polyA selection. The libraries were sequenced on an Illumina HiSeq 2500 machine, as single-end reads.

RNA-seq data processing

The RNA-seq reads were trimmed to remove 3' end adapter sequences, keeping a maximum read length of 81 bp. The reads were aligned on the hg38 primary assembly (excluding patches and haplotypic sequences) of the human genome, downloaded from the Ensembl(Cunningham et al, 2015) database release 76. The alignments were done using TopHat(Kim et al, 2013) release 2.0.10 and Bowtie(Langmead & Salzberg, 2012) release 2.1.0. We allowed intron sizes between 40 bp and 1 million bp for spliced read alignments, with a minimum anchor size of 8 bp and a maximum of 1 mismatch for each aligned read segment.

Gene model reconstruction with RNA-seq

We used Cufflinks(Trapnell et al, 2010) release 2.2.1 to reconstruct *de novo* gene models from TopHat unique read alignments. Reads with multiple reported alignments were excluded from the dataset prior to *de novo* reconstruction. We kept isoforms with a minimum frequency above 0.05. Intra-intronic transcripts (corresponding to retained introns or unspliced pre-mRNAs) were kept if their frequency was above 0.25. We allowed intron sizes between 40 bp and 500,000 bp. Neighboring transcribed regions were collapsed if they were closer than 40 bp. We performed the gene model reconstruction separately for each RNA-seq sample and then merged them into a single set of gene models using the cuffmerge tool in Cufflinks. We note that *de novo* reconstructed gene models may be fragmented, meaning that a single locus can be split into several predicted gene models, in particular for low expression levels.

Long non-coding RNA dataset

We used genomic annotations from the Ensembl(Cunningham et al, 2015) database release 82 as a basis for our analyses, to which we added *de novo* gene models reconstructed with Cufflinks. We determined the protein-coding potential of *de novo* gene models based on the codon substitution frequency (CSF) score approach(Lin et al, 2007; Lin et al, 2011) and on sequence similarity with known protein databases (SwissProt(UniProt, 2015)) and protein domains (Pfam-A(Finn et al, 2014)), as previously described(Necsulea et al, 2014). For the CSF approach, to determine the

codon substitution frequencies expected for coding and non-coding regions, we aligned Ensembl-annotated protein-coding sequences and intronic regions, for 9,000 1-1 orthologous gene families for 42 vertebrate species extracted from the Ensembl Compara database(Vilella et al, 2009). We then counted all observed codon substitutions and constructed coding and non-coding substitution matrices. We downloaded whole genome alignments for human and 99 other vertebrate genomes from the UCSC Genome Browser(Rosenbloom et al, 2015) and we computed the CSF score in 75 bp sliding windows along the entire human genome, as described previously(Necsulea et al, 2014). We then extracted all genomic regions with positive CSF scores. As positive CSF scores can appear spuriously on the opposite strand of protein-coding regions(Cabili et al, 2011), for regions with positive CSF scores on both strands we considered only the strand with the highest score. Gene models were classified as potentially protein-coding if had positive CSF scores over at least 90 bp or 25% of their exonic length. In addition, we searched for sequence similarity between exonic sequences and known proteins from and protein domains from the SwissProt(UniProt, 2015) and Pfam-A(Finn et al, 2014) databases, using blastx(Altschul et al, 1990). We kept SwissProt proteins with high confidence annotations (protein existence score 1, 2 or 3). We retained blastx hits with e-values below 0.001. Gene models were classified as potentially protein-coding if they had significant blastx hits with SwissProt or Pfam-A protein sequences over at least 90 bp or 5% of their exonic length. *De novo* reconstructed gene models classified as non-coding with both approaches were kept for further long non-coding RNA analyses.

To avoid annotating alternative untranslated regions or introns of protein-coding genes as independent long non-coding RNAs, we further filtered the set of *de novo*-predicted lncRNAs based on their distance to Ensembl-annotated protein-coding genes. We retained lncRNA candidates that had no sense overlap with Ensembl-annotated protein-coding genes and that were at least 10 kilobases (kb) away from protein-coding gene coordinates. Sense intronic overlaps with other non-coding transcripts were accepted. We discarded loci with an exonic length below 200 bp (for multi-exonic loci) or 500 bp (for mono-exonic loci). We further excluded loci overlapping with RNA repeats or with UCSC-annotated retro-transposed gene copies over more than 10% of their length.

In addition to *de novo* predicted lncRNA candidates, we analyzed Ensembl-annotated transcripts corresponding to gene biotypes “lincRNA”, “processed_transcript” or

“antisense”. For both Ensembl-annotated and *de novo* predicted lncRNAs, we further required support from at least 50 uniquely mapped RNA-seq reads, across all RNA-seq samples pooled together. In total, we analyzed 8,912 candidate lncRNAs, including 4,246 candidates detected *de novo* and 4,666 Ensembl-annotated lncRNAs. The *de novo* annotated lncRNA coordinates are provided with our GEO submission (accession number GSE84346).

Gene expression estimation

We computed expression levels for protein-coding genes and candidate long non-coding RNAs derived from Ensembl annotations or predicted *de novo* with RNA-seq. For genes that had multiple isoforms, we combined exon coordinates from all isoforms into a single “flattened” gene model and computed a single expression level for each gene. For protein-coding genes, only protein-coding isoforms were kept, discarding retained introns and other potentially non-functional isoforms. We used two approaches to estimate gene expression levels. First, we estimated gene-based RPKM (reads per kilobase of exon per million mapped reads) values by counting uniquely mapped RNA-seq reads that overlapped with exon coordinates over at least 5 bp. RNA-seq reads that were mapped to sense-overlapping exonic regions were added to the read count of all corresponding genes. The total number of mapped reads for each sample (corresponding to the M denominator in the RPKM computation) was computed after discarding ambiguously mapped reads and reads that aligned to the mitochondrial genome. We normalized expression levels among samples using a previously described median-scaling procedure, based on the least-varying genes in terms of expression ranks (Brawand et al, 2011). Second, we used Cufflinks to estimate gene expression levels using all TopHat-aligned reads, assigning reads with multiple alignments to each gene depending on gene expression levels estimated with unique reads (default multiple read correction procedure in Cufflinks). All gene expression estimates are provided with our GEO submission (accession number GSE84346).

Differential gene expression

We assessed differential gene expression using methods in the DESeq2 (Love et al, 2014) package (release 1.10.0) in R/Bioconductor (release 3.2.2), starting from the numbers of unambiguous read counts assigned to each gene. To test for differential gene expression following pegIFN α /ribavirin treatment, we used a likelihood ratio test to compare two

generalized linear models: a full model with two explanatory variables (the control/treated condition and the individual) and the reduced model with the individual as a single explanatory variable. To test for differential gene expression between groups of patients (normal liver, CHC high ISG or CHC low ISG), we compared a model with one explanatory variable (the patient group) and the null model, according to which the patient group has no effect. For the comparison between normal liver, CHC high ISG and CHC low ISG patients, we further selected the samples based on their METAVIR score for inflammation and fibrosis (A1/F1, A1/F2 and A2/F2 samples were kept for further analyses). We also excluded one sample (identifier A707), which had high expression levels for inflammatory markers despite its A2/F2 METAVIR classification. The sets of patients analyzed for each test are provided in Supplementary Table 1. P-values were corrected for multiple testing using the Benjamini-Hochberg method, as implemented in DESeq2. Note that for some genes, the resulting false discovery rate (FDR) is set to “NA”, if the expression levels are too low or too variable to ensure reliable differential expression estimates (Love et al, 2014). For further analyses, we selected genes for which the RPKM level was above 1 in at least one of the compared samples.

Resampling to control for outlier effects in differential expression analyses

The level of endogenous IFN system activation can vary among patients classified as high ISG (Figure 1). In addition, our dataset included different number of patients in the control (6), low ISG (7) and high ISG (7) categories, which may affect the statistical power of the analysis. To avoid outlier effects in our differential expression analyses for these comparisons (contrasting non-CHC, low ISG and high ISG patients), we resampled 6 out of 7 patients for the low ISG and high ISG categories and we performed differential expression analyses with the reduced number of samples. All possible patient combinations were tested separately. We then selected gene expression differences based on their average false discovery rates (FDR) and average log₂-fold expression change level across all resampling replicates. The analyses presented in the manuscript correspond to this resampling correction. Similar conclusions were reached when differential expression analyses were performed with all samples (results provided in Supplementary Table 2). For these comparisons, we considered that genes are differentially expressed if the FDR was below 0.1 and the absolute fold change above 1.5. We voluntarily chose slightly less restrictive FDR and fold change thresholds for these

analyses than for the pegIFNa treatment analysis, to avoid a loss of sensitivity associated with this resampling procedure.

Gene ontology enrichment

We performed gene ontology enrichment analyses using the GOrilla webserver (Eden et al, 2009). We contrasted a focus set of genes (e.g., genes that were up-regulated in a set of patients or at one time point during treatment) with a background set of genes expressed at in the same samples. We set the false discovery rate for the GO enrichment analysis at 0.1. Only protein-coding genes were used for this analysis. We also downloaded GO associations for each Ensembl-annotated gene from the Ensembl 82 database, using BioMart. For the principal component analysis (PCA) presented in Supplementary Fig. 1, we selected genes associated with the categories: "type I interferon production", "response to type I interferon", "response to interferon-gamma".

Transcription factor binding enrichment analysis

We used HOMER (Heinz et al, 2010) to assess the enrichment of transcription factor binding motifs in the promoter regions of differentially expressed protein-coding genes, compared to the genomic background. We searched for motifs in a 500 bp region, starting 400 bp upstream of the transcription start site and ending 100 bp downstream. For each analysis, we display the enriched motif, its frequency among the tested genes and the enrichment with respect to the background.

microRNA expression

To evaluate the involvement of miRNA regulation in the gene expression differences observed between patient categories or following treatment, we first obtained a dataset of miRNAs expressed in the relevant samples. We downloaded miRNA expression values evaluated with RNA sequencing and measured as TPM (tags per million mapped reads) from a previous publication (Hou et al, 2011). This dataset included expression levels for normal liver, hepatitis B virus (HBV)-infected and HCV-infected liver and hepatocellular carcinoma from HBV and HCV-infected livers. For comparability with our samples, we retained only expression levels from normal liver and HCV-infected, non-carcinoma samples. We summed the TPM values across all relevant samples and ranked miRNAs based on their combined expression values. For miRNA target analyses, we retained miRNAs with a combined TPM value of at least 100.

microRNA target prediction

We used two sources for miRNA target predictions. First, we extracted computational target predictions from the TargetScan v7.1 human dataset (Agarwal et al, 2015). To enrich in reliable target predictions, we kept only gene-miRNA associations that had a cumulative context++ score (Agarwal et al, 2015) below 0. We analyzed separately miRNA-target gene relationships for which at least one conserved binding site was predicted. Second, we used target predictions determined experimentally with HITS-CLIP in Huh7 cells (Luna et al, 2015). This dataset included binding sites for 50 miRNAs expressed in Huh7 cells. We filtered this dataset to keep only binding sites found in the 3' UTR region and we excluded 6mer binding sites. For the TargetScan dataset, we analyzed only miRNAs that were expressed in normal and HCV-infected liver, as defined above. All data are provided in Supplementary Table 4. For the analysis of miRNA targets and their expression patterns, we always exclusively analyzed genes that are expressed at an RPKM level of at least 1 in at least one of the relevant samples. For the analysis presented in Fig. 8, we computed confidence intervals for the median expression fold change (following pegIFN α /ribavirin treatment at the 16h time point) with a bootstrap approach, by resampling the same number of genes 100 times with replacement. We then extracted the 2.5% and 97.5% quantiles of the resulting distribution, which are displayed as confidence intervals in Fig. 8.

Definition of microRNA host genes

Our RNA-seq dataset allows us to estimate expression levels for all long, poly-adenylated transcripts, thus in principle including miRNA primary transcripts. We extracted coordinates of miRNA transcripts from Ensembl 82 (Cunningham et al, 2015) and we analyzed their overlap with exons of Ensembl-annotated or *de novo*-detected non-coding RNA genes. We found a total of 70 lncRNAs that had exonic overlap with miRNAs, that we classified as potential “miRNA host genes” and included in further analyses (Supplementary Table 11). We did not include in this analysis genes with intronic overlap with miRNAs.

Antiviral effector datasets

We specifically analyzed the expression patterns of a subset of ISGs that were previously proposed to act as antiviral effectors through a large-scale over-expression screening approach in Huh-7.5 cells (Schoggins et al, 2011). We extracted the list of genes whose

over-expression had a negative on HCV replication in this experimental setup, at both 48h and 72h time points, and matched them with current Ensembl annotations by gene names. Genes that appeared as having both positive and negative effects on HCV replication (depending on the time-points) were excluded. We added to this list of genes a dataset of ISG antiviral effectors previously described (Metz et al, 2013), including genes whose antiviral properties were predicted with a knockdown approach (Metz et al, 2012). The gene lists are provided in Supplementary Table 10.

Differentially expressed genes in HCV-infected Huh7 cells

We also analyzed a set of genes previously shown to be differentially expressed following HCV infection in Huh-7.5 cells (Walters et al, 2009). We matched the list of genes with Ensembl 82 annotations using the RefSeq accession number provided in this dataset (Walters et al, 2009). The gene lists and their differential expression patterns are provided in Supplementary Table 5.

Tissue expression patterns from GTEx

We analyzed the spatial expression patterns of the various gene lists identified in our study, using the gene expression dataset of the GTEx consortium, release v6 (Mele et al, 2015). We downloaded the pre-computed median RPKM values *per* tissue from the GTEx server. We used this dataset to estimate the tissue in which each gene reaches its maximum expression, for genes for which the maximum RPKM value in GTEx tissues was at least 1.

Statistics and graphics

All data analyses and graphical representations were done in R. The principal component analyses were performed with functions implemented in the ade4 library.

Data availability

All raw and processed RNA-seq data, including *de novo* gene annotations obtained with Cufflinks and all expression estimations, are available in the GEO database (accession number GSE84346). **The data is available during the review process at the following link:**

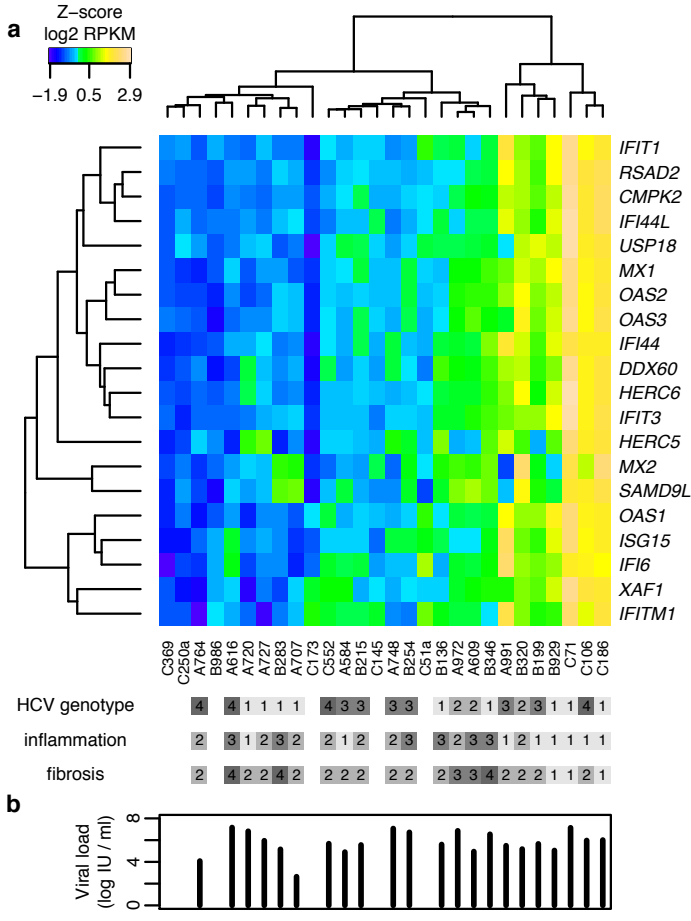
<http://www.ncbi.nlm.nih.gov/geo/query/acc.cgi?token=kjkfsqiexqjlen&acc=GSE84346>

Acknowledgements

This work was supported by Swiss National Science Foundation (SNF) grant 310030B_147089 and 310030_166202 to M.H. Heim, SNF Ambizione grant PZ00P3_142636 to Anamaria Necsulea, SNF MD-PhD stipend 323530_145255 to Tujana Boldanova, and a SCIEX grant 13.296 to Aleksei Suslov. The computations were performed at the Vital-IT (<http://www.vital-it.ch>) Center for high-performance computing of the SIB Swiss Institute of Bioinformatics.

Figures

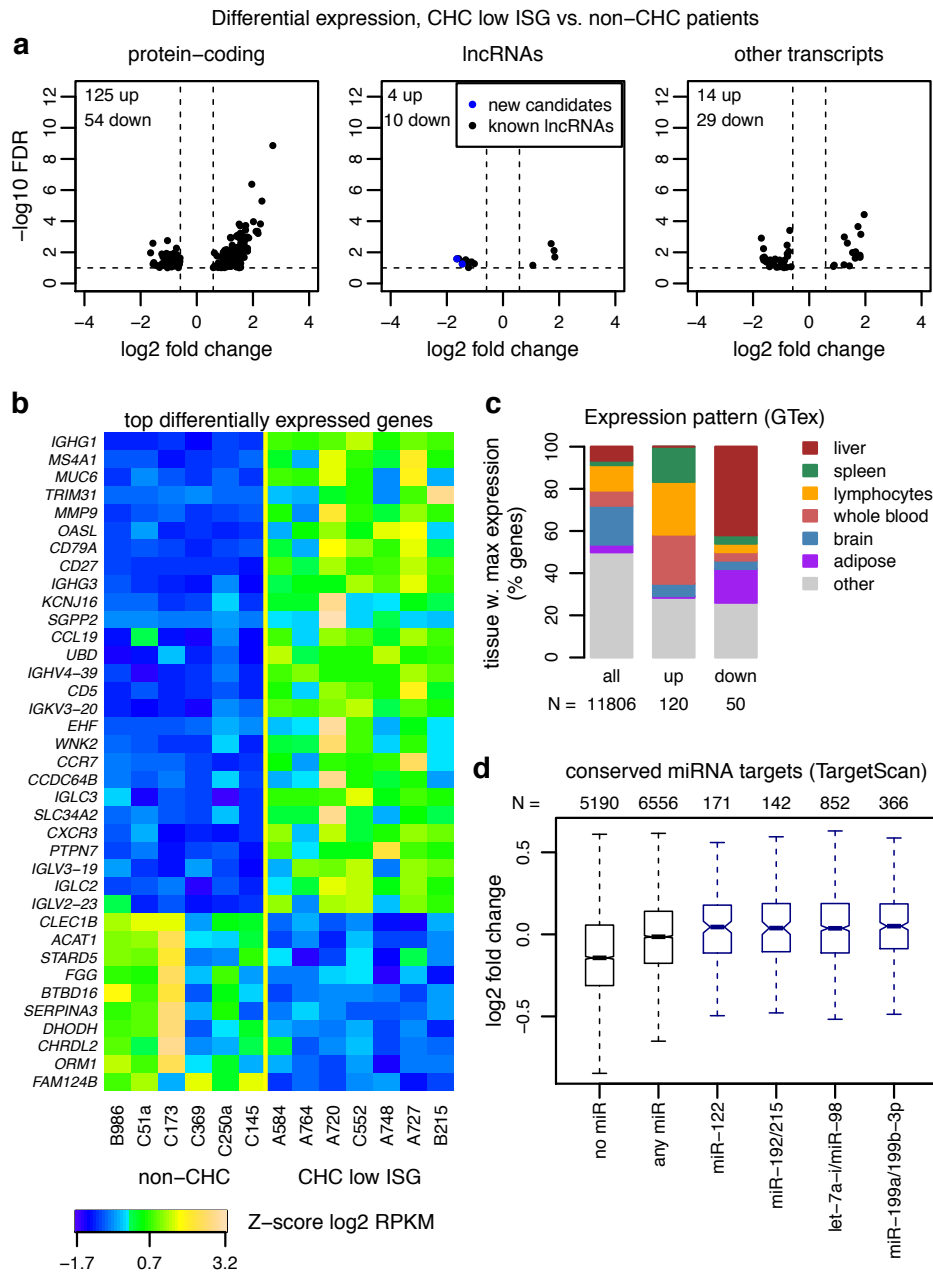
Figure 1.



a. Expression levels of 20 interferon-stimulated genes (ISGs) in 28 liver biopsies from HCV and non-HCV patients, in the absence of treatment. These ISGs were previously detected as consistently stimulated by pegIFNa across 5 time points between 4h and 144h, in chronic hepatitis C (CHC) patients(Dill et al, 2014). The heatmap represents the Z-score (centered and scaled values) of log₂-transformed RPKM (reads per kilobase of exon per million mapped reads) expression levels, normalized based on housekeeping genes (Methods). The samples (columns) and genes (rows) were hierarchically clustered based on pairwise Euclidean distances. The HCV genotype, the METAVIR scores for inflammation (A0 to A3) and fibrosis (F0 to F4) are displayed for each patient. Blank rectangles correspond to non-infected samples.

b. Barplot of the HCV viral load for each patient, ordered as in A. Blank spaces correspond to non-infected samples.

Figure 2.



a. Volcano plot for the differential expression analysis between non-CHC patients and CHC patients with low levels of endogenous ISG activation (CHC low ISG). The X-axis represents the \log_2 fold expression change in CHC low ISG patients compared to non-CHC patients. The Y-axis represents the false discovery rate (with a $-\log_{10}$ transformation) of the differential expression test. Protein-coding genes, candidate long non-coding RNAs (lncRNAs) and other gene categories (including pseudogenes and transcripts with unclear coding potential, Methods) are represented separately. Genes with false discovery rate (FDR) $< 10\%$ and with fold expression change ≥ 1.5 are shown.

b. Heatmap of the expression patterns of the top differentially expressed protein-coding genes. We set a fold change threshold of 3 for up-regulated genes and of 0.5 for down-

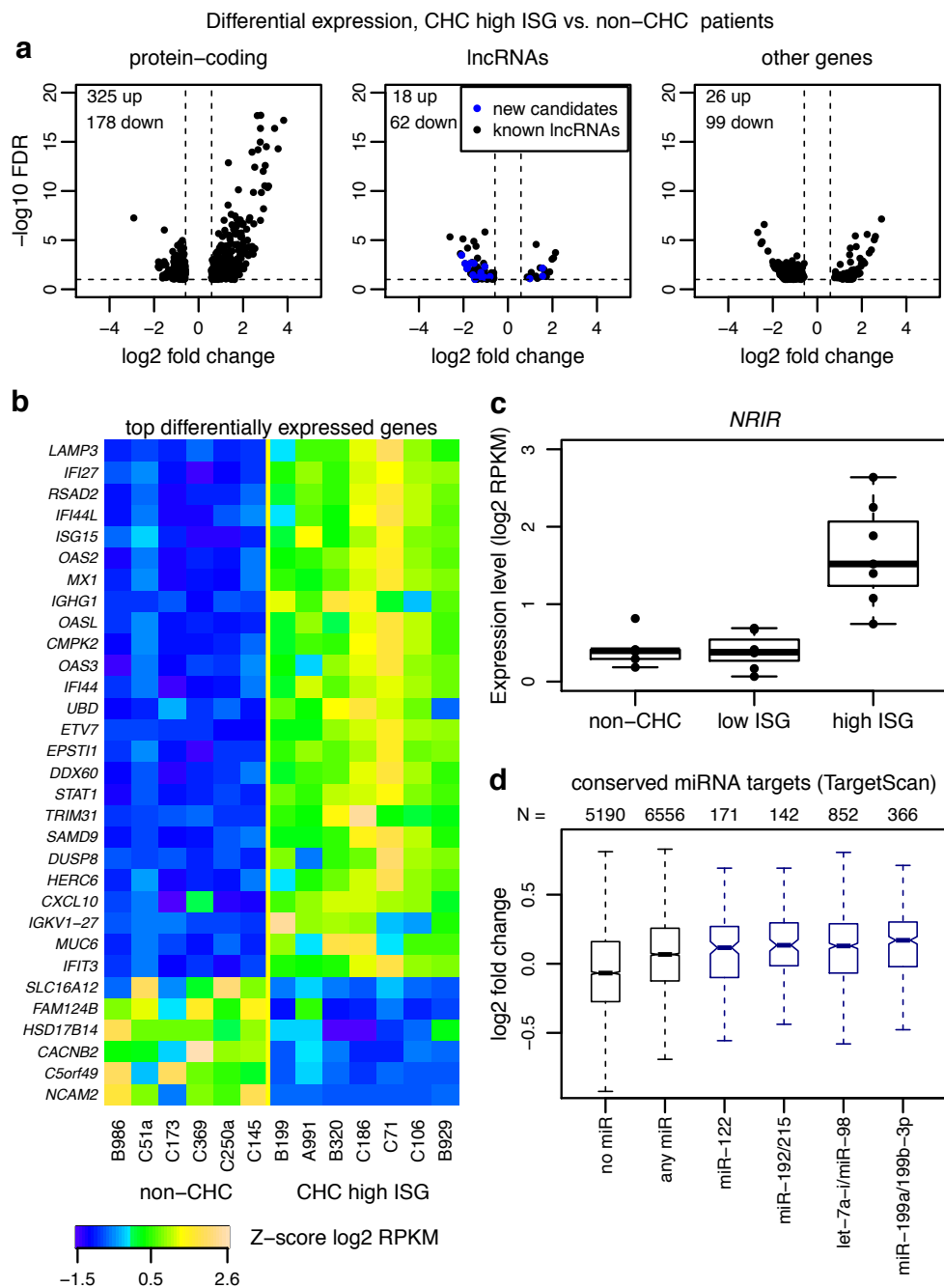
regulated genes. The heatmap represents the Z-score of the log₂-transformed RPKM (reads per kilobase of exon per million mapped reads) gene expression levels, normalized based on housekeeping genes (Methods).

c. Barplots representing the expression patterns of three categories of genes (all expressed genes, genes up-regulated in CHC low ISG samples, and genes down-regulated in CHC low ISG samples compared to control non-CHC samples), in the GTEx tissue transcriptome collection. For each expressed gene, we scored the tissue or cell type in which its maximum expression level was reached (Methods). The height of the rectangles represents the percentage of genes that reaches maximum expression in each of the tissues.

d. Boxplots of the intensity of the expression change (log₂ fold) between non-CHC patients and CHC low ISG patients, for different categories of protein-coding genes defined based on the miRNAs that are predicted to target them. Only miRNAs with high expression in normal or HCV-infected liver were analyzed (Hou et al, 2011).

Evolutionarily conserved miRNA target predictions were extracted from TargetScan v7.1 (Agarwal et al, 2015) (Methods). From left to right: genes that are not conserved targets of any expressed miRNA; genes that are targeted by at least one expressed miRNA; genes that are targeted by miR-122-5p, miR-192/215, let7a-i/miR-98 and miR-199a/199b, respectively.

Figure 3.



a. Volcano plot for the differential expression analysis between non-CHC patients and CHC patients with high levels of endogenous ISG activation (CHC high ISG). The X-axis represents the log₂ fold expression change in CHC high ISG compared to non-CHC patients. The Y-axis represents the false discovery rate (with a $-\log_{10}$ transformation) of the differential expression test. Protein-coding genes, candidate long non-coding RNAs (lncRNAs) and other gene categories (including pseudogenes and transcripts with unclear coding potential, Methods) are represented separately. Only genes with false discovery rate (FDR) < 10% and with fold expression change > 1.5 are shown.

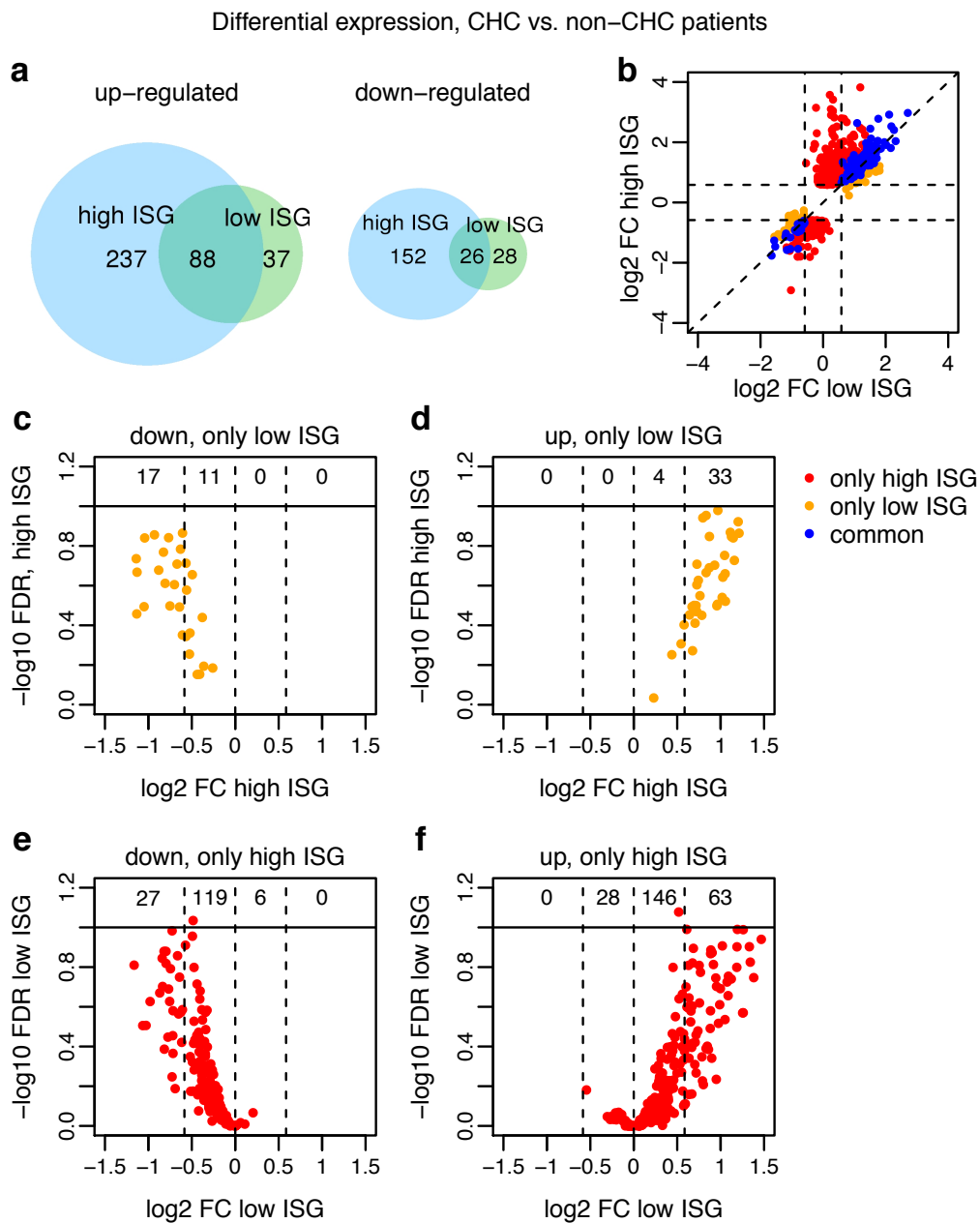
b. Heatmap of the expression patterns of the top differentially expressed genes between non-CHC and CHC high ISG patients. To select the top differentially expressed genes, we set a fold change threshold of 5 for up-regulated genes and of 1/3 for down-regulated genes. The heatmap represents the Z-score of the log₂-transformed RPKM (reads per kilobase of exon per million mapped reads) gene expression levels, normalized based on housekeeping genes (Methods).

c. Example of a lncRNA (*NR1R*(Kambara et al, 2014)) significantly up-regulated in high ISG patients. The boxplots represent the distribution of expression levels (log₂-transformed RPKM) for the three categories of samples. Each point represents an individual sample.

d. Boxplots of the intensity of the expression change (log₂ fold) between non-CHC patients and CHC high ISG patients, for different categories of protein-coding genes defined based on the miRNAs that are predicted to target them. Only miRNAs with high expression in normal or HCV-infected liver were analyzed(Hou et al, 2011).

Evolutionarily conserved miRNA target predictions were extracted from TargetScan v7.1(Agarwal et al, 2015) (Methods). From left to right: genes that are not conserved targets of any expressed miRNA; genes that are targeted by at least one expressed miRNA; genes that are targeted by miR-122-5p, miR-192/215, let7a-i/miR-98 and miR-199a/199b, respectively.

Figure 4.



a. Venn diagram depicting the intersection between protein-coding genes that are differentially expressed (FDR < 10%, minimum absolute fold change 1.5) between non-CHC patients, CHC patients with low endogenous ISG levels (CHC low ISG) and CHC patients with high endogenous ISG levels (CHC high ISG). Up-regulated and down-regulated genes are analyzed separately.

b. Comparison of the log₂-fold expression change for the two differential expression analyses: X-axis, CHC low ISG compared with non-CHC patients; Y-axis, CHC high ISG compared with non-CHC patients. Blue: genes significant in both comparisons; red: genes significant only for high ISG patients; orange: genes significant only for low ISG patients. Only protein-coding genes are displayed.

c. Similar to **b**, for genes that are down-regulated only in the comparison between non-CHC and CHC low ISG patients. The vertical dotted lines represent the absolute fold

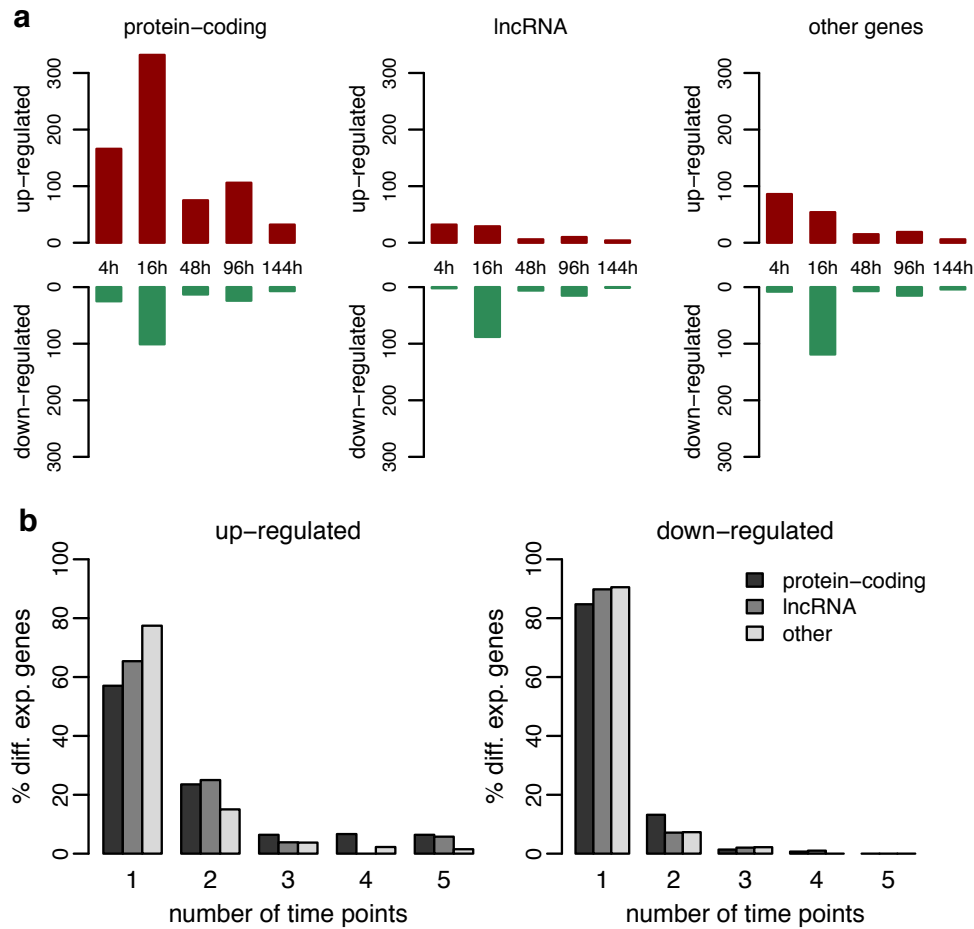
change threshold of 1.5 (0.58 in log₂ scale). The numbers depicted at the top of the plot represent the number of genes in each expression fold change interval (below 1/1.5, between 1/1.5 and 1, between 1 and 1.5 and above 1.5). X-axis: log₂ fold expression change in high ISG patients compared to controls. Y-axis: log₂ fold expression change in low ISG patients compared to controls.

d. Similar to **c**, for genes that are up-regulated only in the comparison between non-CHC and CHC low ISG patients. X-axis: log₂ fold expression change in high ISG patients compared to controls. Y-axis: log₂ fold expression change in low ISG patients compared to controls.

e. Similar to **c**, for genes that are down-regulated only in the comparison between non-CHC and CHC high ISG patients. X-axis: log₂ fold expression change in low ISG patients compared to controls. Y-axis: log₂ fold expression change in high ISG patients compared to controls.

f. Similar to **c**, for genes that are up-regulated only in the comparison between non-CHC and CHC high ISG patients. X-axis: log₂ fold expression change in low ISG patients compared to controls. Y-axis: log₂ fold expression change in high ISG patients compared to controls.

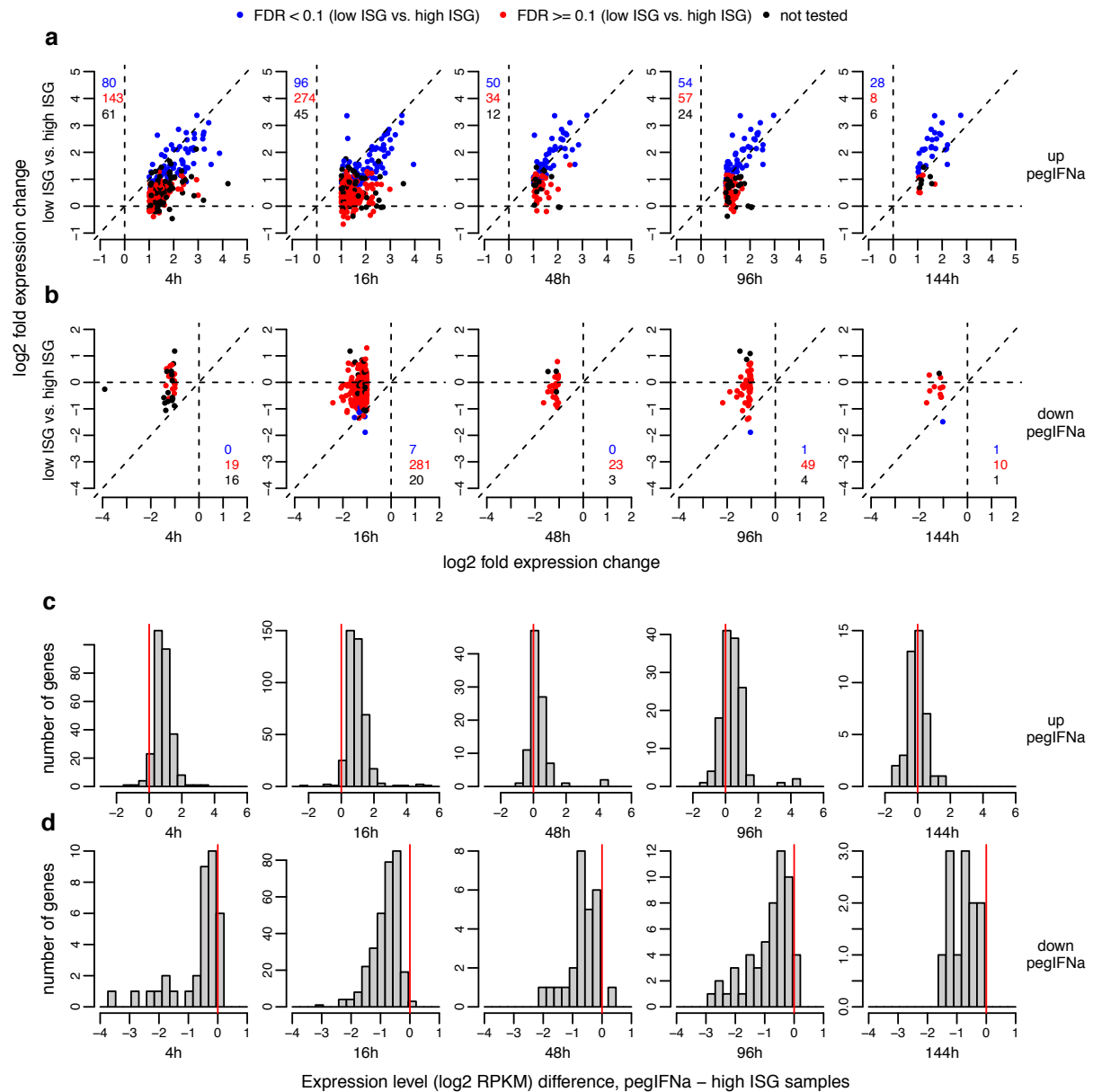
Figure 5.



a. Numbers of differentially expressed genes following pegIFNa/ribavirin treatment in liver biopsies of CHC patients. Gene expression changes were tested between paired biopsies from the same patients, before and after treatment. Protein-coding genes, lncRNAs and other gene categories (including pseudogenes, transcripts with unclear coding potential etc.) are displayed separately. We retained genes with a false discovery rate (FDR) < 0.05, a minimum absolute fold change of 2 and expression level (RPKM) > 1 in at least one sample.

b. Barplot representing the proportion of genes that are up-regulated (left) or down-regulated (right) upon pegIFNa treatment at 1, 2, 3, 4 or 5 time points. Different categories of genes are color-coded.

Figure 6.

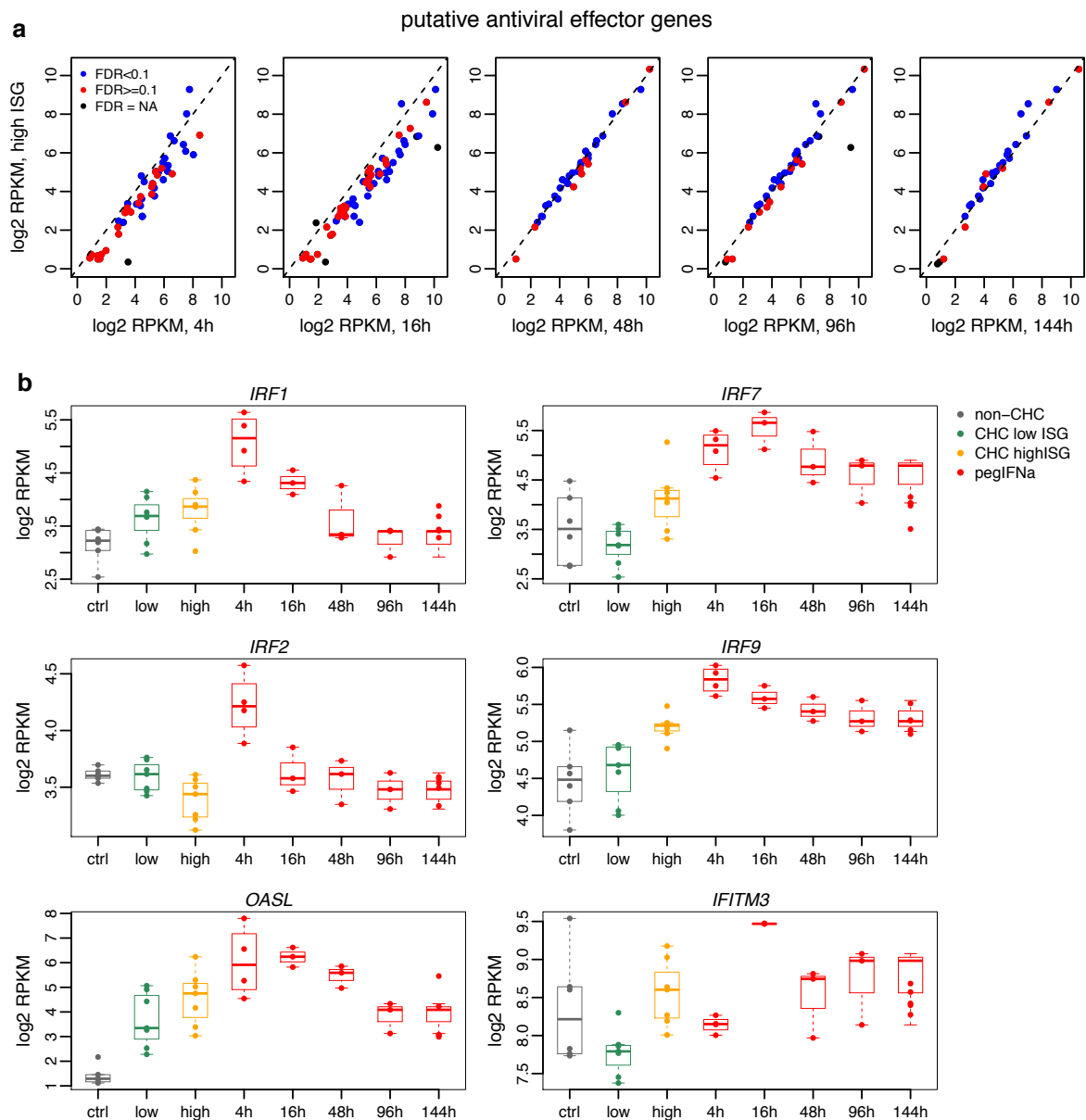


a. Differential expression patterns of the genes that are significantly up-regulated (FDR < 0.05 and minimum absolute fold change 2) following pegIFNa/ribavirin treatment at different time points, in the comparison between CHC low ISG and CHC high ISG patients. X-axis: log₂ fold expression change in pegIFNa-treated compared to control biopsies. Y-axis: log₂ fold expression change in high ISG patients compared to low ISG patients. Blue dots: genes also significantly differentially expressed in the low ISG vs. high ISG comparison (FDR < 0.1); red dots: genes significant only in the pegIFNa analysis; black dots: genes not tested in low ISG vs. high ISG comparison due to low or highly variable expression levels (Methods). The numbers of the genes in each category are depicted on the plot area, with the same color code.

b. Similar to **a**, for genes that are significantly down-regulated (FDR < 0.05 and minimum absolute fold change 2) following pegIFNa treatment at different time points.

- c.** Histogram of the difference in expression levels (log₂-transformed RPKM) between samples treated with pegIFN α /ribavirin and CHC high ISG samples, for the genes that are significantly up-regulated (FDR < 0.05 and minimum absolute fold change 2) following pegIFN α /ribavirin treatment at different time points. The differences were computed between expression levels averaged across all relevant samples.
- d.** Similar to **c**, for genes that are significantly down-regulated (FDR < 0.05 and minimum absolute fold change 2) following pegIFN α /ribavirin treatment at different time points.

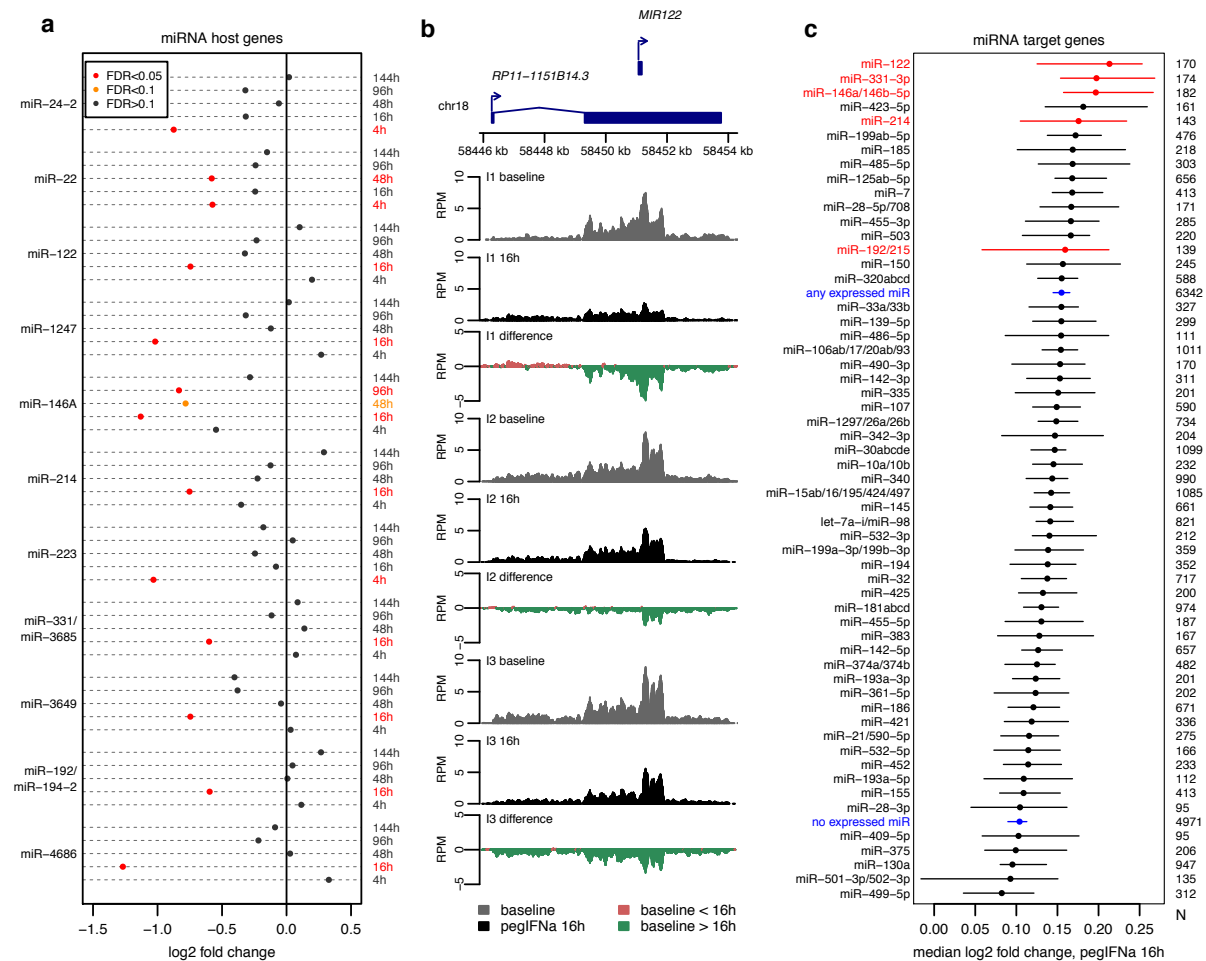
Figure 7.



a. Comparison between expression levels (log₂-transformed RPKM values) in samples obtained after pegIFNa/ribavirin treatment and in high ISG patients (in the absence of treatment), for genes predicted to act as antiviral effectors based on experiments in Huh7.5 cells (Metz et al, 2013; Schoggins et al, 2011). Only genes that are significantly up-regulated (FDR<0.05, no fold change threshold) following pegIFNa/ribavirin treatment are shown. Blue: genes that are also significantly differentially expressed (FDR<0.1) between low ISG and high ISG patients. Red: genes that are not significant in the comparison between low ISG and high ISG patients (FDR>=0.1). Black: genes not tested in the comparison between low ISG and high ISG patients due to low or variable expression levels (Methods).

b. Expression patterns of 6 putative antiviral effector genes that are not significantly different between low ISG and high ISG patients ($FDR \geq 0.1$). We selected genes reported in both publications (Metz et al, 2013; Schoggins et al, 2011), which were significantly up-regulated following pegIFN α /ribavirin treatment in our samples, but not between low ISG and high ISG patients. All resulting genes are shown. Y-axis: log₂-transformed RPKM levels. X-axis: different categories of samples. Gray: control, non-CHC patients; green: CHC low ISG samples; orange: CHC high ISG samples; red: biopsies obtained after pegIFN α /ribavirin treatment, at different time points. The dots represent individual samples. Boxplots are super-imposed over the individual expression levels.

Figure 8.

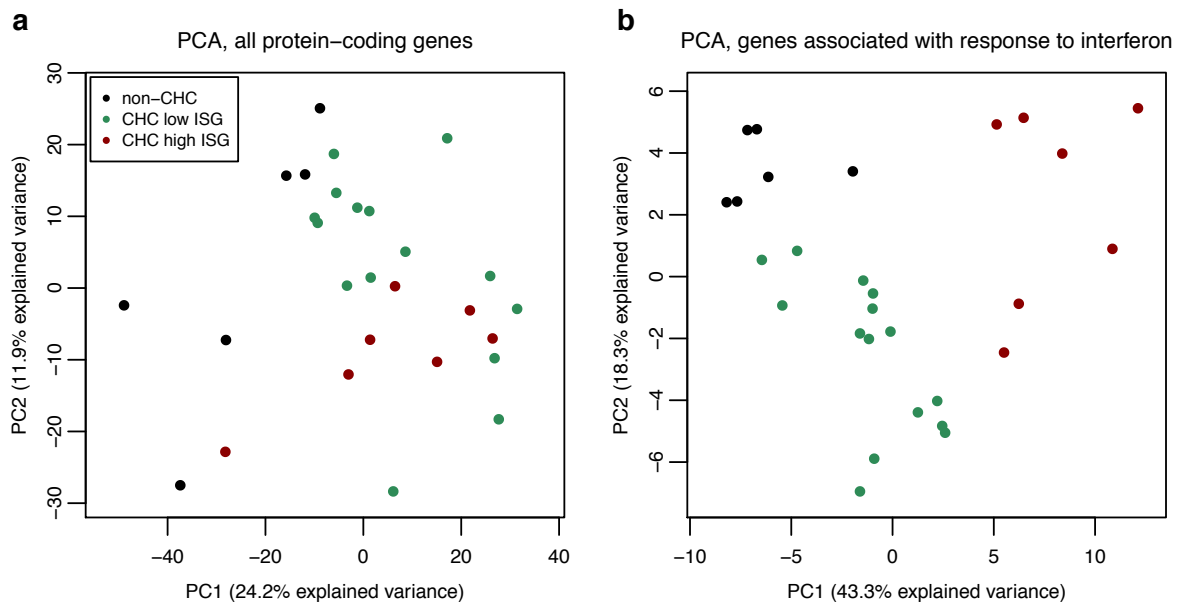


a. Dot-chart representing the expression changes of 11 miRNA host genes following pegIFNa treatment, at different time points. Red: significant changes, FDR<0.05; orange: FDR between 0.05 and 0.1; black: FDR>0.1.

b. RNA-seq coverage profiles along the miR-122 host gene, for pre-treatment and post-treatment biopsies at the 16h time point, for the three analyzed individuals (here termed I1, I2 and I3). Gray: normalized read coverage for baseline/pre-treatment biopsies. Black: normalized read coverage for post-treatment biopsies. Red: positive difference between post-treatment and pre-treatment biopsies. Green: negative difference between post-treatment and pre-treatment biopsies.

c. Dot-chart of the median fold expression change following pegIFNa/ribavirin treatment at the 16h time point, for predicted targets of miRNAs whose hosts are down-regulated (red dots) or of other miRNAs (black dots). We show 57 miRNA families with at least 100 conserved target genes. As a control, we show the median fold expression change for all genes predicted to be targets of any liver-expressed miRNAs or of genes not predicted to be targeted by these miRNAs (blue dots). The horizontal bars represent 95% confidence intervals of the median, constructed with a bootstrap resampling approach (Methods). Only miRNAs with high expression in normal or HCV-infected liver were analyzed (Hou et al, 2011). Evolutionarily conserved miRNA target predictions were extracted from TargetScan v7.1 (Agarwal et al, 2015) (Methods).

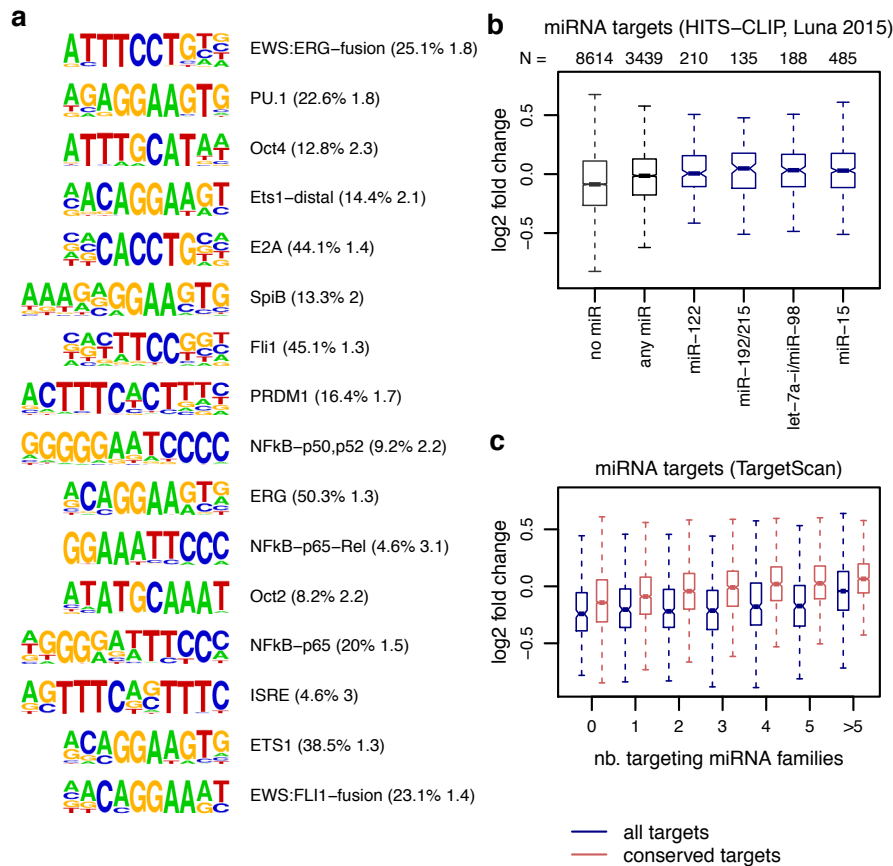
Supplementary Figure 1.



a. Principal component analysis (PCA) of protein-coding gene expression levels, for untreated CHC and control samples. The log₂-transformed RPKM levels of all expressed protein-coding genes were used as input for the PCA (Methods). Black: non-CHC; green: CHC low ISG; red: CHC high ISG samples.

b. Same as **a**, for protein-coding genes associated with “response to interferon” Gene Ontology terms (Methods).

Supplementary Figure 2.

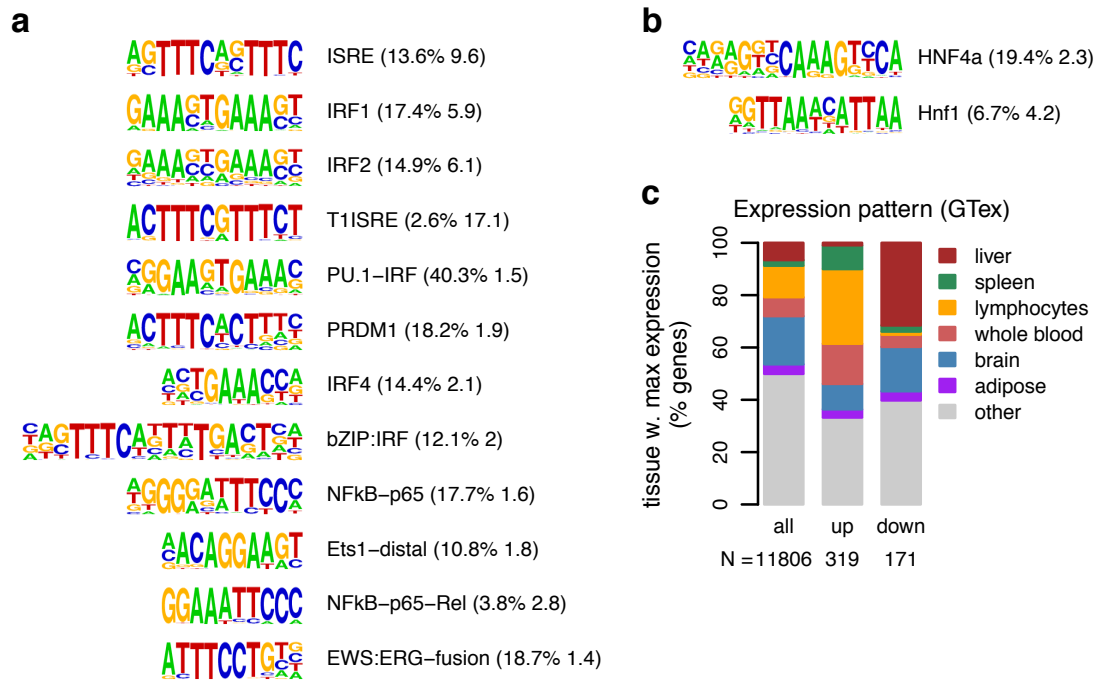


a. Results of the Homer transcription factor binding enrichment analysis (Methods), for protein-coding genes that are up-regulated in CHC low ISG compared to control non-CHC samples. The numbers in parentheses represent the percentage of genes that have this motif in the promoter region and the estimated enrichment with respect to the genomic background.

b. Boxplots of the intensity of the expression change (\log_2 fold) between non-CHC patients and CHC low ISG patients, for different categories of protein-coding genes defined based on the miRNAs that are predicted to target them. Target predictions were determined with HITS-CLIP in Huh7 cells (Luna et al, 2015). From left to right: genes that are not conserved targets of any expressed miRNA; genes that are targeted by at least one expressed miRNA; genes that are targeted by miR-122-5p, miR-192/215, let7a-i/miR-98 and miR-15, respectively.

c. Boxplots of the intensity of the expression change (\log_2 fold) between non-CHC patients and CHC low ISG patients, for different categories of protein-coding genes defined based on the number of miRNA families that are predicted to target them. Only miRNAs with high expression in normal or HCV-infected liver were analyzed (Hou et al, 2011). Evolutionarily conserved miRNA target predictions were extracted from TargetScan v7.1 (Agarwal et al, 2015) (Methods).

Supplementary Figure 3.

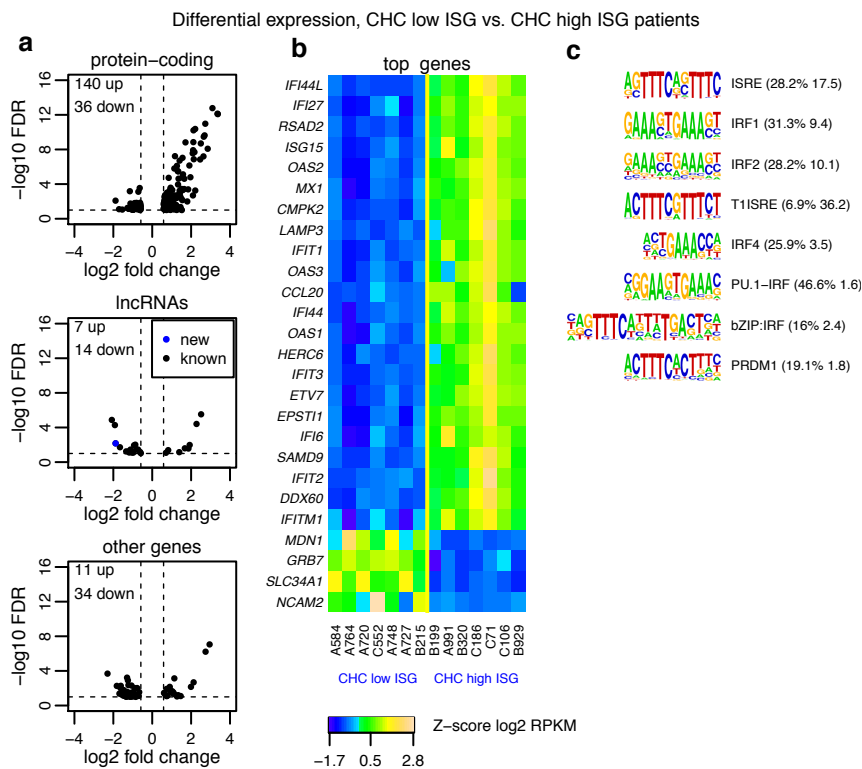


a. Results of the Homer transcription factor binding enrichment analysis (Methods), for protein-coding genes that are up-regulated in CHC high ISG compared to control non-CHC samples. The numbers in parentheses represent the percentage of genes that have this motif in the promoter region and the estimated enrichment with respect to the genomic background.

b. Same as **a**, for genes down-regulated in CHC high ISG compared to control non-CHC samples.

c. Barplots representing the expression patterns of three categories of genes (all expressed genes, genes up-regulated in CHC high ISG patients, and genes down-regulated in CHC high ISG patients compared to control non-CHC samples), in the GTEx tissue transcriptome collection. For each expressed gene, we scored the tissue or cell type in which its maximum expression level was reached. The height of the rectangles represents the percentage of genes that reaches maximum expression in each of the tissues.

Supplementary Figure 4.

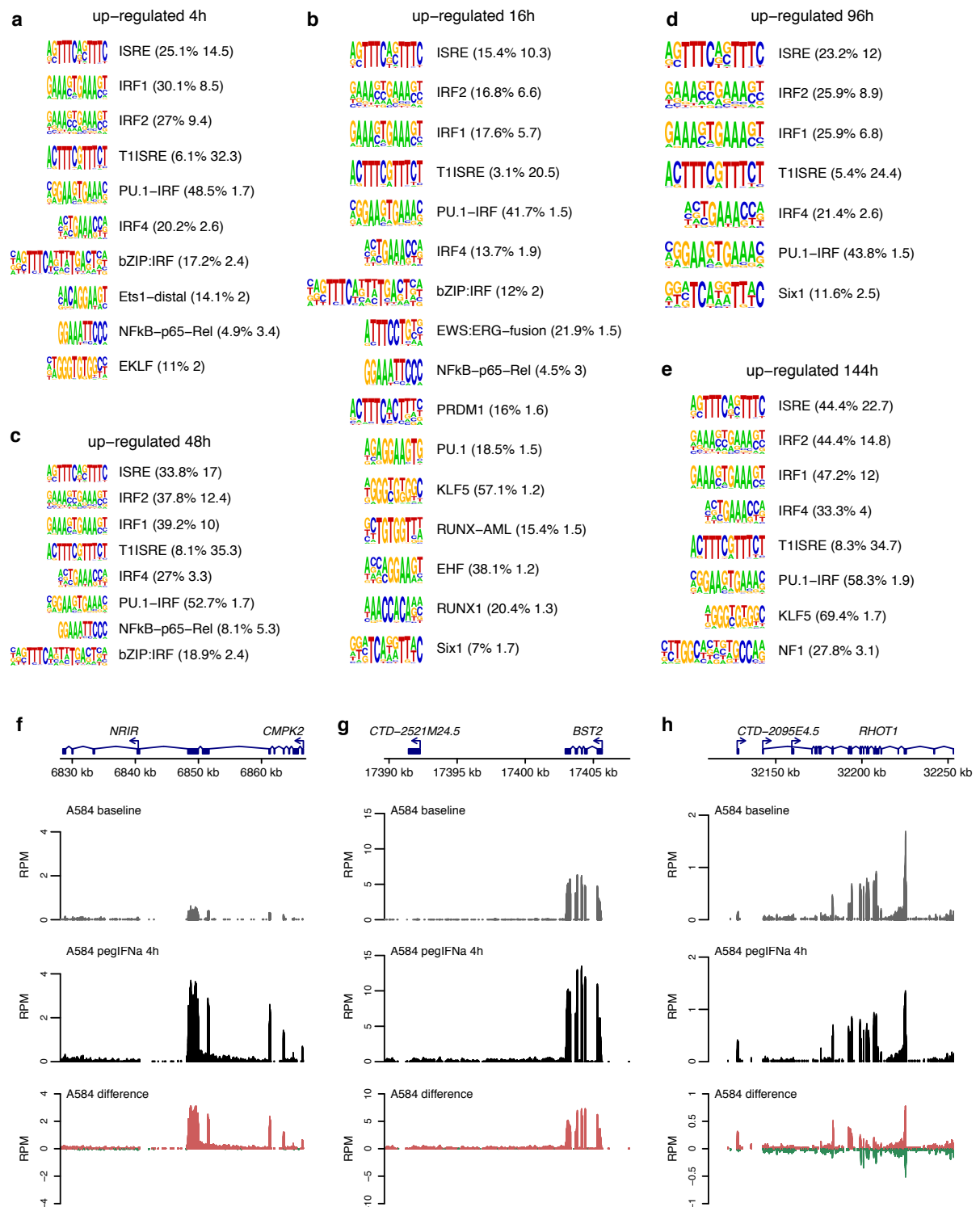


a. Volcano plot for the differential expression analysis between CHC patients with low levels of endogenous ISG activation (CHC low ISG) and CHC patients with high levels of endogenous ISG activation (CHC high ISG). The X-axis represents the log₂ fold expression change in CHC high ISG compared to CHC low patients. The Y-axis represents the false discovery rate (with a -log₁₀ transformation) of the differential expression test. Protein-coding genes, candidate long non-coding RNAs (lncRNAs) and other gene categories (including pseudogenes and transcripts with unclear coding potential, Methods) are represented separately. Only genes with false discovery rate (FDR) < 10% and with fold expression change > 1.5 are shown.

b. Heatmap of the expression patterns of the top differentially expressed genes between CHC low ISG and CHC high ISG patients. To select the top differentially expressed genes, we set a minimum absolute fold change threshold of 3.5 for up-regulated genes and of 2 for down-regulated genes. The heatmap represents the Z-score of the log₂-transformed RPKM (reads per kilobase of exon per million mapped reads) gene expression levels, normalized based on housekeeping genes (Methods).

c. Results of the Homer transcription factor binding enrichment analysis (Methods), for protein-coding genes that are up-regulated in CHC high ISG compared to CHC low ISG samples. The numbers in parentheses represent the percentage of genes that have this motif in the promoter region and the estimated enrichment with respect to the genomic background.

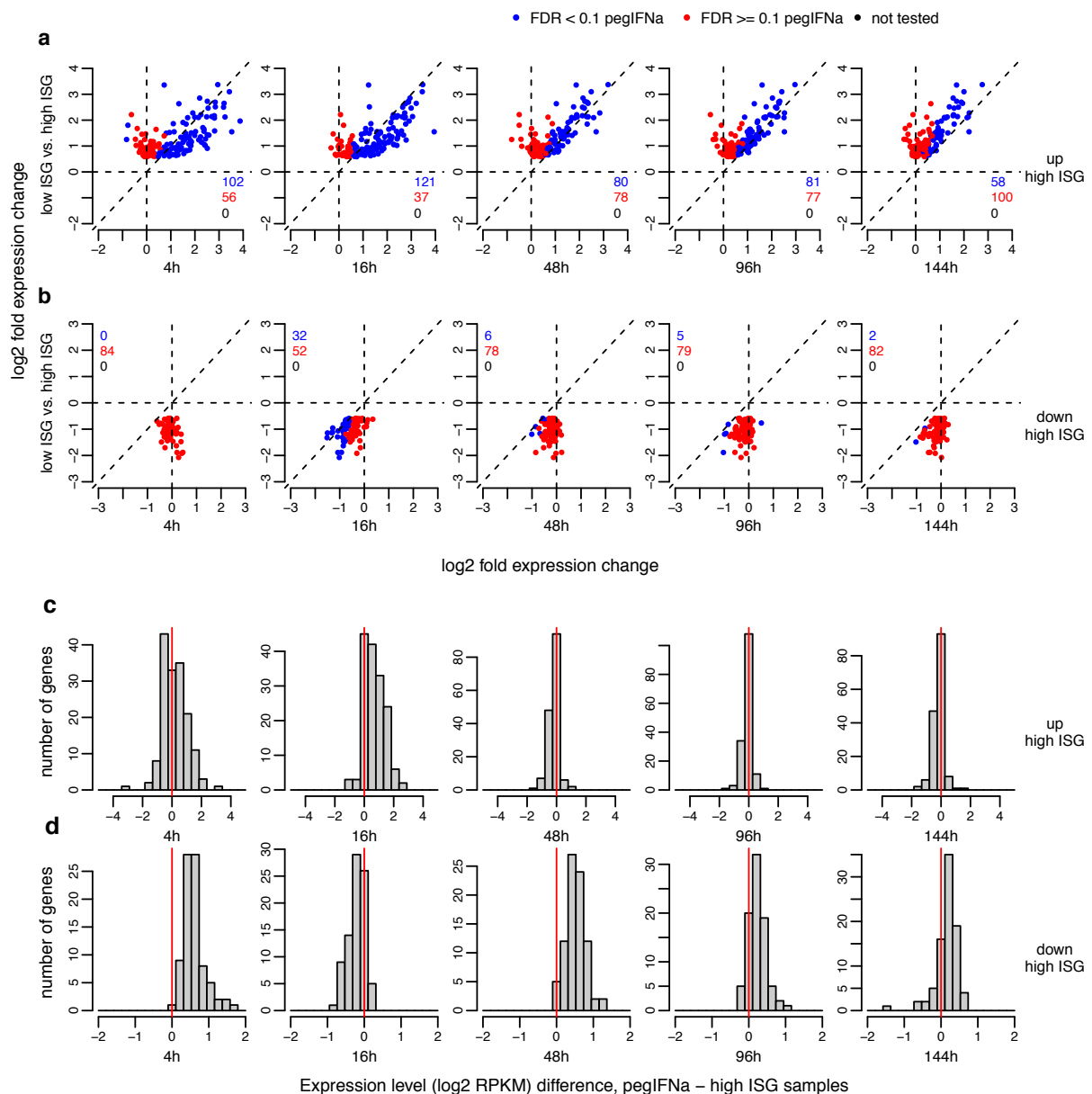
Supplementary Figure 5.



a. Results of the Homer transcription factor binding enrichment analysis (Methods), for protein-coding genes that are up-regulated following 4h of pegIFNa/ribavirin treatment. The numbers in parentheses represent the percentage of genes that have this motif in the promoter region and the estimated enrichment with respect to the genomic background.

- b.** Same as **a**, for genes that are up-regulated following 16h of pegIFNa/ribavirin treatment.
- c.** Same as **a**, for genes that are up-regulated following 48h of pegIFNa/ribavirin treatment.
- d.** Same as **a**, for genes that are up-regulated following 96h of pegIFNa/ribavirin treatment.
- e.** Same as **a**, for genes that are up-regulated following 144h of pegIFNa/ribavirin treatment.
- f.** RNA-seq profiles along the *NRIR* lncRNA, for pre-treatment and post-treatment biopsies at the 4h time point. Gray: normalized read coverage for baseline/pre-treatment biopsies. Black: normalized read coverage for post-treatment biopsies. Red: positive difference between post-treatment and pre-treatment biopsies. Green: negative difference between post-treatment and pre-treatment biopsies.
- g.** Same as **f**, for the lncRNA *CTD-2521M24.5*.
- h.** Same as **f**, for the lncRNA *CTD-2095E4.5*.

Supplementary Figure 6.



a. Differential expression patterns of the genes that are significantly up-regulated (FDR < 0.1 and minimum absolute fold change 1.5) in CHC high ISG patients compared to CHC low ISG patients. Blue dots: genes also significantly differentially expressed following pegIFNa/ribavirin treatment (FDR < 0.05); red dots: genes significant only in the comparison between low ISG and high ISG samples; black dots: genes not tested in the pegIFNa/ribavirin comparison due to low or highly variable expression levels (Methods). X-axis: log₂ fold expression change in pegIFNa-treated compared to control biopsies. Y-axis: log₂ fold expression change in high ISG patients compared to low ISG patients. The numbers of the genes in each category are depicted on the plot area, with the same color code.

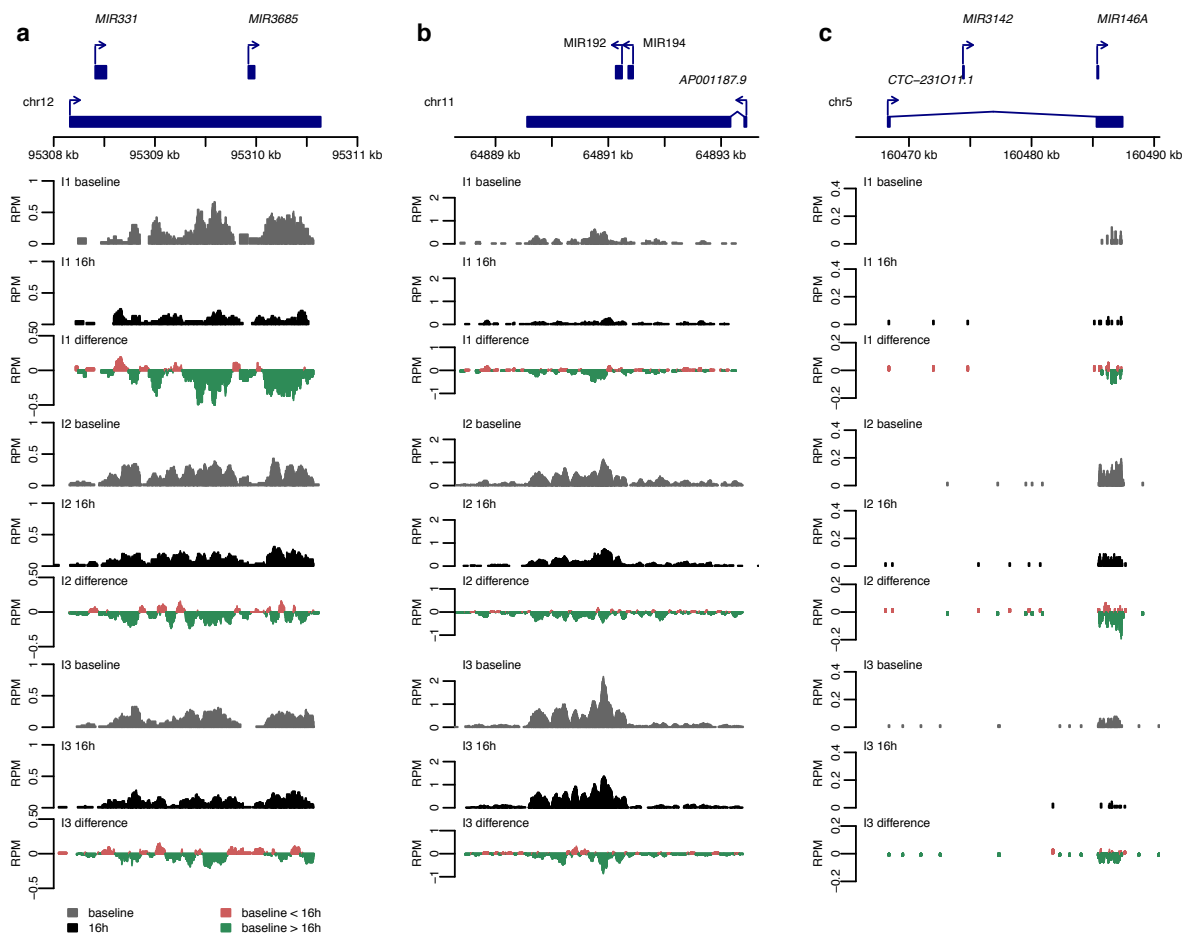
b. Similar to **a**, for genes that are significantly down-regulated (FDR < 0.1 and minimum absolute fold change 1.5) in CHC low ISG and CHC high ISG patients.

c. Histogram of the difference in expression levels (log₂-transformed RPKM) between samples treated with pegIFNa/ribavirin and CHC high ISG samples, for the genes that

are up-regulated (FDR < 0.1 and minimum absolute fold change 1.5) in CHC high ISG patients compared to CHC low ISG patients. The differences were computed between expression levels averaged across all relevant samples.

d. Similar to **c**, for genes that are significantly down-regulated (FDR < 0.1 and minimum absolute fold change 1.5) in CHC high ISG patients compared to CHC low ISG patients.

Supplementary Figure 7.



a. RNA-seq profiles along the miR-331/miR-3685 host gene, for pre-treatment and post-treatment biopsies at the 16h time point, for the three analyzed individuals (I1, I2 and I3). Gray: normalized read coverage for baseline/pre-treatment biopsies. Black: normalized read coverage for post-treatment biopsies. Red: positive difference between post-treatment and pre-treatment biopsies. Green: negative difference between post-treatment and pre-treatment biopsies.

b. Same as **a**, for the miR-192/miR-194 host gene.

c. Same as **a**, for the miR-146a host gene.

Supplementary Table Legends

Supplementary Table 1.

Biopsy No	Patient No	Age	Sex	Patient classification	HCV GT	Viral load, log IU/mL	METAVIR	Comment
A584	1	37	m	CHC low ISG	3	4.9	A1/F2	
A764	3	38	m	CHC low ISG	4	4.08	A2/F2	
A720	4	51	f	CHC low ISG	1	6.82	A1/F2	
C552	5	49	f	CHC low ISG	4	5.68	A2/F2	
A748	8	30	m	CHC low ISG	3	7.07	A2/F2	
A727	9	57	f	CHC low ISG	1	5.95	A2/F2	
B215	16	34	m	CHC low ISG	3	5.56	A2/F2	
A991	6	42	f	CHC high ISG	3	5.49	A1/F2	
B199	7	41	m	CHC high ISG	3	5.66	A1/F2	
B320	17	57	f	CHC high ISG	2	5.18	A2/F2	
B929	19	38	f	CHC high ISG	1	5.05	A1/F1	no therapy
C71	20	41	f	CHC high ISG	1	7.14	A1/F1	no therapy
C106	21	51	m	CHC high ISG	4	5.97	A1/F2	no therapy
C186	22	47	f	CHC high ISG	1	6.01	A1/F1	SVR 24 after triple therapy with pegIFN, Ribavirin and boceprevir
B986	23	49	m	control (non-CHC)				unclear hepatopathie, isolated GGT elevation, normal histology
C51a	24	63	f	control (non-CHC)				paired tumor and non-tumor biopsy, metastase of brest cancer, normal histology of non-tumor biopsy
C145	25	43	f	control (non-CHC)				unclear hepatopathie, isolated GGT elevation, normal histology
C173	26	62	m	control (non-CHC)				unclear hepatopathie, isolated GGT elevation, normal histology
C250a	27	80	m	control (non-CHC)				paired tumor and non-tumor biopsy, metastase of lung cancer, normal histology of non-tumor biopsy
C369	28	37	m	control (non-CHC)				unclear hepatopathie, isolated GGT elevation, normal histology

Biopsy No	Patient No	Patient No (Dill et al., JC, 2014)	Age	Sex	HCV GT	Viral load, log IU/mL			Response			METAVIR	Time point	Medication	
						Baseline	4-week	12-week	4-week	12-week	Follow-up				
A 584	A 584-2	1	2	37	m	3	4.9	neg	neg	RVR	CEVR	SVR	A1/F2	4h	pegIFN-α2b
A 609	A 609-2	2	3	54	f	2	4.95	neg	neg	RVR	CEVR	SVR	A3/F3	4h	pegIFN-α2b
A 764	A 764-2	3	5	38	m	4	4.08	1.66	neg	non-RVR	CEVR	SVR	A2/F2	4h	pegIFN-α2b
A 720	A 720-2	4	6	51	f	1	6.82	3.52	neg	non-RVR	CEVR	SVR	A1/F2	4h	pegIFN-α2b
C552	C591	5	-	49	f	4	5.68	2.75	neg	non-RVR	CEVR	ongoing	A2/F2	16h	pegIFN-α2b
A 991	A991-2	6	8	42	f	3	5.49	neg	neg	RVR	CEVR	SVR	A1/F2	16h	pegIFN-α2b
B 199	B 217	7	9	41	m	3	5.66	neg	neg	RVR	CEVR	SVR	A1/F2	16h	pegIFN-α2b
A 748	A 748-2	8	10	30	m	3	7.07	neg	neg	RVR	CEVR	SVR	A2/F2	48h	pegIFN-α2b
A 727	A 727-2	9	11	57	f	1	5.95	neg	neg	RVR	CEVR	SVR	A2/F2	48h	pegIFN-α2b
B 254	B 284	10	12	37	m	3	6.72	1.28	neg	non-RVR	CEVR	SVR	A3/F2	48h	pegIFN-α2b
A 616	A 616-2	11	13	62	m	4	7.16	neg	neg	RVR	CEVR	SVR	A3/F4	96h	pegIFN-α2b
B 136	B 178	12	14	43	m	1	5.6	1.63	neg	non-RVR	CEVR	SVR	A3/F2	96h	pegIFN-α2b
B 283	B 304	13	15	40	m	1	5.16	1.41	neg	non-RVR	CEVR	SVR	A3/F4	96h	pegIFN-α2b
A 707	A 707-2	14	16	25	f	1	2.64	neg	neg	RVR	CEVR	SVR	A2/F2	144h	pegIFN-α2b
A 972	A 972-2	15	17	70	m	2	6.86	1.84	neg	non-RVR	CEVR	SVR	A2/F3	144h	pegIFN-α2b
B 215	B 247	16	18	34	m	3	5.56	neg	neg	RVR	CEVR	SVR	A2/F2	144h	pegIFN-α2b
B 320	B 371	17	19	57	f	2	5.18	neg	neg	RVR	CEVR	SVR	A2/F2	144h	pegIFN-α2b
B 346	B 401	18	20	57	m	1	6.54	4.59	3.33	non-RVR	EV	Interrupted	A3/F4	144h	pegIFN-α2b

This table describes the patient characteristics. The first Excel sheet ("Patients - endogenous ISG") contains the characteristics of the patients classified as "CHC low ISG", "CHC high ISG" and of control (non-CHC) patients. The second Excel sheet presents the characteristics of the patients analyzed in the pegIFNa time series.

Supplementary Table 2.

This table presents the results of the differential expression analyses comparing control non-CHC samples, CHC low ISG samples and CHC high ISG samples. Each analysis is presented in a separate Excel sheet.

Supplementary Table 3.

This table provides the gene ontology enrichment results for the comparison between non-CHC patients, CHC low ISG and CHC high ISG patients. These results were obtained with GOrilla (Eden et al., Bioinformatics, 2009). The enrichment test was performed only for the "biological process" GO category.

Supplementary Table 4.

This table provides information regarding the set of liver-expressed miRNAs and their targets predicted by TargetScan that we analyzed in this manuscript (Methods). We also provide miRNA target predictions from a previous publication (Luna et al, 2015) in a separate Excel sheet.

Supplementary Table 5.

This table presents a comparison between genes that are differentially expressed following HCV infection in Huh7.5 cells (previously published dataset (Walters et al, 2009)) and those that we found to be differentially expressed following HCV infection in liver biopsies.

Supplementary Table 6.

This table presents the results of the differential expression analyses comparing pre-treatment and post-treatment biopsies at different time points during the pegIFNa/ribavirin treatment. Each analysis is presented in a separate Excel sheet.

Supplementary Table 7.

This table provides the gene ontology enrichment results for the differential expression analyses comparing pre-treatment and post-treatment biopsies at different time points during the pegIFNa/ribavirin treatment. Each analysis is presented in a separate Excel sheet.

Supplementary Table 8.

This table provides the list of genes that are differentially expressed following IFNa treatment, at one or more time points. For each gene, we extract the time-points in which it is up-regulated or down-regulated.

Supplementary Table 9.

This table provides a comparison between genes that are differentially expressed between low ISG and high ISG patients and following pegIFNa/ribavirin treatment, at different time points.

Supplementary Table 10.

This table presents the results of the differential expression analyses (between low ISG and high ISG patients, or following pegIFNa/ribavirin treatment biopsies) for lists of genes previously shown to have a negative effect on HCV replication in Huh7.5 cells (Metz et al, 2013; Schoggins et al, 2011).

Supplementary Table 11.

This table presents the list of miRNA host genes analyzed in this manuscript, highlighting those that are differentially expressed following pegIFNa/ribavirin treatment (FDR<0.05).

References

- Agarwal V, Bell GW, Nam JW, Bartel DP (2015) Predicting effective microRNA target sites in mammalian mRNAs. *eLife* **4**
- Altschul SF, Gish W, Miller W, Myers EW, Lipman DJ (1990) Basic local alignment search tool. *Journal of molecular biology* **215**: 403-410
- Asselah T, Bieche I, Narguet S, Sabbagh A, Laurendeau I, Ripault MP, Boyer N, Martinot-Peignoux M, Valla D, Vidaud M, Marcellin P (2008) Liver gene expression signature to predict response to pegylated interferon plus ribavirin combination therapy in patients with chronic hepatitis C. *Gut* **57**: 516-524
- Bedossa P, Poinard T (1996) An algorithm for the grading of activity in chronic hepatitis C. The METAVIR Cooperative Study Group. *Hepatology* **24**: 289-293
- Bibert S, Roger T, Calandra T, Bochud M, Cerny A, Semmo N, Duong FH, Gerlach T, Malinverni R, Moradpour D, Negro F, Mullhaupt B, Bochud PY, Swiss Hepatitis CCS (2013) IL28B expression depends on a novel TT/-G polymorphism which improves HCV clearance prediction. *The Journal of experimental medicine* **210**: 1109-1116
- Bigger CB, Guerra B, Brasky KM, Hubbard G, Beard MR, Luxon BA, Lemon SM, Lanford RE (2004) Intrahepatic gene expression during chronic hepatitis C virus infection in chimpanzees. *Journal of virology* **78**: 13779-13792
- Brawand D, Soumillon M, Necsulea A, Julien P, Csardi G, Harrigan P, Weier M, Liechti A, Aximu-Petri A, Kircher M, Albert FW, Zeller U, Khaitovich P, Grutzner F, Bergmann S, Nielsen R, Paabo S, Kaessmann H (2011) The evolution of gene expression levels in mammalian organs. *Nature* **478**: 343-348
- Cabili MN, Trapnell C, Goff L, Koziol M, Tazon-Vega B, Regev A, Rinn JL (2011) Integrative annotation of human large intergenic noncoding RNAs reveals global properties and specific subclasses. *Genes & development* **25**: 1915-1927
- Chen L, Borozan I, Feld J, Sun J, Tannis LL, Coltescu C, Heathcote J, Edwards AM, McGilvray ID (2005) Hepatic gene expression discriminates responders and nonresponders in treatment of chronic hepatitis C viral infection. *Gastroenterology* **128**: 1437-1444
- Colpitts CC, El-Saghire H, Pochet N, Schuster C, Baumert TF (2015) High-throughput approaches to unravel hepatitis C virus-host interactions. *Virus Res*
- Cunningham F, Amode MR, Barrell D, Beal K, Billis K, Brent S, Carvalho-Silva D, Clapham P, Coates G, Fitzgerald S, Gil L, Giron CG, Gordon L, Hourlier T, Hunt SE, Janacek SH, Johnson N, Juettemann T, Kahari AK, Keenan S, Martin FJ, Maurel T, McLaren W, Murphy DN, Nag R, Overduin B, Parker A, Patricio M, Perry E, Pignatelli M, Riat HS, Sheppard D, Taylor K, Thormann A, Vullo A, Wilder SP, Zadissa A, Aken BL, Birney E, Harrow J, Kinsella R, Muffato M, Ruffier M, Searle SM, Spudich G, Trevanion SJ, Yates A, Zerbino DR, Flicek P (2015) Ensembl 2015. *Nucleic acids research* **43**: D662-669

Dill MT, Duong FH, Vogt JE, Bibert S, Bochud PY, Terracciano L, Papassotiropoulos A, Roth V, Heim MH (2011) Interferon-induced gene expression is a stronger predictor of treatment response than IL28B genotype in patients with hepatitis C. *Gastroenterology* **140**: 1021-1031

Dill MT, Makowska Z, Trincucci G, Gruber AJ, Vogt JE, Filipowicz M, Calabrese D, Krol I, Lau DT, Terracciano L, van Nimwegen E, Roth V, Heim MH (2014) Pegylated IFN-alpha regulates hepatic gene expression through transient Jak/STAT activation. *The Journal of clinical investigation* **124**: 1568-1581

Eden E, Navon R, Steinfeld I, Lipson D, Yakhini Z (2009) GOrilla: a tool for discovery and visualization of enriched GO terms in ranked gene lists. *BMC bioinformatics* **10**: 48

Finn RD, Bateman A, Clements J, Coggill P, Eberhardt RY, Eddy SR, Heger A, Hetherington K, Holm L, Mistry J, Sonnhammer EL, Tate J, Punta M (2014) Pfam: the protein families database. *Nucleic acids research* **42**: D222-230

Hamming OJ, Terczynska-Dyla E, Vieyres G, Dijkman R, Jorgensen SE, Akhtar H, Siupka P, Pietschmann T, Thiel V, Hartmann R (2013) Interferon lambda 4 signals via the IFNlambda receptor to regulate antiviral activity against HCV and coronaviruses. *The EMBO journal* **32**: 3055-3065

Heim MH (2013) 25 years of interferon-based treatment of chronic hepatitis C: an epoch coming to an end. *Nature reviews Immunology* **13**: 535-542

Heim MH, Thimme R (2014) Innate and adaptive immune responses in HCV infections. *Journal of hepatology* **61**: S14-S25

Heinz S, Benner C, Spann N, Bertolino E, Lin YC, Laslo P, Cheng JX, Murre C, Singh H, Glass CK (2010) Simple combinations of lineage-determining transcription factors prime cis-regulatory elements required for macrophage and B cell identities. *Molecular cell* **38**: 576-589

Ho BC, Yu IS, Lu LF, Rudensky A, Chen HY, Tsai CW, Chang YL, Wu CT, Chang LY, Shih SR, Lin SW, Lee CN, Yang PC, Yu SL (2014) Inhibition of miR-146a prevents enterovirus-induced death by restoring the production of type I interferon. *Nature communications* **5**: 3344

Hou J, Lin L, Zhou W, Wang Z, Ding G, Dong Q, Qin L, Wu X, Zheng Y, Yang Y, Tian W, Zhang Q, Wang C, Zhang Q, Zhuang SM, Zheng L, Liang A, Tao W, Cao X (2011) Identification of miRNomes in human liver and hepatocellular carcinoma reveals miR-199a/b-3p as therapeutic target for hepatocellular carcinoma. *Cancer cell* **19**: 232-243

Hou J, Wang P, Lin L, Liu X, Ma F, An H, Wang Z, Cao X (2009) MicroRNA-146a feedback inhibits RIG-I-dependent Type I IFN production in macrophages by targeting TRAF6, IRAK1, and IRAK2. *Journal of immunology* **183**: 2150-2158

Ikushima H, Negishi H, Taniguchi T (2013) The IRF family transcription factors at the interface of innate and adaptive immune responses. *Cold Spring Harbor symposia on quantitative biology* **78**: 105-116

Jopling CL, Norman KL, Sarnow P (2006) Positive and negative modulation of viral and cellular mRNAs by liver-specific microRNA miR-122. *Cold Spring Harbor symposia on quantitative biology* **71**: 369-376

Jopling CL, Yi M, Lancaster AM, Lemon SM, Sarnow P (2005) Modulation of hepatitis C virus RNA abundance by a liver-specific MicroRNA. *Science* **309**: 1577-1581

Kambara H, Niazi F, Kostadinova L, Moonka DK, Siegel CT, Post AB, Carnero E, Barriocanal M, Fortes P, Anthony DD, Valadkhan S (2014) Negative regulation of the interferon response by an interferon-induced long non-coding RNA. *Nucleic acids research* **42**: 10668-10680

Kim D, Pertea G, Trapnell C, Pimentel H, Kelley R, Salzberg SL (2013) TopHat2: accurate alignment of transcriptomes in the presence of insertions, deletions and gene fusions. *Genome biology* **14**: R36

Langmead B, Salzberg SL (2012) Fast gapped-read alignment with Bowtie 2. *Nature methods* **9**: 357-359

Lavanchy D (2011) Evolving epidemiology of hepatitis C virus. *Clin Microbiol Infect* **17**: 107-115

Lin MF, Carlson JW, Crosby MA, Matthews BB, Yu C, Park S, Wan KH, Schroeder AJ, Gramates LS, St Pierre SE, Roark M, Wiley KL, Jr., Kulathinal RJ, Zhang P, Myrick KV, Antone JV, Celniker SE, Gelbart WM, Kellis M (2007) Revisiting the protein-coding gene catalog of *Drosophila melanogaster* using 12 fly genomes. *Genome research* **17**: 1823-1836

Lin MF, Jungreis I, Kellis M (2011) PhyloCSF: a comparative genomics method to distinguish protein coding and non-coding regions. *Bioinformatics* **27**: i275-282

Lindenbach BD, Evans MJ, Syder AJ, Wolk B, Tellinghuisen TL, Liu CC, Maruyama T, Hynes RO, Burton DR, McKeating JA, Rice CM (2005) Complete replication of hepatitis C virus in cell culture. *Science* **309**: 623-626

Love MI, Huber W, Anders S (2014) Moderated estimation of fold change and dispersion for RNA-seq data with DESeq2. *Genome biology* **15**: 550

Luna JM, Scheel TK, Danino T, Shaw KS, Mele A, Fak JJ, Nishiuchi E, Takacs CN, Catanese MT, de Jong YP, Jacobson IM, Rice CM, Darnell RB (2015) Hepatitis C virus RNA functionally sequesters miR-122. *Cell* **160**: 1099-1110

Mele M, Ferreira PG, Reverter F, DeLuca DS, Monlong J, Sammeth M, Young TR, Goldmann JM, Pervouchine DD, Sullivan TJ, Johnson R, Segre AV, Djebali S, Niarchou A, Consortium GT, Wright FA, Lappalainen T, Calvo M, Getz G, Dermitzakis ET, Ardlie KG,

- Guigo R (2015) Human genomics. The human transcriptome across tissues and individuals. *Science* **348**: 660-665
- Metz P, Dazert E, Ruggieri A, Mazur J, Kaderali L, Kaul A, Zeuge U, Windisch MP, Trippler M, Lohmann V, Binder M, Frese M, Bartenschlager R (2012) Identification of type I and type II interferon-induced effectors controlling hepatitis C virus replication. *Hepatology* **56**: 2082-2093
- Metz P, Reuter A, Bender S, Bartenschlager R (2013) Interferon-stimulated genes and their role in controlling hepatitis C virus. *Journal of hepatology* **59**: 1331-1341
- Motawi TK, Shaker OG, El-Maraghy SA, Senousy MA (2015) Serum interferon-related microRNAs as biomarkers to predict the response to interferon therapy in chronic hepatitis C genotype 4. *PloS one* **10**: e0120794
- Necsulea A, Soumillon M, Warnefors M, Liechti A, Daish T, Zeller U, Baker JC, Grutzner F, Kaessmann H (2014) The evolution of lncRNA repertoires and expression patterns in tetrapods. *Nature* **505**: 635-640
- Pedersen IM, Cheng G, Wieland S, Volinia S, Croce CM, Chisari FV, David M (2007) Interferon modulation of cellular microRNAs as an antiviral mechanism. *Nature* **449**: 919-922
- Prokunina-Olsson L, Muchmore B, Tang W, Pfeiffer RM, Park H, Dickensheets H, Hergott D, Porter-Gill P, Mumy A, Kohaar I, Chen S, Brand N, Tarway M, Liu L, Sheikh F, Astemborski J, Bonkovsky HL, Edlin BR, Howell CD, Morgan TR, Thomas DL, Rehermann B, Donnelly RP, O'Brien TR (2013) A variant upstream of IFNL3 (IL28B) creating a new interferon gene IFNL4 is associated with impaired clearance of hepatitis C virus. *Nature genetics* **45**: 164-171
- Rosenbloom KR, Armstrong J, Barber GP, Casper J, Clawson H, Diekhans M, Dreszer TR, Fujita PA, Guruvadoo L, Haeussler M, Harte RA, Heitner S, Hickey G, Hinrichs AS, Hubley R, Karolchik D, Learned K, Lee BT, Li CH, Miga KH, Nguyen N, Paten B, Raney BJ, Smit AF, Speir ML, Zweig AS, Haussler D, Kuhn RM, Kent WJ (2015) The UCSC Genome Browser database: 2015 update. *Nucleic acids research* **43**: D670-681
- Sarasin-Filipowicz M, Krol J, Markiewicz I, Heim MH, Filipowicz W (2009) Decreased levels of microRNA miR-122 in individuals with hepatitis C responding poorly to interferon therapy. *Nat Med* **15**: 31-33
- Sarasin-Filipowicz M, Oakeley EJ, Duong FH, Christen V, Terracciano L, Filipowicz W, Heim MH (2008) Interferon signaling and treatment outcome in chronic hepatitis C. *Proc Natl Acad Sci U S A* **105**: 7034-7039
- Schoggins JW, Wilson SJ, Panis M, Murphy MY, Jones CT, Bieniasz P, Rice CM (2011) A diverse range of gene products are effectors of the type I interferon antiviral response. *Nature* **472**: 481-485
- Stiffler JD, Nguyen M, Sohn JA, Liu C, Kaplan D, Seeger C (2009) Focal distribution of hepatitis C virus RNA in infected livers. *PloS one* **4**: e6661

Terczynska-Dyla E, Bibert S, Duong FH, Krol I, Jorgensen S, Collinet E, Kutalik Z, Aubert V, Cerny A, Kaiser L, Malinverni R, Mangia A, Moradpour D, Mullhaupt B, Negro F, Santoro R, Semela D, Semmo N, Swiss Hepatitis CCSG, Heim MH, Bochud PY, Hartmann R, Swiss Hepatitis CCSG (2014) Reduced IFNlambda4 activity is associated with improved HCV clearance and reduced expression of interferon-stimulated genes. *Nature communications* **5**: 5699

Trapnell C, Williams BA, Pertea G, Mortazavi A, Kwan G, van Baren MJ, Salzberg SL, Wold BJ, Pachter L (2010) Transcript assembly and quantification by RNA-Seq reveals unannotated transcripts and isoform switching during cell differentiation. *Nature biotechnology* **28**: 511-515

UniProt C (2015) UniProt: a hub for protein information. *Nucleic acids research* **43**: D204-212

Vilella AJ, Severin J, Ureta-Vidal A, Heng L, Durbin R, Birney E (2009) EnsemblCompara GeneTrees: Complete, duplication-aware phylogenetic trees in vertebrates. *Genome research* **19**: 327-335

Wakita T, Pietschmann T, Kato T, Date T, Miyamoto M, Zhao Z, Murthy K, Habermann A, Krausslich HG, Mizokami M, Bartenschlager R, Liang TJ (2005) Production of infectious hepatitis C virus in tissue culture from a cloned viral genome. *Nat Med* **11**: 791-796

Walters KA, Syder AJ, Lederer SL, Diamond DL, Paeper B, Rice CM, Katze MG (2009) Genomic analysis reveals a potential role for cell cycle perturbation in HCV-mediated apoptosis of cultured hepatocytes. *PLoS Pathog* **5**: e1000269

Wieland S, Makowska Z, Campana B, Calabrese D, Dill MT, Chung J, Chisari FV, Heim MH (2014) Simultaneous detection of hepatitis C virus and interferon stimulated gene expression in infected human liver. *Hepatology* **59**: 2121-2130

Zhong J, Gastaminza P, Cheng G, Kapadia S, Kato T, Burton DR, Wieland SF, Uprichard SL, Wakita T, Chisari FV (2005) Robust hepatitis C virus infection in vitro. *Proc Natl Acad Sci USA* **102**: 9294-9299

4. Conclusion

In the liver, cell-intrinsic adaptive changes to HCV infections are difficult to detect because of the gene expression changes induced by the innate immune response, mainly through IFNs, can mask the more subtle cell-intrinsic changes induced by HCV directly in infected cells. Due to a genetic polymorphism in the IFNL4 gene, ISG induction in humans is highly variable^{110, 116}. To specifically identify dysregulated genes other than IFN stimulated genes, we selected a set of liver biopsies from patients without endogenous ISG induction and compared gene expression in these “ISG low” samples with global gene expression in a set of control samples from non-infected patients with a normal liver. We found that gene expression changes between uninfected liver samples and biopsies without detectable ISG expression mainly reflect the presence of immune cell infiltrates in the latter group. Contrary to our expectations, we could not detect expression changes of genes involved in cellular responses to HCV described in cell culture. For example, a previous large-scale analysis of differential gene expression in HCV-infected Huh-7.5 cells revealed that 860 genes showed a 2-fold or higher change in expression. Gene ontology analysis revealed that many of them are involved in DNA damage/oxidative stress response, cytochrome c release, cell death, cell cycle and cytokine/growth factor signalling¹²². Unlike this *in vitro* analysis, our *in vivo* differential expression analyses did not reveal enrichments for these functional categories of genes. Using a targeted approach by specifically analysing genes previously reported to be changed in HCV-infected Huh-7.5 cells¹²², we could indeed identify a core set of 25 genes that are differentially expressed following HCV infection in both Huh 7.5 cells and in liver samples from patients without IFN system activation. This common gene set included several cell cycle associated genes, such as *UBD*, *ITIH1* and *BIRC3*. 25 out of 860 genes seems to be a very low number, but statistical analysis of the data revealed that this is significantly more than expected by chance alone. We conclude that our *in vivo* analysis confirms the induction of a small but significant number of genes that have been described to be induced by HCV in cell culture experiments. The huge differences between *in vivo* and *in vitro* could be due to the very high viral concentration in cell culture: the number of HCV virions per infected cell is between 1 and 8 in the human liver, but can be as high as 500 to 1000 in the Huh-7.5 cell culture model. Moreover only 1-55% of the hepatocytes in the human liver are HCV positive¹⁰⁹. Therefore, changes in

infected hepatocytes could be masked by unchanged gene expression in non-infected hepatocytes and non-parenchymal liver cells.

The second aim of the work was to characterize IFN stimulated changes in the liver transcriptome of patients with chronic hepatitis C (CHC) and an activated endogenous IFN system. To do this, we contrasted gene expression levels between non-CHC control samples and CHC samples with high ISG expression (“ISG high”). We observed 503 protein-coding genes, 80 candidate long non-coding RNAs and 125 other genes differentially expressed genes in the latter group. As expected, the most highly up-regulated protein-coding genes were known ISGs. The up-regulated long non-coding RNAs included a previously described interferon-inducible transcript, *NRIR*¹²³. However, most of the lnc RNAs have not been described previously in the context of HCV infections, and their function, if any, remains to be explored.

The third aim of the work addressed a longstanding conundrum in the field: Despite a strong induction of hundreds of ISGs the endogenous IFN system is ineffective against HCV, whereas therapies with pegIFN α were curative in many patients. Two alternative explanations were explored: Either some critical ISGs are exclusively induced by pegIFN α , or pegIFN α induces the same ISGs but at a higher level than the endogenous IFNs. Our data clearly indicate that the second explanation is more likely. The same set of ISGs was induced by pegIFN α and the endogenous IFN system, but with lower induction levels in the latter.

The fourth aim of the study was to characterize the expression dynamics of non-coding genes, including long non-coding RNAs and miRNA transcripts in response to HCV infections and to pegIFN α treatments. Our analysis revealed that numerous non-coding transcripts are down-regulated, in particular at the 16h time point. These down-regulated genes include 11 miRNA “host” genes. Most interesting of them is miR-122, because it is an essential host factor for HCV replication²⁹. Detailed functional experiments in Huh7 cells brought evidence that HCV infection leads to significant depression of miR-122 target genes due to this sponging effect¹. At first sight, our *in vivo* transcriptomic analysis appeared to confirm this observation, as miR-122 target genes had higher expression levels in HCV-infected compared to control biopsies. However, a closer look revealed the same pattern for other miRNAs highly expressed in the liver

(e.g., miR-192, let-7). Because HCV does not bind these other miRNAs, this observation cannot be simply explained by a sponging effect.

It has been reported, that hundreds of lncRNAs are induced by pegIFN α treatment in Huh7 cells¹²⁴ and PHH¹²³. RNA-Seq analysis of Huh7 cells infected with the JFH-1 strain of HCV revealed that the expression of more than 500 lncRNAs is altered in infected cells¹²⁵. We could not confirm this huge impact of HCV on lncRNA expression *in vivo*. In our analysis we found only 14 lncRNAs in “ISG low” and 80 lncRNAs, including the previously published NRIR¹²³ in “ISG high” samples to be altered upon HCV infection. Moreover, even in the samples with maximal stimulation during pegIFN α treatment, only 88 lncRNAs were differentially expressed. As with cell-intrinsic changes discussed above, a possible explanation lies in the massive “over-infection” of cells present in the fully infectious HCV cell culture system. In addition, these differences between *in vitro* and *in vivo* experiments could also result from a different definition of lncRNAs, since we used very stringent criteria. To avoid annotating alternative un-translated regions or introns of protein-coding genes as independent lncRNAs, we filtered the set of *de novo*-predicted lncRNAs based on their distance to Ensembl-annotated protein-coding genes. We retained only lncRNA candidates that had no sense overlap with Ensembl-annotated protein-coding genes and that were at least 10 kilobases (kb) away from protein-coding gene coordinates. We also discarded loci with an exonic length below 200 bp (for multi-exonic loci) or 500 bp (for mono-exonic loci). We further excluded loci overlapping with RNA repeats or with UCSC-annotated retro-transposed gene copies over more than 10% of their length. These stringent criteria might have missed some lncRNAs, but we are convinced that many of the previously reported HCV induced lncRNAs were not bona-fide lncRNAs according to current bio-informatic standards.

In conclusion, our comprehensive transcriptome analysis of liver biopsy from patients with CHC revealed that HCV has no strong effect on the homeostasis of infected cells, that the endogenous IFN response is qualitatively similar to pegIFN α treatment but too weak to clear the infection and that IFN down-regulates miRNA precursor transcripts, thereby fine-tuning ISG expression.

5. References:

1. Luna, J.M. *et al.* Hepatitis C virus RNA functionally sequesters miR-122. *Cell* **160**, 1099-1110 (2015).
2. Lavanchy, D. Evolving epidemiology of hepatitis C virus. *Clin Microbiol Infect* **17**, 107-115 (2011).
3. Choo, Q.L. *et al.* Isolation of a cDNA clone derived from a blood-borne non-A, non-B viral hepatitis genome. *Science* **244**, 359-362 (1989).
4. Mohd Hanafiah, K., Groeger, J., Flaxman, A.D. & Wiersma, S.T. Global epidemiology of hepatitis C virus infection: new estimates of age-specific antibody to HCV seroprevalence. *Hepatology* **57**, 1333-1342 (2013).
5. van de Laar, T.J., Matthews, G.V., Prins, M. & Danta, M. Acute hepatitis C in HIV-infected men who have sex with men: an emerging sexually transmitted infection. *AIDS* **24**, 1799-1812 (2010).
6. Grebely, J. *et al.* The effects of female sex, viral genotype, and IL28B genotype on spontaneous clearance of acute hepatitis C virus infection. *Hepatology* **59**, 109-120 (2014).
7. Wang, C.C. *et al.* Acute hepatitis C in a contemporary US cohort: modes of acquisition and factors influencing viral clearance. *J Infect Dis* **196**, 1474-1482 (2007).
8. Yeung, L.T., To, T., King, S.M. & Roberts, E.A. Spontaneous clearance of childhood hepatitis C virus infection. *J Viral Hepat* **14**, 797-805 (2007).
9. Wiese, M., Berr, F., Lafrenz, M., Porst, H. & Oesen, U. Low frequency of cirrhosis in a hepatitis C (genotype 1b) single-source outbreak in germany: a 20-year multicenter study. *Hepatology* **32**, 91-96 (2000).
10. Tong, M.J., el-Farra, N.S., Reikes, A.R. & Co, R.L. Clinical outcomes after transfusion-associated hepatitis C. *N Engl J Med* **332**, 1463-1466 (1995).
11. Thein, H.H., Yi, Q., Dore, G.J. & Krahn, M.D. Estimation of stage-specific fibrosis progression rates in chronic hepatitis C virus infection: a meta-analysis and meta-regression. *Hepatology* **48**, 418-431 (2008).
12. Watanabe, H. *et al.* Spontaneous elimination of serum hepatitis C virus (HCV) RNA in chronic HCV carriers: a population-based cohort study. *J Med Virol* **71**, 56-61 (2003).

13. Westbrook, R.H. & Dusheiko, G. Natural history of hepatitis C. *J Hepatol* **61**, S58-68 (2014).
14. Poynard, T. *et al.* Slow regression of liver fibrosis presumed by repeated biomarkers after virological cure in patients with chronic hepatitis C. *J Hepatol* **59**, 675-683 (2013).
15. Heim, M.H. 25 years of interferon-based treatment of chronic hepatitis C: an epoch coming to an end. *Nat Rev Immunol* **13**, 535-542 (2013).
16. Goutagny, N. *et al.* Evidence of viral replication in circulating dendritic cells during hepatitis C virus infection. *J Infect Dis* **187**, 1951-1958 (2003).
17. Neumann, A.U. *et al.* Hepatitis C viral dynamics in vivo and the antiviral efficacy of interferon-alpha therapy. *Science* **282**, 103-107 (1998).
18. Powdrill, M.H. *et al.* Contribution of a mutational bias in hepatitis C virus replication to the genetic barrier in the development of drug resistance. *Proc Natl Acad Sci U S A* **108**, 20509-20513 (2011).
19. Smith, D.B. *et al.* Expanded classification of hepatitis C virus into 7 genotypes and 67 subtypes: updated criteria and genotype assignment web resource. *Hepatology* **59**, 318-327 (2014).
20. Moradpour, D., Penin, F. & Rice, C.M. Replication of hepatitis C virus. *Nat Rev Microbiol* **5**, 453-463 (2007).
21. Andre, P. *et al.* Characterization of low- and very-low-density hepatitis C virus RNA-containing particles. *J Virol* **76**, 6919-6928 (2002).
22. Egger, D. *et al.* Expression of hepatitis C virus proteins induces distinct membrane alterations including a candidate viral replication complex. *J Virol* **76**, 5974-5984 (2002).
23. Gosert, R. *et al.* Identification of the hepatitis C virus RNA replication complex in Huh-7 cells harboring subgenomic replicons. *J Virol* **77**, 5487-5492 (2003).
24. Barba, G. *et al.* Hepatitis C virus core protein shows a cytoplasmic localization and associates to cellular lipid storage droplets. *Proc Natl Acad Sci U S A* **94**, 1200-1205 (1997).
25. Boulant, S., Targett-Adams, P. & McLauchlan, J. Disrupting the association of hepatitis C virus core protein with lipid droplets correlates with a loss in production of infectious virus. *J Gen Virol* **88**, 2204-2213 (2007).
26. Targett-Adams, P., Hope, G., Boulant, S. & McLauchlan, J. Maturation of hepatitis C virus core protein by signal peptide peptidase is required for virus production. *J Biol Chem* **283**, 16850-16859 (2008).

27. Gastaminza, P., Kapadia, S.B. & Chisari, F.V. Differential biophysical properties of infectious intracellular and secreted hepatitis C virus particles. *J Virol* **80**, 11074-11081 (2006).
28. Huang, H. *et al.* Hepatitis C virus production by human hepatocytes dependent on assembly and secretion of very low-density lipoproteins. *Proc Natl Acad Sci U S A* **104**, 5848-5853 (2007).
29. Jopling, C.L., Yi, M., Lancaster, A.M., Lemon, S.M. & Sarnow, P. Modulation of hepatitis C virus RNA abundance by a liver-specific MicroRNA. *Science* **309**, 1577-1581 (2005).
30. Henke, J.I. *et al.* microRNA-122 stimulates translation of hepatitis C virus RNA. *EMBO J* **27**, 3300-3310 (2008).
31. Shimakami, T. *et al.* Stabilization of hepatitis C virus RNA by an Ago2-miR-122 complex. *Proc Natl Acad Sci U S A* **109**, 941-946 (2012).
32. Li, Y., Masaki, T., Yamane, D., McGivern, D.R. & Lemon, S.M. Competing and noncompeting activities of miR-122 and the 5' exonuclease Xrn1 in regulation of hepatitis C virus replication. *Proc Natl Acad Sci U S A* **110**, 1881-1886 (2013).
33. Colpitts, C.C., El-Saghire, H., Pochet, N., Schuster, C. & Baumert, T.F. High-throughput approaches to unravel hepatitis C virus-host interactions. *Virus Res* (2015).
34. Kolykhalov, A.A. *et al.* Transmission of hepatitis C by intrahepatic inoculation with transcribed RNA. *Science* **277**, 570-574 (1997).
35. Yanagi, M., Purcell, R.H., Emerson, S.U. & Bukh, J. Transcripts from a single full-length cDNA clone of hepatitis C virus are infectious when directly transfected into the liver of a chimpanzee. *Proc Natl Acad Sci U S A* **94**, 8738-8743 (1997).
36. Bukh, J. *et al.* Mutations that permit efficient replication of hepatitis C virus RNA in Huh-7 cells prevent productive replication in chimpanzees. *Proc Natl Acad Sci U S A* **99**, 14416-14421 (2002).
37. Wakita, T. *et al.* Production of infectious hepatitis C virus in tissue culture from a cloned viral genome. *Nat Med* **11**, 791-796 (2005).
38. Zhong, J. *et al.* Robust hepatitis C virus infection in vitro. *Proc Natl Acad Sci U S A* **102**, 9294-9299 (2005).
39. Lindenbach, B.D. *et al.* Complete replication of hepatitis C virus in cell culture. *Science* **309**, 623-626 (2005).
40. Li, Y.P. *et al.* Robust full-length hepatitis C virus genotype 2a and 2b infectious cultures using mutations identified by a systematic approach applicable to patient strains. *Proc Natl Acad Sci U S A* **109**, E1101-1110 (2012).

41. Li, Y.P. *et al.* Highly efficient full-length hepatitis C virus genotype 1 (strain TN) infectious culture system. *Proc Natl Acad Sci U S A* **109**, 19757-19762 (2012).
42. Marukian, S. *et al.* Hepatitis C virus induces interferon-lambda and interferon-stimulated genes in primary liver cultures. *Hepatology* **54**, 1913-1923 (2011).
43. Roelandt, P. *et al.* Human pluripotent stem cell-derived hepatocytes support complete replication of hepatitis C virus. *J Hepatol* **57**, 246-251 (2012).
44. Yoshida, T. *et al.* Use of human hepatocyte-like cells derived from induced pluripotent stem cells as a model for hepatocytes in hepatitis C virus infection. *Biochem Biophys Res Commun* **416**, 119-124 (2011).
45. Bukh, J. A critical role for the chimpanzee model in the study of hepatitis C. *Hepatology* **39**, 1469-1475 (2004).
46. Deinhardt, F., Holmes, A.W., Capps, R.B. & Popper, H. Studies on the transmission of human viral hepatitis to marmoset monkeys. I. Transmission of disease, serial passages, and description of liver lesions. *J Exp Med* **125**, 673-688 (1967).
47. Stapleton, J.T., Fong, S., Muerhoff, A.S., Bukh, J. & Simmonds, P. The GB viruses: a review and proposed classification of GBV-A, GBV-C (HGV), and GBV-D in genus Pegivirus within the family Flaviviridae. *J Gen Virol* **92**, 233-246 (2011).
48. Vercauteren, K., de Jong, Y.P. & Meuleman, P. Animal models for the study of HCV. *Curr Opin Virol* **13**, 67-74 (2015).
49. Bitzegeio, J. *et al.* Adaptation of hepatitis C virus to mouse CD81 permits infection of mouse cells in the absence of human entry factors. *PLoS Pathog* **6**, e1000978 (2010).
50. Mercer, D.F. *et al.* Hepatitis C virus replication in mice with chimeric human livers. *Nat Med* **7**, 927-933 (2001).
51. Dorner, M. *et al.* A genetically humanized mouse model for hepatitis C virus infection. *Nature* **474**, 208-211 (2011).
52. van der Meer, A.J. *et al.* Association between sustained virological response and all-cause mortality among patients with chronic hepatitis C and advanced hepatic fibrosis. *JAMA* **308**, 2584-2593 (2012).
53. Fried, M.W. *et al.* Peginterferon alfa-2a plus ribavirin for chronic hepatitis C virus infection. *N Engl J Med* **347**, 975-982 (2002).
54. Manns, M.P. *et al.* Peginterferon alfa-2b plus ribavirin compared with interferon alfa-2b plus ribavirin for initial treatment of chronic hepatitis C: a randomised trial. *Lancet* **358**, 958-965 (2001).
55. Poordad, F. *et al.* Boceprevir for untreated chronic HCV genotype 1 infection. *N Engl J Med* **364**, 1195-1206 (2011).

56. Poynard, T. *et al.* Effect of treatment with peginterferon or interferon alfa-2b and ribavirin on steatosis in patients infected with hepatitis C. *Hepatology* **38**, 75-85 (2003).
57. Hoofnagle, J.H. *et al.* Treatment of chronic non-A,non-B hepatitis with recombinant human alpha interferon. A preliminary report. *N Engl J Med* **315**, 1575-1578 (1986).
58. Davis, G.L. *et al.* Treatment of chronic hepatitis C with recombinant interferon alfa. A multicenter randomized, controlled trial. Hepatitis Interventional Therapy Group. *N Engl J Med* **321**, 1501-1506 (1989).
59. Di Bisceglie, A.M. *et al.* Recombinant interferon alfa therapy for chronic hepatitis C. A randomized, double-blind, placebo-controlled trial. *N Engl J Med* **321**, 1506-1510 (1989).
60. McHutchison, J.G. *et al.* Interferon alfa-2b alone or in combination with ribavirin as initial treatment for chronic hepatitis C. Hepatitis Interventional Therapy Group. *N Engl J Med* **339**, 1485-1492 (1998).
61. Zeuzem, S. *et al.* Peginterferon alfa-2a in patients with chronic hepatitis C. *N Engl J Med* **343**, 1666-1672 (2000).
62. Lindsay, K.L. *et al.* A randomized, double-blind trial comparing pegylated interferon alfa-2b to interferon alfa-2b as initial treatment for chronic hepatitis C. *Hepatology* **34**, 395-403 (2001).
63. Larner, A.C., Chaudhuri, A. & Darnell, J.E., Jr. Transcriptional induction by interferon. New protein(s) determine the extent and length of the induction. *J Biol Chem* **261**, 453-459 (1986).
64. Makowska, Z., Duong, F.H., Trincucci, G., Tough, D.F. & Heim, M.H. Interferon-beta and interferon-lambda signaling is not affected by interferon-induced refractoriness to interferon-alpha in vivo. *Hepatology* **53**, 1154-1163 (2011).
65. Sarasin-Filipowicz, M. *et al.* Alpha interferon induces long-lasting refractoriness of JAK-STAT signaling in the mouse liver through induction of USP18/UBP43. *Mol Cell Biol* **29**, 4841-4851 (2009).
66. Ploss, A. & Dubuisson, J. New advances in the molecular biology of hepatitis C virus infection: towards the identification of new treatment targets. *Gut* **61 Suppl 1**, i25-35 (2012).
67. Jacobson, I.M. *et al.* Telaprevir for previously untreated chronic hepatitis C virus infection. *N Engl J Med* **364**, 2405-2416 (2011).
68. Feld, J.J. *et al.* Sofosbuvir and Velpatasvir for HCV Genotype 1, 2, 4, 5, and 6 Infection. *N Engl J Med* **373**, 2599-2607 (2015).

69. Foster, G.R. *et al.* Sofosbuvir and Velpatasvir for HCV Genotype 2 and 3 Infection. *N Engl J Med* **373**, 2608-2617 (2015).
70. Isaacs, A. & Lindenmann, J. Virus interference. I. The interferon. *Proc R Soc Lond B Biol Sci* **147**, 258-267 (1957).
71. Pestka, S., Krause, C.D. & Walter, M.R. Interferons, interferon-like cytokines, and their receptors. *Immunol Rev* **202**, 8-32 (2004).
72. Croll, A.D., Wilkinson, M.F. & Morris, A.G. Gamma-interferon production by human low-density lymphocytes induced by T-cell mitogens. *Immunology* **58**, 641-646 (1986).
73. Handa, K., Suzuki, R., Matsui, H., Shimizu, Y. & Kumagai, K. Natural killer (NK) cells as a responder to interleukin 2 (IL 2). II. IL 2-induced interferon gamma production. *J Immunol* **130**, 988-992 (1983).
74. Aguet, M., Dembic, Z. & Merlin, G. Molecular cloning and expression of the human interferon-gamma receptor. *Cell* **55**, 273-280 (1988).
75. Hemmi, S., Bohni, R., Stark, G., Di Marco, F. & Aguet, M. A novel member of the interferon receptor family complements functionality of the murine interferon gamma receptor in human cells. *Cell* **76**, 803-810 (1994).
76. Soh, J. *et al.* Identification and sequence of an accessory factor required for activation of the human interferon gamma receptor. *Cell* **76**, 793-802 (1994).
77. Kotenko, S.V. *et al.* IFN-lambdas mediate antiviral protection through a distinct class II cytokine receptor complex. *Nat Immunol* **4**, 69-77 (2003).
78. Donnelly, R.P., Sheikh, F., Kotenko, S.V. & Dickensheets, H. The expanded family of class II cytokines that share the IL-10 receptor-2 (IL-10R2) chain. *J Leukoc Biol* **76**, 314-321 (2004).
79. Heim, M.H. & Thimme, R. Innate and adaptive immune responses in HCV infections. *J Hepatol* **61**, S14-S25 (2014).
80. Ank, N. *et al.* Lambda interferon (IFN-lambda), a type III IFN, is induced by viruses and IFNs and displays potent antiviral activity against select virus infections in vivo. *J Virol* **80**, 4501-4509 (2006).
81. Iwasaki, A. & Medzhitov, R. Toll-like receptor control of the adaptive immune responses. *Nat Immunol* **5**, 987-995 (2004).
82. Akira, S., Uematsu, S. & Takeuchi, O. Pathogen recognition and innate immunity. *Cell* **124**, 783-801 (2006).
83. Yoneyama, M. & Fujita, T. Function of RIG-I-like receptors in antiviral innate immunity. *J Biol Chem* **282**, 15315-15318 (2007).

84. Sadler, A.J. & Williams, B.R. Interferon-inducible antiviral effectors. *Nat Rev Immunol* **8**, 559-568 (2008).
85. Darnell, J.E., Jr., Kerr, I.M. & Stark, G.R. Jak-STAT pathways and transcriptional activation in response to IFNs and other extracellular signaling proteins. *Science* **264**, 1415-1421 (1994).
86. Decker, T., Lew, D.J., Mirkovitch, J. & Darnell, J.E., Jr. Cytoplasmic activation of GAF, an IFN-gamma-regulated DNA-binding factor. *EMBO J* **10**, 927-932 (1991).
87. Strehlow, I. & Decker, T. Transcriptional induction of IFN-gamma-responsive genes is modulated by DNA surrounding the interferon stimulation response element. *Nucleic Acids Res* **20**, 3865-3872 (1992).
88. Darnell, J.E., Jr. STATs and gene regulation. *Science* **277**, 1630-1635 (1997).
89. Zhou, Z. *et al.* Type III interferon (IFN) induces a type I IFN-like response in a restricted subset of cells through signaling pathways involving both the Jak-STAT pathway and the mitogen-activated protein kinases. *J Virol* **81**, 7749-7758 (2007).
90. Heim, M.H., Kerr, I.M., Stark, G.R. & Darnell, J.E., Jr. Contribution of STAT SH2 groups to specific interferon signaling by the Jak-STAT pathway. *Science* **267**, 1347-1349 (1995).
91. Der, S.D., Zhou, A., Williams, B.R. & Silverman, R.H. Identification of genes differentially regulated by interferon alpha, beta, or gamma using oligonucleotide arrays. *Proc Natl Acad Sci U S A* **95**, 15623-15628 (1998).
92. Marcello, T. *et al.* Interferons alpha and lambda inhibit hepatitis C virus replication with distinct signal transduction and gene regulation kinetics. *Gastroenterology* **131**, 1887-1898 (2006).
93. Sarasin-Filipowicz, M. *et al.* Interferon signaling and treatment outcome in chronic hepatitis C. *Proc Natl Acad Sci U S A* **105**, 7034-7039 (2008).
94. Krebs, D.L. & Hilton, D.J. SOCS proteins: negative regulators of cytokine signaling. *Stem Cells* **19**, 378-387 (2001).
95. Fenner, J.E. *et al.* Suppressor of cytokine signaling 1 regulates the immune response to infection by a unique inhibition of type I interferon activity. *Nat Immunol* **7**, 33-39 (2006).
96. Alexander, W.S. *et al.* SOCS1 is a critical inhibitor of interferon gamma signaling and prevents the potentially fatal neonatal actions of this cytokine. *Cell* **98**, 597-608 (1999).
97. Malakhova, O.A. *et al.* UBP43 is a novel regulator of interferon signaling independent of its ISG15 isopeptidase activity. *EMBO J* **25**, 2358-2367 (2006).

98. Stetson, D.B. & Medzhitov, R. Type I interferons in host defense. *Immunity* **25**, 373-381 (2006).
99. Thimme, R. *et al.* Determinants of viral clearance and persistence during acute hepatitis C virus infection. *J Exp Med* **194**, 1395-1406 (2001).
100. Bigger, C.B., Brasky, K.M. & Lanford, R.E. DNA microarray analysis of chimpanzee liver during acute resolving hepatitis C virus infection. *J Virol* **75**, 7059-7066 (2001).
101. Su, A.I. *et al.* Genomic analysis of the host response to hepatitis C virus infection. *Proc Natl Acad Sci U S A* **99**, 15669-15674 (2002).
102. Major, M.E. *et al.* Hepatitis C virus kinetics and host responses associated with disease and outcome of infection in chimpanzees. *Hepatology* **39**, 1709-1720 (2004).
103. Thomas, E. *et al.* HCV infection induces a unique hepatic innate immune response associated with robust production of type III interferons. *Gastroenterology* **142**, 978-988 (2012).
104. Park, H. *et al.* IL-29 is the dominant type III interferon produced by hepatocytes during acute hepatitis C virus infection. *Hepatology* **56**, 2060-2070 (2012).
105. Takahashi, K. *et al.* Plasmacytoid dendritic cells sense hepatitis C virus-infected cells, produce interferon, and inhibit infection. *Proc Natl Acad Sci U S A* **107**, 7431-7436 (2010).
106. Thimme, R., Binder, M. & Bartenschlager, R. Failure of innate and adaptive immune responses in controlling hepatitis C virus infection. *FEMS Microbiol Rev* **36**, 663-683 (2012).
107. Rehmann, B. Pathogenesis of chronic viral hepatitis: differential roles of T cells and NK cells. *Nat Med* **19**, 859-868 (2013).
108. Thimme, R. *et al.* Viral and immunological determinants of hepatitis C virus clearance, persistence, and disease. *Proc Natl Acad Sci U S A* **99**, 15661-15668 (2002).
109. Wieland, S. *et al.* Simultaneous detection of hepatitis C virus and interferon stimulated gene expression in infected human liver. *Hepatology* **59**, 2121-2130 (2014).
110. Terczynska-Dyla, E. *et al.* Reduced IFN λ 4 activity is associated with improved HCV clearance and reduced expression of interferon-stimulated genes. *Nat Commun* **5**, 5699 (2014).
111. Honda, M. *et al.* Hepatic ISG expression is associated with genetic variation in interleukin 28B and the outcome of IFN therapy for chronic hepatitis C. *Gastroenterology* **139**, 499-509 (2010).

112. Urban, T.J. *et al.* IL28B genotype is associated with differential expression of intrahepatic interferon-stimulated genes in patients with chronic hepatitis C. *Hepatology* **52**, 1888-1896 (2010).
113. Chen, L. *et al.* Hepatic gene expression discriminates responders and nonresponders in treatment of chronic hepatitis C viral infection. *Gastroenterology* **128**, 1437-1444 (2005).
114. Asselah, T. *et al.* Liver gene expression signature to predict response to pegylated interferon plus ribavirin combination therapy in patients with chronic hepatitis C. *Gut* **57**, 516-524 (2008).
115. Dill, M.T. *et al.* Interferon-gamma-stimulated genes, but not USP18, are expressed in livers of patients with acute hepatitis C. *Gastroenterology* **143**, 777-786 e771-776 (2012).
116. Prokunina-Olsson, L. *et al.* A variant upstream of IFNL3 (IL28B) creating a new interferon gene IFNL4 is associated with impaired clearance of hepatitis C virus. *Nature genetics* **45**, 164-171 (2013).
117. Thomas, D.L. *et al.* Genetic variation in IL28B and spontaneous clearance of hepatitis C virus. *Nature* **461**, 798-801 (2009).
118. Rauch, A. *et al.* Genetic variation in IL28B is associated with chronic hepatitis C and treatment failure: a genome-wide association study. *Gastroenterology* **138**, 1338-1345, 1345 e1331-1337 (2010).
119. Tanaka, Y. *et al.* Genome-wide association of IL28B with response to pegylated interferon-alpha and ribavirin therapy for chronic hepatitis C. *Nature genetics* **41**, 1105-1109 (2009).
120. Bibert, S. *et al.* IL28B expression depends on a novel TT/-G polymorphism which improves HCV clearance prediction. *J Exp Med* **210**, 1109-1116 (2013).
121. Wack, A., Terczynska-Dyla, E. & Hartmann, R. Guarding the frontiers: the biology of type III interferons. *Nat Immunol* **16**, 802-809 (2015).
122. Walters, K.A. *et al.* Genomic analysis reveals a potential role for cell cycle perturbation in HCV-mediated apoptosis of cultured hepatocytes. *PLoS Pathog* **5**, e1000269 (2009).
123. Kambara, H. *et al.* Negative regulation of the interferon response by an interferon-induced long non-coding RNA. *Nucleic Acids Res* **42**, 10668-10680 (2014).
124. Barriocanal, M., Carnero, E., Segura, V. & Fortes, P. Long Non-Coding RNA BST2/BISPR is Induced by IFN and Regulates the Expression of the Antiviral Factor Tetherin. *Front Immunol* **5**, 655 (2014).

125. Carnero, E. & Fortes, P. HCV infection, IFN response and the coding and non-coding host cell genome. *Virus Res* **212**, 85-102 (2016).

6. Curriculum Vitae

Personal Details:

Family Name: Boldanova
Given Name: Tuyana
Date of Birth: 18th of December 1981
Nationality: Russian
Address: Riehenring 9, CH-4058 Basel
Email: t.boldanova@gmx.ch

Work Experience:

Since 7/2015	Residency at Gastroenterology and Hepatology Division	University Hospital Basel, Switzerland
1/2008-12/2011	Internal Medicine Residency (inpatient and outpatient medicine, emergency room, Cardiology, Gastroenterology and Hepatology, cardiac and intensiv care unit, cardiac surgery)	University Hospital Basel, Switzerland
09/2006 - 12/2007	Research Fellowship at Cardiology Division (Participation in 5 clinical trials)	University Hospital Basel, Switzerland
09/2004 - 06/2006	Intern in the Internal Medicine and Surgery	Irkutsk State Hospital, Russia

Education:

Since 1/2012 03/2007-5/2009	MD-PhD in Hepatology group, Biomedicine Department of the University of Basel, Switzerland Doctoral candidate (Doktorandin) in Graduation Subject Human Medicine (Promotionsfach Humanmedizin) in the University of Basel, Switzerland
06/2004	Diploma as Medical Doctor
1998 - 2004	State Medicine University of Irkutsk, Russia Faculty: Human Medicine
06/1998	General qualification for University entrance
1996 -1998	Medical - biology gymnasium

1988 -1996 Primary school

Further education:

12/2010	Basis training: Contrast-enhanced ultrasound	Thun, Switzerland
2/2010	Basic training: Ultrasound, SGUM	Winterthur, Switzerland
11/2009	BLS-Course	Basel, Switzerland
1/2008	Diabetes-Course	Basel, Switzerland
6/2007	European language certificate, German	Goethe-Institut, Frankfurt/Main
5/2007	Presentation training course	Liestal, Switzerland

Dissertation:

5/2009	Impact of history of heart failure on diagnostic and prognostic value of BNP: Results from the B-type Natriuretic Peptide for Acute Shortness of Breath Evaluation (BASEL) Study	Prof. Dr. Christian Müller Universitätsspital Basel
--------	--	---

Conference contributions:

1. National MD-PhD Conference and General Assembly of the Swiss MD-PhD 2015: Long non-coding RNAs and interferon-regulated gene expression
2. Hepatobiliary and Gastrointestinal Research Retreat 2015, Vulpera (GR), Switzerland: Hepatocellular carcinoma project: overview
3. Gastroenterology-Region Meeting 2014, Strasbourg, France: Mechanisms of Evasive Resistance in Cancer (MERiC): Overview of the project
4. Gastroenterology-Region Meeting 2012, Freiburg, Germany: LncRNA-AC122108.1 is required to genes repress a subset of IFN α -regulated

Awards:

9/2012: MD/PhD stipend of the Swiss National Science Foundation

Publication List:

1. **Boldanova T**, Suslov A, Heim MH and Necsulea A. Transcriptional response to hepatitis C virus infection and interferon alpha treatment in the human liver. Submitted
2. Makowska Z, **Boldanova T**, Adametz D, Quagliata L, Vogt JE, Dill MT, Matter MS, Roth V, Terracciano L, Heim MH. Gene expression analysis of biopsy samples reveals critical limitations of transcriptome-based molecular classifications of hepatocellular carcinoma. *J Pathol Clin Res*. 2016 Feb 5;2(2):80-92.
3. Dazert E, Colombi M, **Boldanova T**, Moes S, Adametz D, Quagliata L, Roth V, Terracciano L, Heim MH, Jenoe P, Hall MN. Quantitative proteomics and phosphoproteomics on serial tumor biopsies from a sorafenib-treated HCC patient. *Proc Natl Acad Sci U S A*. 2016 Feb 2;113(5):1381-6.
4. Frey RS, **Boldanova T**, Heim M. Ultrasound surveillance for hepatocellular carcinoma: real-life performance in a hepatology outpatient clinic. *Swiss Med Wkly*. 2015 Nov 20;145:w14200.
5. Anggakusuma, Romero-Brey I, Berger C, Colpitts CC, **Boldanova T**, Engelmann M, Todt D, Perin PM, Behrendt P, Vondran FW, Xu S, Goffinet C, Schang LM, Heim MH, Bartenschlager R, Pietschmann T, Steinmann E. Interferon-inducible cholesterol-25-hydroxylase restricts hepatitis C virus replication through blockage of membranous web formation. *Hepatology*. 2015 Sep;62(3):702-14.
6. Duong FH, Trincucci G, **Boldanova T**, Calabrese D, Campana B, Krol I, Durand SC, Heydmann L, Zeisel MB, Baumert TF, Heim MH. IFN- λ receptor 1 expression is induced in chronic hepatitis C and correlates with the IFN- λ 3 genotype and with nonresponsiveness to IFN- α therapies. *J Exp Med*. 2014 May 5;211(5):857-68.
7. Schaub N, **Boldanova T**, Noveanu M, Arenja N, Hermann H, Twerenbold R, Frei R, Bingisser R, Trampuz A, Mueller C. Incremental value of multiplex real-time PCR for the early diagnosis of sepsis in the emergency department. *Swiss Med Wkly*. 2014 Feb 4;144:w13911.
8. Quagliata L, Matter MS, Piscuoglio S, Arabi L, Ruiz C, Procino A, Kovac M, Moretti F, Makowska Z, **Boldanova T**, Andersen JB, Hämmerle M, Tornillo L, Heim MH, Diederichs S, Cillo C, Terracciano LM. Long noncoding RNA HOTTIP/HOXA13 expression is associated with disease progression and predicts outcome in hepatocellular carcinoma patients. *Hepatology*. 2014 Mar;59(3):911-23.
9. Clément S, Fauvelle C, Branche E, Kaddai V, Conzelmann S, **Boldanova T**, Bartosch B, Minehira K, Negro F. Role of seipin in lipid droplet morphology and hepatitis C virus life cycle. *J Gen Virol*. 2013 Oct;94(Pt 10):2208-14
10. Potocki M, Breidhardt T, Reichlin T, Hartwiger S, Morgenthaler NG, Bergmann A, Noveanu M, Freidank H, Taegtmeier AB, Wetzl K, **Boldanova T**, Stelzig C, Bingisser R, Christ M, Mueller C. Comparison of midregional pro-atrial natriuretic

peptide with N-terminal pro-B-type natriuretic peptide in the diagnosis of heart failure. *J Intern Med.* 2010 Jan;267(1):119-29.

11. Reichlin T, Hochholzer W, Stelzig C, Laule K, Freidank H, Morgenthaler NG, Bergmann A, Potocki M, Noveanu M, Breidhardt T, Christ A, **Boldanova T**, Merki R, Schaub N, Bingisser R, Christ M, Mueller C. Incremental value of copeptin for rapid rule out of acute myocardial infarction. *J Am Coll Cardiol.* 2009 Jun 30;54(1):60-8.
12. **Boldanova T**, Noveanu M, Breidhardt T, Potocki M, Reichlin T, Taegtmeyer A, Christ M, Laule K, Stelzig C, Mueller C. Impact of history of heart failure on diagnostic and prognostic value of BNP: results from the B-type Natriuretic Peptide for Acute Shortness of Breath Evaluation (BASEL) study. *Int J Cardiol.* 2010 Jul 23;142(3):265-72.
13. Breidhardt T, Christ M, Matti M, Schrafl D, Laule K, Noveanu M, **Boldanova T**, Klima T, Hochholzer W, Perruchoud AP, Mueller C. QRS and QTc interval prolongation in the prediction of long-term mortality of patients with acute destabilised heart failure. *Heart.* 2007 Sep;93(9):1093-7.